Spring 2022

ANISOTROPY AND ITS EFFECTS ON STORMWATER SUBSURFACE GRAVEL TRENCH DESIGN

David Joseph Tarushka
University of New Hampshire, Durham

ANISOTROPY AND ITS EFFECTS ON STORMWATER SUBSURFACE GRAVEL TRENCH DESIGN

BY

DAVID TARUSHKA

BS Civil Engineering, University of New Hampshire, 2015

THESIS

Submitted to the University of New Hampshire

In Partial Fulfillment of

The Requirements for the Degree of

Master of Science

in

Civil Engineering

May 2022

This thesis/dissertation has been examined and approved in partial fulfillment of the requirements for the degree of Master of Science in Civil Engineering by:

Thesis/Dissertation Director, Thomas Ballestero, Ph.D. Civil and Environmental Engineering

Ernst Linder, Ph.D. Statistics

Alison Watts, Ph.D. Civil and Environmental Engineering

On April 13, 2022

Original approval signatures are on file with the University of New Hampshire Graduate School.

DEDICATION

In loving memory of my grandfather, Joseph.

"It doesn't matter how long you take, as long as you never stop."

ACKNOWLEDGEMENTS

This research was funded by the EPA STAR project (Grant Number RD 83555801) and the city of Philadelphia, and conducted by the University of New Hampshire Stormwater Center, as led by Dr. Thomas Ballestero and Dr. James Houle.

I wish to thank the people who helped me through this process including Dr. Tom Ballestero, Dr. Ernst Linder, John Chagnon and the associates of Ambit Engineering, Daniel Macadam, Phani Kidambi, Betsy, and my ever-patient family.

TABLE OF CONTENTS

Dedication iii

Acknowledgements iv

List of Tables vii

List of Figures viii

List of Appendices xi

Abstract xii

Introduction 1

Literature Review 6

1. Infiltration and Subsurface Performance 6

2. Stormwater Parameters and Concepts 9

3. Statistical Concepts 12

Methods 15

1.Site Analysis 15

A. Trench Design 15

B. Other Considerations of Subsurface Conditions 21

C. Monitoring Equipment 23

D. Site Borings 26

2. Storms 27

3. Trench Analysis 29

A. Modelling Process 29

B. Layer Equations 33

C. Automated Correction and Detection 50

D. Manual Data Removal 59

E. Time Series 63

F. Drainage Prediction 70

G. Primary Knot Points 73

H. Splines 78

I. Hydrograph Consolidation and Knot Tuning 84

Results 93

1. Recreating Original Data with Model 93

2. Field Workflow 109

3. Future Recommendations 111

Conclusion 114

List of References 120

LIST OF TABLES

Table 1: GA-1 boring results, Golder Associates 27

Table 2: Infiltration rate profile of Lot-A subsurface gravel trench estimated from HydroCAD 105

LIST OF FIGURES

Figure 1: One-inch storm hydrograph volume estimation, UNH A-Lot 4

Figure 2: Plan view of UNH Lot A Tree Trench system 16

Figure 3: Cross sectional diagram of UNH Lot A Tree Trench system 17

Figure 4: Time history of depth of water in trench and precipitation, A-Lot 19

Figure 5: A Lot Gravel Trench Construction after rain 23

Figure 6: 9/19/2016 Storm, Monitoring Wells in A-Lot, Mounding, 1.24 in. 25

Figure 7: A depiction of the bulb of saturation surrounding a subsurface gravel trench 34

Figure 8: The conceptual model of infiltration from a subsurface gravel trench 34

Figure 9: Uneven versus calculated depth profile for partially filled gravel trench 38

Figure 10: Example of finding discontinuities, part 1 40

Figure 11: Example of finding discontinuities, part 2 41

Figure 12: Example of finding discontinuities, part 3 41

Figure 13: Example of finding discontinuities, part 4 42

Figure 14: Illustration of Darcy's Law 45

Figure 15: Complete dataset, pre-drift correction, UNH A-Lot 50

Figure 16: Drift corrected complete dataset, UNH A-Lot 53

Figure 17: Complete dataset, post-drift correction, UNH A-Lot, depth of water in gravel trench 53

Figure 18: Partial dataset and peak detection, UNH A-Lot 56

Figure 19: Partial dataset with cropped recession limbs, UNH A-Lot 58

Figure 20: Discarded storm hydrograph, algorithm irregularities, UNH A-Lot 60

Figure 21: Discarded storm hydrograph, bad data, UNH A-Lot 61

Figure 22: Discarded storm hydrograph, extensive reaction delay, UNH A-Lot 62

Figure 23: Chosen dataset for initial regression (Oct. 9, 2016, 0.884 inches of rain), UNH A-Lot 63

Figure 24: Comparing a linear spline to a general trendline 66

Figure 25: Predicted versus actual trench hydrograph, R-squared, UNH A-Lot 67

Figure 26: EARTH results for hydrograph peak prediction 67

Figure 27: EARTH model selection, UNH A-Lot 70

Figure 28: EARTH residuals (ft) versus fitted water height values (ft), UNH A-Lot 71

Figure 29: An example of a master curve and a derivative secondary curve 72

Figure 30: All water depth hydrographs overlapped, UNH Lot A gravel trench 74

Figure 31: Demonstration of knot points on hydrograph, UNH A-Lot 77

Figure 32: First knot characteristic curve, UNH A-Lot 81

Figure 33: Second knot characteristic curve, UNH A-Lot 81

Figure 34: Third knot characteristic curve, UNH A-Lot 82

Figure 35: Practice storm fitting, A-Lot 84

Figure 36: Infiltration rates from practice storm fitting, A-Lot 85

Figure 37: Master curve after adjustment iteration 8, UNH A-Lot 86

Figure 38: Comparison of adjusted aggregate data to EARTH model, UNH A-Lot 88

Figure 39: EARTH model for master curve 89

Figure 40: EARTH model selection, UNH A-Lot 90

Figure 41: Trench height EARTH residuals (ft) versus fitted trench height values (ft), UNH A-Lot 91

Figure 42: Predicted versus observed water height in trench, UNH A-Lot 92

Figure 43: Comparison of EARTH to actual data, partial dataset, UNH A-Lot 96

Figure 44: Sidewall infiltration as a percentage of total infiltration 97

Figure 45: Rainfall depth (log10-inches) versus percent sidewall infiltration, UNH A-Lot 98

Figure 46: Synthetic hydrograph versus actual data, UNH A-Lot 100

Figure 47: Synthetic and actual hydrograph of UNH A-Lot, partial dataset 101

Figure 48: One-inch storm hydrograph estimation, UNH A-Lot 102

Figure 49: One-inch storm hydrograph infiltration rate, UNH A-Lot 103

Figure 50: Height in gravel trench vs. system average infiltration rate, UNH A-Lot 104

Figure 51: HydroCAD infiltration through bottom of gravel trench, A-Lot 107

Figure 52: HydroCAD infiltration through bottom and sides of gravel trench, A-Lot 107

LIST OF APPENDICES

Appendix A: UNH Tax Map

Appendix B: UNH Flood Map

Appendix C: UNH A-Lot Soil Map and Report

Appendix D: UNH A-Lot Extreme Precipitation Report

Appendix E: UNH A-Lot HydroCAD Analysis

Appendix F: Compiled Anisotropy Code

Appendix G: UNH A-Lot As-Built diagrams

Appendix H: UNH A-Lot Boring Logs

Appendix I: Trench Design Calculations

Appendix J: Infiltrometer Testing Data

Appendix K: Monitoring Well Installation Log

Appendix L: HOBO U20 Specifications

Appendix M: CS450 Specifications

ABSTRACT

ANISOTROPY AND ITS EFFECTS ON STORMWATER SUBSURFACE GRAVEL TRENCH DESIGN

By

David Tarushka

University of New Hampshire, May 2022

Currently, one of the fastest growing fields in infrastructure is stormwater. Stormwater systems are the first line of defense in protecting cities from flooding and overburdening wastewater treatment facilities. Since stormwater infrastructure will continue to grow for the foreseeable future, any reduction in construction requirements may result in a considerable reduction in spending. The most immediate way to reduce construction costs would be to reduce the size of the system itself.

The focus of this thesis will be infiltration characteristics of stormwater systems, using the ongoing research of parking lot A at the University of New Hampshire in Durham, NH. The research consists of calculating the infiltration rates of a subsurface stormwater gravel trench. It is believed that the system experiences higher than expected infiltration rates due to an unusually high rate of lateral flow, characterized by the soil's anisotropy. This research discusses how anisotropy can potentially be obtained in situ, how this can be used when modelling the system's hydraulic performance, and how this relates to reducing stormwater system sizes. This paper theorizes that sudden changes in performance in a gravel trench can be used to distinguish soil horizon elevations, and estimate lateral infiltration rates using splicing techniques such as EARTH and linear modelling. With those practices, the Lot-A gravel trench is believed to have

lateral infiltration rates spanning 0.150 inches per hour at the bottom of the trench to 124 inches per hour at the top of the trench, depending on the soil layer. The models produced were also able to reproduce the water height data of the trench system using only rain gauge data, with an R^2 value of 0.793, and an RMSE of 0.115 feet.

INTRODUCTION

The EPA defines stormwater as follows:

§122.26(b)(13) *Storm water* means storm water runoff, snow melt runoff, and surface runoff and drainage (ECFR, 2022).

This paper will define stormwater as any runoff resultant from precipitation, including rainfall and snow melt. Before precipitation that has reached the ground can be qualified as runoff, there are a few ways in which that precipitation can be intercepted. Precipitation can be pooled in small depressions on the ground or obstructed by trees, also known as "initial abstraction," it can be absorbed into the ground through infiltration, or it can be stored on the ground as snow. Surface runoff occurs when all local forms of interception have been exhausted, the infiltrative capacity of the soil has been exceeded, and stored snow (if any) should begin to melt. Impervious surfaces, like roads and buildings, have very little interception quality, and as such are known to produce greater amounts of runoff, and consequentially, produce higher velocity runoff (HydroCAD, 2020). In great enough quantities, and without proper reduction techniques, surface runoff has the potential to cause a multitude of problems with infrastructure and local habitat. Larger volumes of runoff, for example, cause the water to run at higher velocities, carrying larger diameter sediments and causing erosion. Runoff exposed to pavement and agricultural land can also carry pollutants into streams, causing problems with the local wildlife (Tsihrintzis, 1997). That same stormwater could also be carried by a drainage system, taxing that system's limited capacity for treatment or conveyance. Therefore, it is the purpose of modern green stormwater infrastructure to act as an additional stormwater interception, one with the potential to treat stormwater so it may be in balance with the surrounding ecosystem, and not

overburden the environment or local infrastructure (New Hampshire Stormwater Manual Part 2, 2008).

There are many interception techniques, but one of the most common is routing the water, via culverts and catch basins, to the nearest, most appropriate water body. Sometimes, stormwater can be intercepted and infiltrated into the surrounding soil. There are tradeoffs to be considered when comparing different methods of runoff facilitation. It may prove more cost effective to use on-site stormwater management systems, which can divert and treat stormwater in an environmentally safer manner than letting stormwater run into a stream unabated (Tsihrintzis, 1997). However, depending on the type of system proposed, stormwater systems may have hidden costs and different functionalities that make them impractical for the desired effect (Alfakih, 1999). Any proposed stormwater systems will require those considerations.

The green stormwater infrastructure management system (GSI) discussed in this thesis is a subsurface gravel trench system (New Hampshire Stormwater Manual Part 2, 2008, page 84). A subsurface gravel trench is a trench dug near the outlet of a desired subcatchment. The trench has geotextiles affixed to the side walls and is filled with uniformly graded gravel. The gravel has a high void ratio, estimated at 0.40 (New Hampshire Stormwater Manual Part 2, 2008, page 87), which serves several purposes: allowing for the free flow of water through the GSI, providing storage space for water, provides surface area for biogeochemical reactions for pollutant reduction, and dependent on design criteria, can provide extra infiltration into the surrounding soil. During a storm, when runoff reaches the outlet of the subcatchment, it will flow into the GSI inlet, from the inlet then into a system of slotted pipes running near the top of the gravel, through the gravel medium, into a second set of slotted pipes called the “underdrain,” and from the underdrain to the outlet of the system. The outlet can be connected to any local drainage

infrastructure, or to the stormwater's ultimate destination. In addition to any stormwater exiting the underdrain, if the GSI is designed as an infiltration practice, it is expected that some of the stormwater contained within the gravel medium will infiltrate into the surrounding native soil. If the trench overflows, the water will start flowing out of a high flow bypass (HFB) and into the surrounding drainage network. The volume of water that exits the system due to infiltration can be considered volume reduction, as that stormwater will reach a different destination than it otherwise would have without the GSI.

When discussing a stormwater system with infiltration capacity, like the subsurface gravel trench, it is important to remember that once water infiltrates into the location's native soil, the water does not "go away." Water will always flow from an area of high energy to an area of low energy. The water's flow path is influenced by gravity but can flow in any direction dependent on the forces acting on it. Once in soil, water can flow sideways or even upwards. Such a consideration is often ignored in the subsurface design process, which only considers flow in the vertical direction (Green, 1911). In a trench system, infiltration is often only considered out the bottom of the trench, and not through the sidewalls (New Hampshire Stormwater Manual Part 2, 2008, page 86). It may be the case that certain design variables, particularly the maximum drain time (New Hampshire Stormwater Manual Part 2, 2008, page 87) would benefit considerably with the addition of accurate sidewall infiltration estimates.

This paper seeks to determine the influence of soil layering effects and lateral infiltration rates on the performance of a subsurface gravel trench system located at the University of New Hampshire's parking lot A.

Figure 1 shows an estimated hydrograph of the system in question. The y-axis represents the volume of water in the gravel trench, which is directly related to the height of water in the

trench. The x-axis represents time. There are multiple segments in the hydrograph, as can be found in any of the observed hydrographs. This thesis posits that the segmentation is due to layering effects in the soil surrounding the gravel trench, that each kink in the graph is representative of a soil horizon, and that each segment of the falling branch of every hydrograph can be deconstructed into a composite of infiltration through every layer exposed to saturation both horizontally and vertically at the bottom of the trench. Figure 1 shows a diagram to that effect.

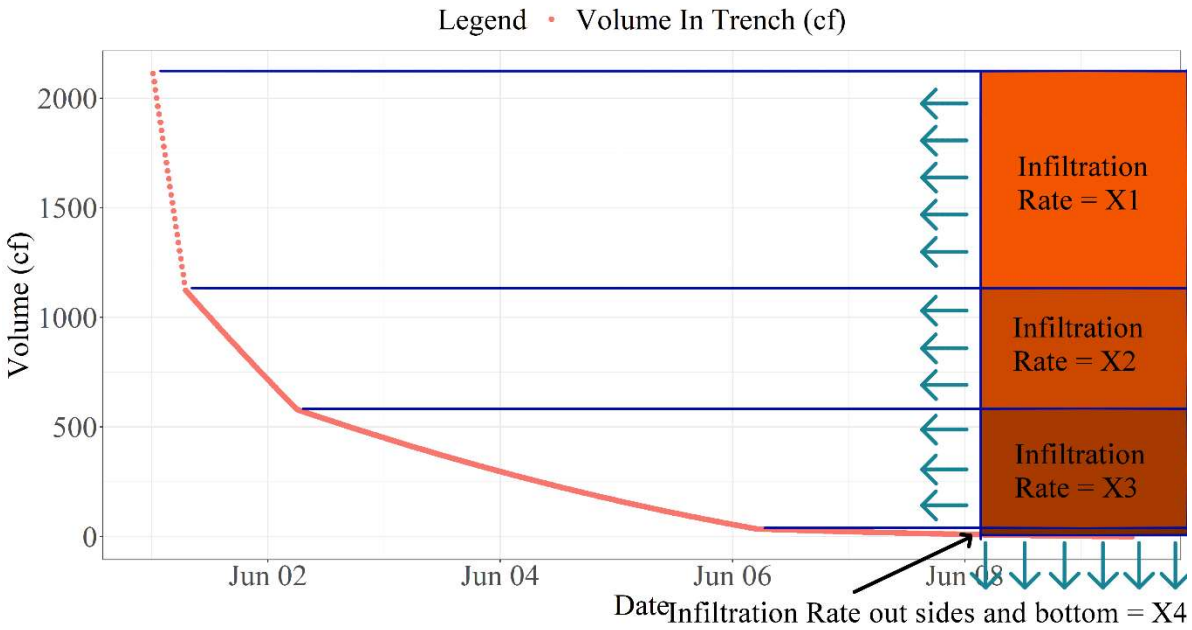

Figure 1: One-inch storm hydrograph volume estimation, UNH A-Lot

This thesis seeks to consider the inclusion of soil layering characteristics into the analysis of the subsurface gravel trench by using field observations of water depths in an analogous system with linear models. The current design procedures for a subsurface gravel trench only considers infiltration out the bottom surface of the trench, and not the sides. If infiltration out the sides was being considered, a trench might be able to infiltrate the required Water Quality Volume (WQV), or volume produced by 1 inch of rainfall over the relevant subcatchment, into

the surrounding soil within the required time allotment of 72 hours while using less area than the area proposed by more traditional methods. If the designed trench's dimensions have the possibility of being reduced, then that may lead to saving money on construction costs.

The methodology utilized in this thesis uses a statistical analysis of a subsurface gravel trench water level data. A set of measurements from one location of the height of water in the trench are taken into consideration and utilized in a statistical framework, such that water out the sides of the trench can be analyzed separately from water out the bottom of the trench. The different components can then be analyzed for their net contribution to the time it takes for water in the trench to infiltrate the surrounding soil. The methodology can then be compared to other methods of infiltration so that their water balances and estimates for infiltration can be directly compared. The desired result is an estimation for every storm's trench water level hydrograph, specifically where the water height is falling over time, which can then be compared to the observed data set.

Hypothesis: Provided a soil profile with horizontal anisotropic conditions and a high rate of lateral flow, as well as an explanatory model, sidewall infiltration can be used to explain subsurface gravel trench performance that vertical infiltration could not by itself.

LITERATURE REVIEW

The literature review can be subdivided in three specific parts. The first part is "Infiltration and Subsurface Performance," where performance and on-site tests specific to the subsurface gravel trench are explored. The second section is "Stormwater Parameters and Concepts" which discusses the broader concepts surrounding the field of stormwater, as well as more abstract soil hydraulic equations. The third section, "Statistical Concepts" will discuss statistical approaches to modelling real world phenomenon, not necessarily to do with stormwater directly, but useful for that purpose nonetheless. Of the sections researched, the area that provided the least suitable information was "Infiltration and Subsurface Performance." The amount of information available about lateral infiltration, testing procedures, the subsurface gravel trench, and any numerical data therein was very limited. Most papers found were presented in terms of abstract equations that would be difficult for those without specific knowledge of the subject to understand, let alone replicate. Some of the search terms for this thesis included anisotropy, lateral infiltration, gravel trench, hydraulic conductivity, infiltration testing, groundwater programs, smoothing filters, spline regressions, polynomial regressions, and various R language related queries.

1. Infiltration and Subsurface Performance

Literature on infiltration practices in regards to lateral hydraulic performance of soil was limited, particularly in regards to testing. "Discrepancies Between Analytical Solutions of Two

Borehole Permeameters for Estimating Field-Saturated Hydraulic Conductivity" discussed various methods for estimating hydraulic conductivities using the Guelph permeameter (Jabro, 2006). This paper as well as "An Improved Infiltration Model and Design Sizing Approach for Stormwater Bioretention Filters Including Anisotropy and Infiltration into Native Soils" (Macadam, 2018) proved useful in demonstrating why the guelph permeameter is not a useful device for measuring hydraulic anisotropy in soils, as the device has the potential to return negative flow rates, which given the circumstances is impossible. In "Sequential infiltration analysis of infiltration curves measured with disc infiltrometer in layered soils," however, methods are investigated in regards to how to overcome the inherent errors in the saturated bulb testing procedure (D. Moret-Fernández, 2021). This article proposes that an increasing time series analysis can potentially solve for the properties of the top layer of soil when using a disc infiltrometer. The article discusses computational methods and lab testing used to estimate saturated conductivity, as well as the thickness of the top layer of soil and sorptivity. The only downside is that this method can only solve for the properties of the first layer of soil, and not an entire profile.

The test with the most literature, the double ring infiltrometer, did not provide estimates for lateral infiltration rates. "Measuring Horizontal and Vertical Hydraulic Conductivity of Soil With the Double-Tube Method" provides a method for solving for the anisotropy of a soil through the use of a double ring infiltrometer (Bouwer, 1964). The double ring infiltrometer is a useful device for in-situ measurements of a soil's vertical infiltration rate. In the event that a soil profile is needed, the double ring infiltrometer would need large holes dug at multiple elevations for the access of the device. The double ring infiltrometer was used during the construction of the Lot A gravel trench to get vertical infiltration estimates on the site.

When adequate information was not found on either testing procedures or the performance of the gravel trench itself, the next step was to look for general equations that might provide lateral infiltration rates through more common methodology and computation. The goal would be to find an equation that was analogous to a subsurface gravel trench. “Solving vertical and horizontal well hydraulics problems analytically in Cartesian coordinates with vertical and horizontal anisotropies” claims to solve for anisotropy in the vertical direction, as well as in cartesian coordinates (Batu, 2012). The defined well modelled for drawdown in the paper is long and thin, and exists across an aquifer of specified width and infinite length. A possible implementation of such a setup might be to mirror the well across the length of the trench. Unfortunately, this system models drawdown in saturated soil, as might occur below the water table, where the system of this thesis involves pumping water into unsaturated soil, so the scenario is not analogous.

In a similar vein of problems with analogy, “Drawdowns due to Intermittent-Pumping Cycles” contains an intermittent cycle pump equation (Singh, 2004). Such a concept is relevant to the given thesis as it explains water introduced to a given system. The equations presented require a measured transmissivity or storativity of a given system. There are also theoretical problems connecting this paper to the presented thesis, as this paper discusses introducing water in a series of regular, equal bursts to a well source with zero volume. An ideal solution set would allow for a single burst to be introduced to a given system, rather than a regular series.

If one is able to procure an estimation for both vertical and horizontal soil conductivity, it may be possible to use the unit gradient flow model as utilized in “Infiltration Characteristics of Subsurface Gravel Filtration Systems for Stormwater Management,” a saturated flow model that utilizes computational methods to solve for individual horizontal and vertical components of

flow out of a system (Ely, 2019). The paper by Macadam mentioned earlier also provided a useful metric for measuring horizontal outflow by using the Green-Ampt method in the horizontal as well as the vertical direction (Macadam, 2018). The method as suggested would have the horizontal Green-Ampt equation resemble the vertical Green-Ampt equation with a couple differences, most importantly that the wetting front not be used as a driving factor, as would be dictated by the direction of gravity.

An additional method worth considering for modelling horizontal infiltration can be found in "A MODFLOW Infiltration Device Package for Simulating Storm Water Infiltration" (Jeppesen, 2015). While the traditional MODFLOW program is conducted in the groundwater table, the additional package mentioned in the paper allows for a system to be measured outside the groundwater table entirely, including the ability to infiltrate out the bottom of the designed system.

2. Stormwater Parameters and Concepts

This section is dedicated to more general knowledge about the subject of stormwater, including the reasons for stormwater practices. The best starting point for this subject is likely the regulatory agency that establishes the need for stormwater regulation. "Title 40: Protection of Environment" which establishes the EPA, the regulatory agency which set up stormwater regulations used across America, provided a definition for stormwater for reference. The EPA's definition of "stormwater" uses the word "stormwater" in the definition, so for clarity, their definition of stormwater was adapted slightly for this thesis. As mentioned in the introduction,

"this paper will define stormwater as any runoff resultant from precipitation, including rainfall and snow melt." This definition was used because it is similar to the EPA definition, but does not include the defined word in the definition. At the local regulatory level, The New Hampshire Stormwater Manual describes the specifications and BMPs used in the design of various stormwater systems in the state of New Hampshire (Burack, 2008). For engineering work, it is particularly useful in that it is the standard for stormwater system design in many town ordinances in the state of New Hampshire. This manual shares design similarities to the Philadelphia design of the subsurface gravel trench in Lot A ("Regulations", 2021).

General information about the field of stormwater is useful for people with no prior insight into the subject. "Modeling and Management of Urban Stormwater Runoff Quality: A Review" provides a useful overview of stormwater treatment in general (Tsihrintzis, 1997). Included are discussions on common types of pollutants, methods of pollutant transport, and types of treatment BMPs. This paper was used to justify some basic statements about the field of stormwater, including the effects of stormwater pollution, and the justification of stormwater detention and treatment. If someone needed to get a basic understanding of the practice of stormwater treatment and management in about 30 pages, this would be a decent resource.

On the infiltration side of stormwater terminology, "Modeling Groundwater Flow and Contaminant Transport" describes a large number of groundwater concepts. In the case of this thesis, the concept of relative importance was the equation for Darcy's Law applied in the horizontal direction. The concept did not prove useful as Darcy's Law requires a column length, while the theoretical framework of this thesis calls for fluid movement through a boundary or surface (Bear, 2010). Darcy's Law is the starting point for another fundamental infiltration estimation, the Green-Ampt method. "Studies of soil physics, part I – the flow of air and water

through soils" details the Green-Ampt method for calculating infiltration through the wetting front (Green, 1911). The understanding of this paper plays well into the subject matter of this thesis, but is imperfect as the wetting front described only occurs in the vertical direction. The equation can be adapted for lateral infiltration, but its accuracy for that purpose is unknown. The Green-Ampt method is not directly used in the HydroCAD model created for this thesis (HydroCAD, 2020), but the constant velocity infiltration method used instead is expected to be analogous to the Green-Ampt method, as in the model infiltration occurs as a block out the bottom of the trench, in the same way as Green-Ampt.

HydroCAD was used in the formulation of this thesis, in order to estimate the difference in performance of a gravel trench with infiltration only occurring out the bottom, versus a gravel trench with infiltration occurring out the bottom as well as the sides. It is a widely used program in New Hampshire due to its robust calculation methods for stormwater design (HydroCAD, 2020). For the subsurface gravel trench in particular, the use of this program was very easy, as only two nodes are required to model the watershed and trench. In the event of a project requiring many nodes, the program might become more laborious, as the complex calculations involved can return invalid results, but the program can handle two nodes very easily. The website also contains a manual that describes the entire process for stormwater modelling in detail, including justifications for every decision one could make with the related program. Even if one did not use this program, the manual alone would be an excellent resource for stormwater design.

3. Statistical Concepts

Of the areas researched for this thesis, the one that provided the most information was statistical methodology. The purpose of this research was to find statistical models that would be able to best mimic the observed trench water height data, while adhering to parameters that would allow analogies to be made between the model and the physical world. The coding language used for the development of this thesis, R (R Core Team, 2020), is well documented, and its statistics packages are cited to relevant papers. "EARTH: Multivariate Adaptive Regression Splines" and the offshoot explanatory documentation for the R modelling package EARTH are essential reading if one wants to understand the products and capabilities of the modelling software (Milborrow, 2011 and Milborrow, 2021). Perhaps the biggest limitations of this particular software are the products themselves. Reading an EARTH model, retrieving variables from the model, and reading the output graphs can be overly complicated and not conducive toward presentation materials. Fortunately, the extra documentation presented is easy to understand, the model is easy to make, and the results are generally very useful toward understanding data. EARTH was used for multiple practices in this thesis, including measuring hydrograph peak heights and estimating the recession limb of each hydrograph.

The EARTH model itself is built on the use of spline fitting, an important component of finding kinks in graphs. For a background in the relevant concepts, "Key Concepts and techniques in GIS" (Albrecht, 2007) provides easy to understand reading complete with graphics on polynomial fitting, discussion on the problems with overfitting, and most importantly, the use of splines in regressions. Splines are segments drawn to describe the variance in data at the local level. The splines utilized in this thesis are not simplistic line segments as detailed in the book,

they are instead compound segments with overlapping sections, designed not just to describe the shape of the trench water height hydrograph, but also to subdivide the hydrograph to estimate the various contributing components of infiltration.

Another R function prevalent in this thesis was the Savitzky-Golay filter. "Smoothing and differentiation of data by simplified least squares procedures" explains the foundations of the Savitzky-Golay filter, a smoothing filter utilized in this thesis (Savitzky,1964). The Savitzky-Golay filter is particularly useful in that it can maintain peaks within a signal better, unlike a more traditional rolling average, which will both dampen peaks more significantly as well as move the location of peaks if those peaks are at all skewed. This type of filter was used in this thesis to reduce noise in the hydrograph data caused by machine imprecisions.

At the foundation of the EARTH model, as well as the drift correction model used in this thesis is the linear model. “Linear models an integrated approach” was used for its definition of linear models, to explain how a linear model can contain a polynomial for the explanatory variable (Sengupta, 2003). This thesis uses predominantly linear models to describe hydrograph characteristics such as peak height and the descending hydrograph limb. In the same vein of the drift correction model, “Why High-Order Polynomials Should Not Be Used in Regression Discontinuity Designs” illustrates some of the limitations of higher order linear polynomial regressions (Gelman, 2014). Of note are pages 5 and 6 of the report, demonstrating that high order polynomial regressions are extremely poor at estimating points outside the typical range of data. In other words, high order polynomial regressions get much less accurate on the fringes of a dataset where data points are more sparce. Therefore in general it is best to keep polynomial regressions to within the 3rd or 4th order, unless there is a good justification for doing so.

Part of the development of the statistical model of the gravel trench was figuring out the specific goals of the model. From the search came several distinctions between direct and indirect inversions, forward and inverse modelling, and predictive and estimation modelling.

An understanding of direct and indirect inversions is that the direct solution takes input data and matches it to a model in the best manner possible (Virieux, 2016). An indirect solution takes guesses to reduce the error between the calculated function and the observed data, closing in on the best possible solution. The direct solution is subject to heavy distortion, as any bias in the relevant coefficients will dramatically change the solution. The indirect method matches the solution to the observation through iteration, meaning that accuracy comes at the expense of the comprehensive nature of the model.

For forward and inverse modelling, "The Double Constraint Inversion Methodology Equations and Applications in Forward and Inverse Modeling of Groundwater Flow" illustrates that the inverse problem solves for an estimation, while the forward problem creates a prediction. A similar process was utilized in this thesis, so this article provided useful terminology and a good overview of the process. The creation of the model that describes the existing gravel trench would be the inverse model in this case, while the forward model would be using the created model to replicate the behavior of the gravel trench using only rain gauge data.

METHODS

1. Site Analysis

A. Trench Design

Depending on the design used, a subsurface gravel trench can have a varying anatomy. This section will describe the system at the University of New Hampshire's parking lot A. The system is 150 feet long and 17 feet wide. The system is located on an island separating the parking lot and the adjacent road, Gables Way. The trench stretches beneath the parking lot, as can be observed by the newer pavement forming a rectangle above the system. The island is across the street from the University's Transportation Center. Most of the monitoring equipment is stored in two brown sheds located on the island and is described in the "Monitoring Equipment" section. The contributing subcatchment for th6e gravel trench system has a time of concentration of six minutes, meaning it takes six minutes for water to flow from the most remote part of the subcatchment to the inlet to the system.

Figure 2 shows a complete plan view of the tree trench system in UNH's Lot A. Figure 3 shows a cross sectional diagram of the tree trench system. The complete plan set for the tree trench system can be found in Appendix G.

The system inlet is a sectioned concrete box. The inlet opening is a large and heavy steel grate located on the pavement, which experiences a high traffic load as evidenced by the bowing visible in the center of the grate. Below the grate is a rectangular, sharp crested weir. Past the weir, water flows into a large opening in the center of the concrete box.

Once the concrete box fills to a certain height, water starts to flow through slotted pipes embedded horizontally across the top of the gravel trench. The slotted, horizontal pipes are the

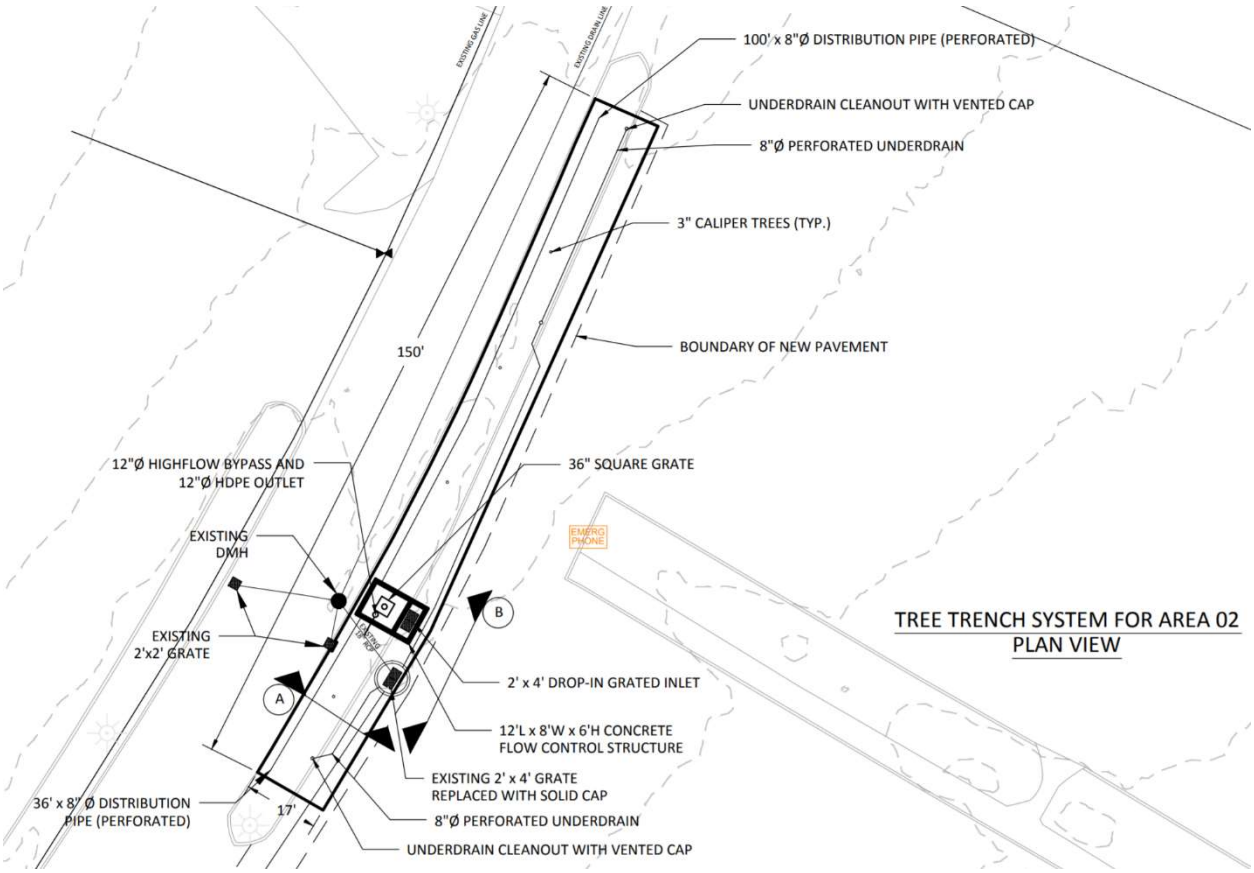

Figure 2: Plan view of UNH Lot A Tree Trench system

inlet to the gravel. The pipes allow for easier flow across the trench, and the slots in the pipes allow the water to exit the pipe to the gravel media. At the bottom of the system are slotted underdrains, leading to the system outlet. Each underdrain pipe has a cleanout. Cleanouts are vertical extensions of the underdrains that go above ground, allowing for access to the pipes in the event of clogging. From a plan view, the distribution box is offset from the middle of the system and the trench is divided in two parts, which means there are inlets and underdrains on each side of the concrete box, for a total of two cleanouts. The trench has geotextiles on all four walls, allowing for some lateral movement of water, but preventing soil piping. The trench does not have geotextiles on the bottom to accommodate infiltration there. Geotextiles in the primary water flow path can become clogged with finer sediments, and over time can reduce the overall

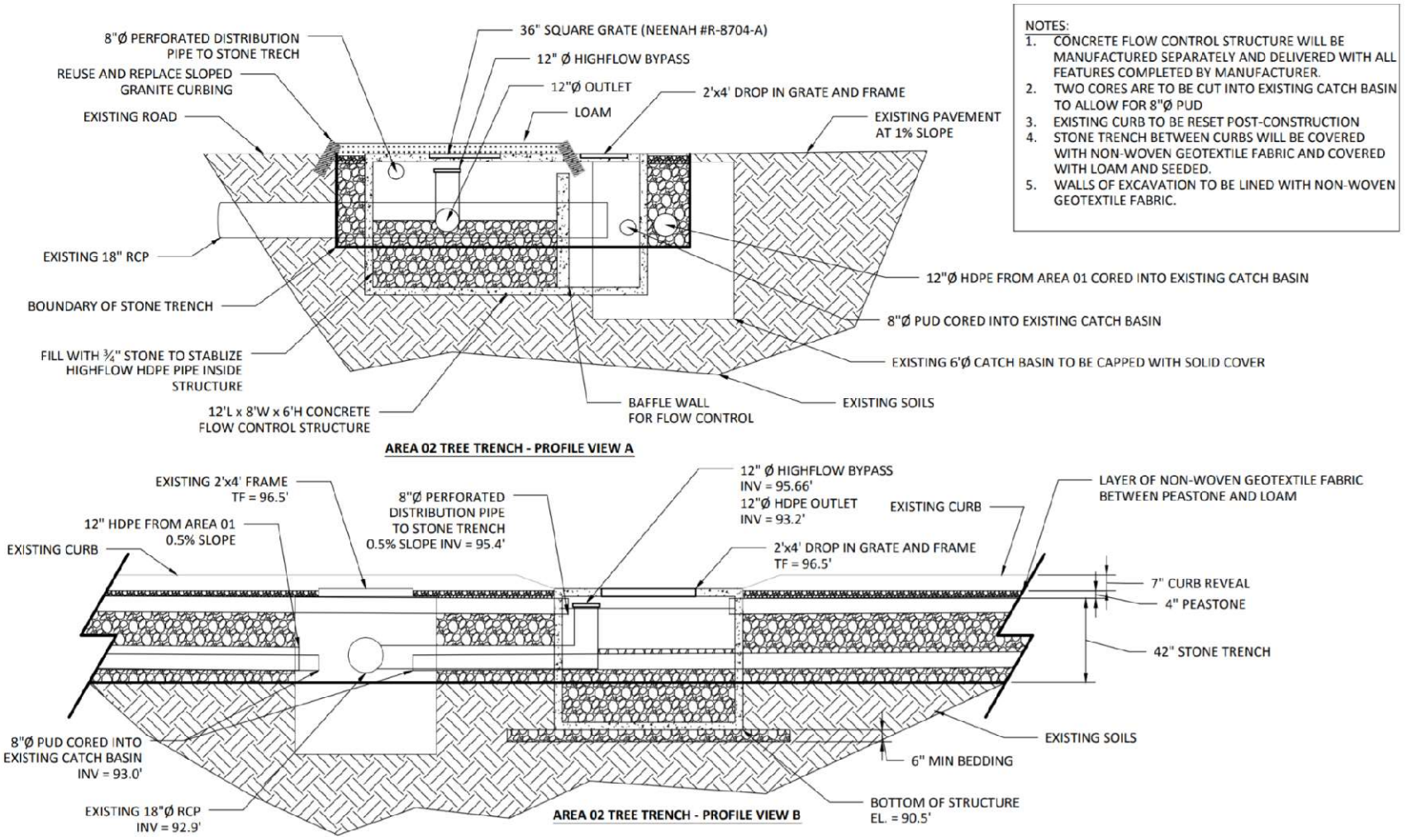

Figure 3: Cross sectional diagram of UNH Lot A Tree Trench system

infiltration rate of the system, which would explain the design choice to not cover the bottom of the trench, where the most infiltration is expected.

If the concrete box should fill past the depth of the gravel, a bypass pipe is seated facing upwards in the inlet concrete box. When the water reaches the appropriate height filling the gravel, the bypass acts like a circular weir, with water flowing in evenly around the whole pipe. This pipe feeds into the Gables Way drainage network. The underdrain end cap was to have an orifice hole drilled in it to drain the system to the Gables Way storm sewer. That hole was never drilled in order to study system infiltration characteristics. The bypass pipe was capped since June 2015, as denoted in Figure 4. Figure 4 is the multi-year water level hydrograph for the system. Also included in Figure 4 is the date the adjacent catch basin, which existed before the construction of the trench and was connected to the trench system, was closed off to the adjacent Gables Way stormwater conveyance infrastructure. Relevant storm rain depths are listed directly on the graph.

It should also be noted that without the underdrain orifice, the A-Lot gravel trench experiences very poor drainage performance at low water depths. For a storm on October 9, 2016 (0.884 inch depth), the trench filled to a depth of 1.09 feet (about half its total depth) and took over 6 days to empty completely. Within the first three days, it had emptied to 0.235 feet, meaning it took 3 days to infiltrate less than 3 inches of water in the trench.

This system was based off design specifications from the Philadelphia Water Department, called the “Philadelphia Tree Trench.” This design differentiates from the typical subsurface gravel trench in terms of the inlet design, but more noticeable is that the system was designed to incorporate several trees along the length of the trench. The tree design feature is useful for city planning as a beautification effort but may face practical problems. During the period of

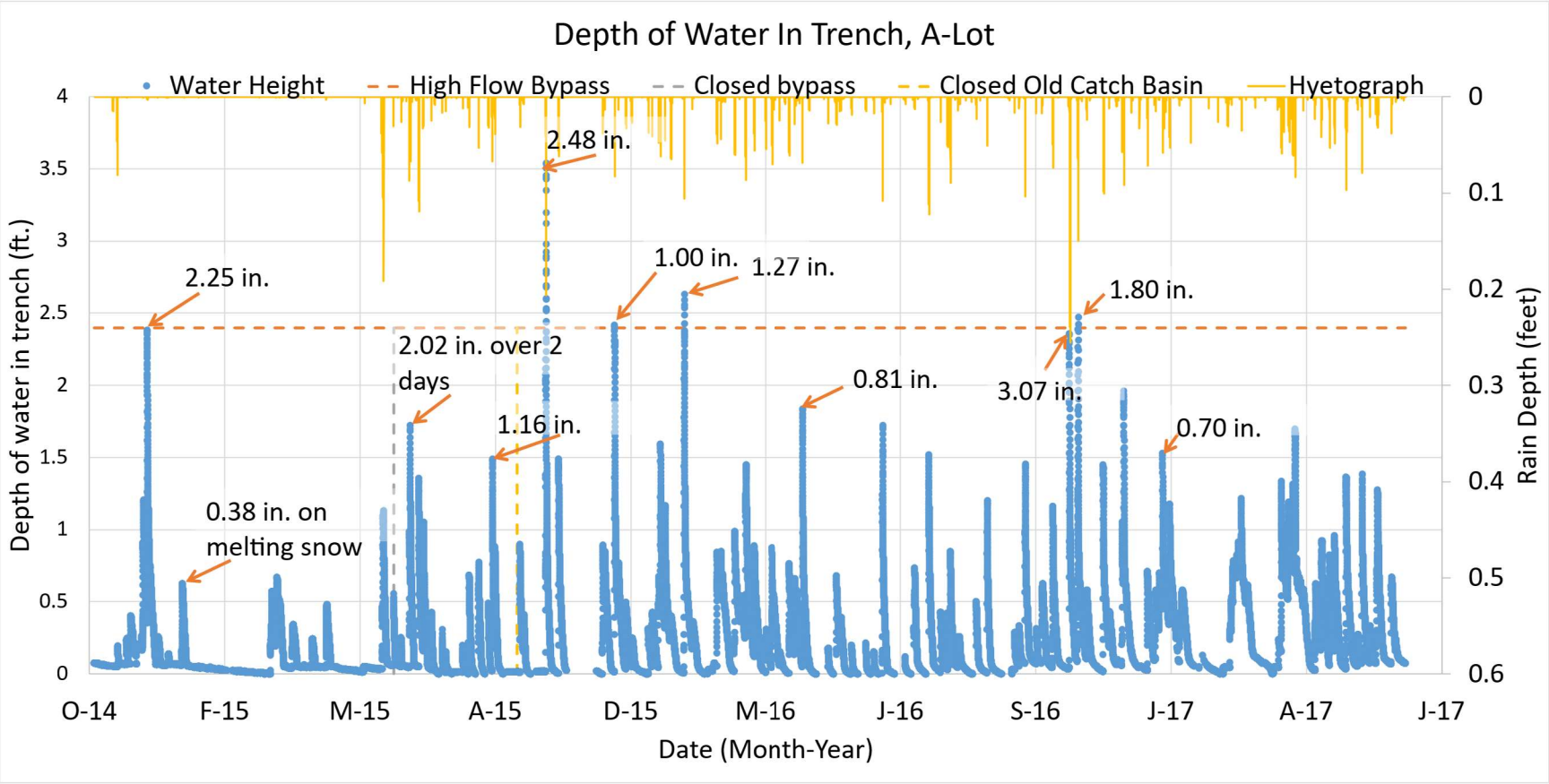

Figure 4: Time history of depth of water in trench and precipitation, A-Lot

observation, several of the A-Lot trees were knocked down by plows, some of the trees died, and all the trees exhibited signs of physiological stress, for example, shoots growing near the ground or bald spots on the trees, known as dieback. To the credit of the system, the trees growing in the system experienced less physiological stress than the control group trees grown nearby, both of which died.

The subsurface gravel trench started recording data on October 10th, 2014 at 2pm, though many of the monitoring wells did not start collecting until June 25th, 2015. Part of the earlier data was not used in the analysis, due to the high flow bypass and old catch basin acting as additional variables. The site contains several monitoring wells containing pressure transducers, four of which measure the groundwater table below and near the system, and three which measure the height of any water in the trench itself. The site also contains a barometer. Some instrumentation is housed on the island between Gables Way and the adjacent parking lot in a small wooden shed. There is some instrumentation located further north, including one device measuring the groundwater table and one device measuring a separate system that was not considered for this research.

According to the plans for the subsurface gravel trench, the contributing watershed area was determined to be 0.58 acres, covering a narrow strip of the parking lot. There is a small, steep area beyond the parking lot that contributes to the watershed but does not have any impermeable surface. The small, permeable surface was not considered in the analyses for this research due to the very small to negligible runoff it produces.

While the SCS Curve Number method dictates that a curve number value of 98 is to be used with an impermeable surface like a parking lot, a visual inspection revealed that the parking

lot surface contains a lot of wear and extensive cracks, so the curve number used was reduced to 94 to compensate for this surface condition.

Close to the distribution box is some pre-existing infrastructure. What used to be an old storm grate has since been replaced with a solid metal plate. The capped storm grate's distribution box is connected to several underdrains at the bottom of the trench, as well as the high flow bypass of the gravel trench's distribution box. This capped box was and still is connected to the Gable's Way storm sewer. The high flow bypass of the system was capped on June 10th, 2015. No data for the analysis presented in this thesis was used from before the bypass was capped, to maintain consistency in the data. Since the high flow bypass is capped, that means the capped storm grate's distribution box is only connected to the underdrain through the gravel medium.

When analyzing the subsurface gravel filter at A-Lot, one must first consider the specifications from which it was designed. The system was designed from specifications from the Philadelphia Water Department (PWD). The system was also designed to hold the WQV. The trench itself is approximately 2.4 feet deep, as designed using the WQV and inlet and outlet elevations. For information on the design procedure of the A-Lot trench, reference the PWD ("Regulations", 2021). For information on how the typical gravel trench is designed in New Hampshire, reference Appendix I.

B. Other Considerations of Subsurface Conditions

In researching parking Lot A, several claims were encountered regarding the site's history. The claims made might contribute to some of the more eccentric hydrological behavior

observed on the site, and consequentially are worth consideration. While there was little documented proof surrounding some of the claims made about the site, there was some evidence that gave credence to several claims. It is advised to take all the following statements with an appropriate degree of skepticism.

1) Lot A was used to bury old automobile parts. Evidence: One of the borings taken by Golder Associates hit refusal between 15 and 20 feet down. The wash water on the site yielded scraps of metal (Appendix H, Boring 5-A).

2) Lot A was a dumping ground for unsuitable construction fill from other sites. Evidence: Figure 2 of Golder Associate's "Exploration Location Plan Parking Lot A" features a shaded area on top of the area around parking Lot A described in the legend as "Approximate location of "landfill area" identified on 1975 Existing conditions plan" (Appendix H, Exploration Location Plan Parking Lot A). The 1975 existing conditions plan was not found.

3) The current parking lot surrounding Lot A was built atop several feet of fill covering a previous parking lot. This is not borne out by the boring logs.

i) Pictures on the trench construction site revealed water pooled on the bottom of the trench the day after a storm, as seen in Figure 5. The boring logs for the site show the presence of clay, which would explain the pooling.

ii) Multiple wells were attempted in the construction of the subsurface gravel trench further into the parking lot area, all of which hit refusal several feet down, but the refusal was not described as asphalt, but rather as pebbles (Appendix K, Monitoring Well Installation Log, MW5 and MW6).

Figure 5: A Lot Gravel Trench Construction after rain

iii) The stratification is consistent with the Golder borings on the site, which revealed stratification of the soil at 3 feet below the surface, and describes the material below the stratification as “Fill.” There was no presence of asphalt in the borings. (Appendix H, Boring GA-1).

C. Monitoring Equipment

In order to form conclusions about possible anisotropy in the subsurface gravel trench, multiple types of data were needed, including the height of water in the trench, the time and date for each measurement (the timestamp), and the depth of rain for any given timestep. The original dataset used was in 15-minute timesteps and ranged from 2015-11-06 23:15:00 to 2017-11-08 16:00:00, for a total of 66,134 data points. This section will describe the instrumentation used in measuring the necessary data, as well as any additional instrumentation on the site.

The Onset HOBO water level data logger is a cylindrical device that receives data by being submerged in a fluid. The model number was a U20, with a depth rating of up to 13 feet, and a typical error of ± 0.075% of FS (Full Scale) (Appendix L, HOBO U20 Water Level Logger). The device measures the absolute pressure of its surrounding through a small hole near the bottom of the instrument. A circumferential line on the device shows the exact depth to the sensor when the device is submerged in water. In order to precisely gauge the elevation of the device in a well, one can subtract the length of the line being fed to the device from the elevation of the highest point of the line, provided the line is taught. If the cap of the HOBO is removed, an embedded optical sensor can both transfer and receive computer data from a corresponding port. Any temporal, pressure (psi), and temperature (Fahrenheit) data stored on the HOBO is downloaded by a program called HOBOware, which can save the data as a .csv (comma delineated) file. In order to calculate the depth of water above a HOBO, an additional sensor is required above the water to measure the atmospheric pressure at that location. The atmospheric pressure is then subtracted from the absolute pressure reading of the submerged probe, and the difference can be divided by the specific weight of water to convert pressure to depth of water above the sensor.

There are multiple HOBO sensors located in or around the subsurface gravel trench at the University of New Hampshire's Lot A. Inside one of the brown storage sheds located on the traffic island is a HOBO measuring barometric pressure. The trench system itself has two piezometric HOBOs measuring the height of the water in the trench directly. Two more wells completed below the system bottom measure the groundwater table, as shown in Figure 6. The data from the groundwater table showed that the groundwater table was too far removed from the bottom of the trench, and not susceptible enough to mounding effects for the table and the

bottom of the trench to hydraulically make contact. In the Figure, Monitoring Well 1 (MW1) measures the height of water in the trench. Monitoring wells 2 and 3 (MW2 and MW3) measure the groundwater table, always multiple feet below the bottom of the trench, which itself is at elevation 92.5 feet. The lines for MW2 and MW3 overlap each other and cannot be easily distinguished. Two devices across Gables Way measure the groundwater table adjacent to the trench. Finally, to the north of the system, is another couple of traffic islands, each with one HOBO monitor. One of the monitors is in a separate stormwater system, and the furthest north monitor measures the groundwater table. Each HOBO monitors three factors: absolute pressure, the timestamp, and the temperature.

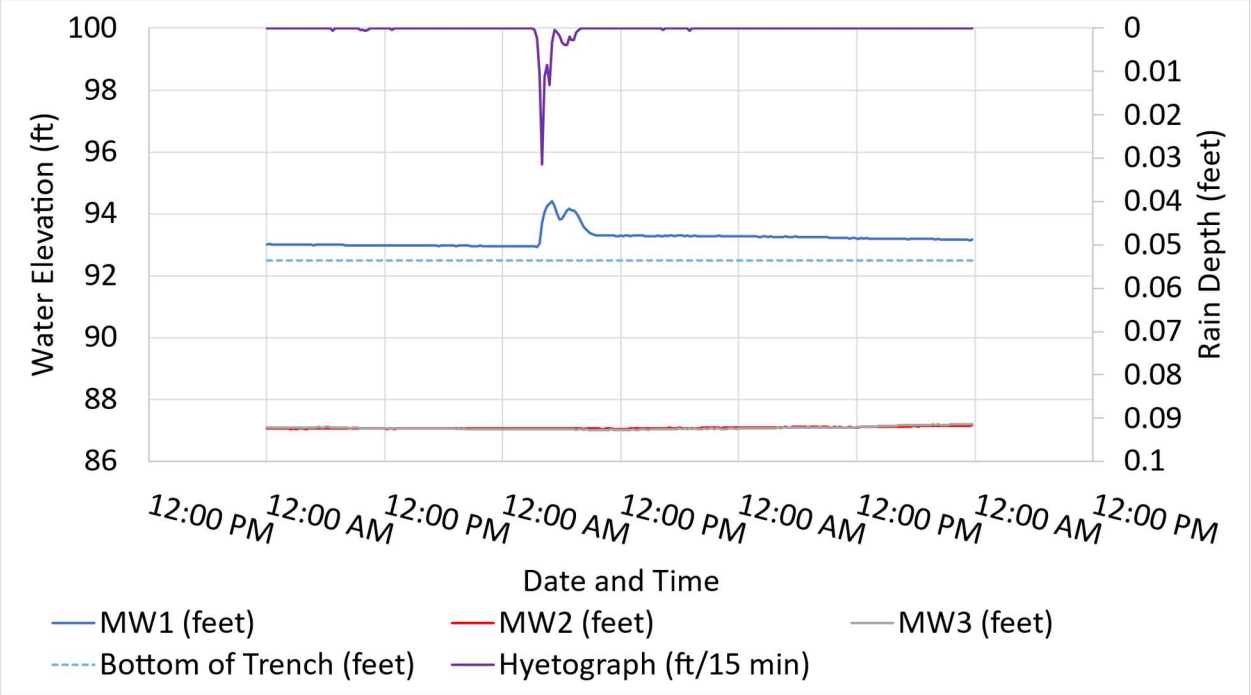

Figure 6: 9/19/2016 Storm, Monitoring Wells in A-Lot, Mounding, 1.24 in.

The CR1000 Campbell Scientific is a data logger that can be attached to a variety of sensors, capable of measuring a variety of data types. The CR1000 for the gravel trench system is attached to a rain sensor, which measures the depth of rainfall in inches during any 15-minute timestep and a CS450 sensor, which directly measures the height of water in the gravel trench, in

feet, with an accuracy of ± 0.1% FS, and a resolution of 0.0035% FS (Appendix M, CS450 and CS455).

The CR1000 is attached to a deep cycle 12V battery. While the battery needs to be checked periodically to ensure it still holds a charge, it generally remains charged since it is attached to a solar panel installed above the storage shed. All devices record in 15-minute intervals. The information can be downloaded to a computer using the PC400 software through a special adapter cord. The PC400 software, as well as the HOBOware software for the HOBO unit, are available as freeware through each company's respective website.

Any weather related values were obtained from the weather station located on top of the University of New Hampshire's Gregg Hall, located on the campus, found at http://www.weather.unh.edu/.

D. Site Borings

Soil layering is an important component to establishing the anisotropy of a given site, so soil borings can provide useful context in determining anisotropic conditions of a given location. One can find a complete history of the soil borings for the University of New Hampshire's Parking Lot A in Appendix H. This section will explain a brief analysis of the results.

Borings for Lot A were advanced at several locations, conducted by the company Eversource, Exeter Environmental Associates, Inc., and Golder Associates in Manchester. The boring closest to the current location of the gravel trench was conducted by Golder (Appendix H, Boring GA-1). The boring log did not include any lab analyses or sieve analyses. Table 1 shows the results of the boring closest to the gravel trench. Note the lack of asphalt present.

Depth from surface (feet)	Soil description
0-3	Engineered fill: compact, tan, coarse-medium-fine sand, with little fine-coarse gravel, and little silt.
3-6.8	Compact, brown, silty coarse-medium-fine sand, with little fine-coarse gravel
6-7	High resistance encountered from pebbles, 50 blows for 3 inches.

Table 1: GA-1 boring results, Golder Associates

The change in soil quality after the first 3 feet is consistent with the construction of the trench, which encountered a very low permeability layer at the bottom of the trench (Appendix J, Infiltrometer Data). The Golder boring does not agree with the presence of asphalt as was the word-of-mouth knowledge that the current lot was built on top of an older parking lot, though the presence of asphalt would be dependent on the layout of the former parking lot.

The double ring infiltrometer tests performed at the bottom of the trench in July 2014 had readings between 0.00 and 0.08 inches/hour (Appendix J, A-Lot Area 2). That low of an infiltration rate alone would require an underdrain to empty the designed system in the specified 72-hour time frame, as was present in the trench design.

2. Storms

Part of the objective of this thesis is to recreate aspects of the performance of a subsurface gravel trench, and relate them to the design process. In statistical analysis, the creation of a model given existing data through the statistical estimation of parameters is called

the “inverse method.” In the case of the gravel trench system, understanding the relation of storm parameters to the reaction of the trench will help in setting up the data for more accurate analysis of more subtle factors in the trench infiltration process, like anisotropy. The design process would be most aided by a predictive process which would estimate the performance of a trench system through storm parameters. For such a translation to occur, storms should be analyzed in addition to the reaction from the subsurface trench, as storms will be used to predict the starting water depth in the trench system. This section will address general storm parameters that can be described at any site. Once the data was collected, multiple common forms of graphing or observing the system's qualities were used. These graphs included:

1) Hyetograph: A graph depicting rainfall depth versus time. Since the data was collected in 15-minute timesteps, the total rainfall for the given 15-minute timestep, in inches, was used as the y-axis.

2) Hydrograph: A graph depicting water height, volume, or discharge versus time. The most common hydrograph in the case of the subsurface gravel trench was the height of water in the trench, but other instances of hydrographs were used, such as the volume of water flowing into the system over time, and outflow from the system over time. The relationship between water height and discharge is easily calculated as the height of water in the trench directly related to the volume of water in the trench. If no water is entering the trench, then to satisfy continuity the system’s change in volume must be directly related to the system’s discharge (infiltration).

3) Cumulative Probability Distribution: Various methods of consolidation can allow rainfall measurements to provide useful long term information. Daily rainfall may be ranked by depth to obtain probabilities. For example, if the rainfall of each individual day was compared and sorted by depth, the total number of days that exceed a certain amount of rainfall could be

counted (this is called the exceedance probability), and the number of days that do not exceed a certain amount of rainfall could be counted (this is called the non-exceedance probability). When any number of non-exceedance days is divided by the total number of days (plus one, to account for the fact that smaller precipitation depths are possible), then a statistic is generated called the non-exceedance probability. The non-exceedance probability can be generated for any given daily rain depth in a dataset, and is useful in reviewing the gradation between storm intensities.

In order to isolate each storm, there must be a defined beginning and end to every hyetograph. Fortunately, the defining feature for both is the presence of rainfall. However, rainfall must itself be discretized into separate storms. For this thesis, a storm will be defined as any period of rainfall with antecedent dry periods no longer than six hours. The process of storm detection is automated, and each individual storm hydrograph is defined by the presence of a unique storm event.

3. Trench Analysis

A. Modelling Process

One of the central components of this thesis is the creation of model estimates and predictions, of which the predictions can be compared to the observed data. Estimation and prediction produce two separate results, but with the method presented in this thesis, the results of the estimation are used as the input model to create a prediction. In statistical theory, the inverse problem and the forward problem are individual analysis for a given system existing in the real world. The inverse problem seeks to estimate real world variables given input data. The forward problem seeks to predict the behavior of a given system utilizing a model. If the results

of the forward problem reflect the observed data accurately, then the prediction is validated (Allaby, 2008). The end result of the inverse solution is to produce a relationship between infiltration rate (L/T) and the height of water in the trench (L). That relationship should yield a chart of infiltration rates per defined soil layers, which can be input into HydroCAD for modelling the performance of different sized systems.

In the case of the gravel trench, the inverse problem model seeks to analyze field data using periods after a storm where the stage of water in the subsurface gravel trench is receding (the falling limb) after surface runoff has ceased. The model uses the observed in-trench water depth hydrograph and replicates it in distinct parts to re-create multiple elements of the hydrograph, such as the height of the hydrograph, the shape of the falling branch, and the distance from the end of the storm to the peak of the storm. The replicating process ends with individual hydrograph factors trained with existing height data. The forward problem model combines all the individual components of the inverse problem model and can be used to estimate future trench performance hydrographs with only rain data. Additionally, rain data may be synthesized to desired parameters to be used with the forward problem model to estimate system hydrologic performance. For example, a 1-inch rain event may be created to simulate how the trench responds to a sudden burst of rain.

The following methodology will mention the use of a "linear model." It should be mentioned that in the most fundamental mathematical sense, linear models do not necessarily represent a straight line on a graph. In the sense used in this paper, a linear model is any model wherein a coefficient is linearly related to the output. For example, a simple equation like "$y=ax^2+bx+c$" (where 'a,' 'b,' and 'c' are all real numbers and 'a' is non-zero) would be

parabolic if ‘y’ was graphed against ‘x,’ but were the coefficients ‘a,’ ‘b,’ or ‘c’ changed, the resultant output ‘y’ would change directly to any change in coefficient. (Sengupta, 2003, page 7)

For the creation of the inverse problem model:

1) The unaltered hydrological data was corrected for sensor drift. A more thorough detailing of the drift correction process may be found in the section “Automated Correction and Detection.”
2) Using the corrected rainfall data, storm periods were estimated so that the rainfall data could be discretized into individual storms. Parameters for defining storm periods included:
    a. Any rainfall with at least six antecedent hours of zero precipitation.
    b. Any subdivided period with a rainfall depth of at least 0.1 inches. Any storm periods with less than 0.1 inches of rainfall were removed from consideration, as they would produce insufficient runoff to make a significant peak in the runoff.
3) The start and end points of a storm period were used to discretize the gravel trench water depth data into periods representative of individual storms.
4) Parts of the discretized storm data were removed for any pre-existing technical problems. Storms were eliminated from consideration which did not meet quality standards. Quality standards will be further addressed in the sections “Automated Correction and Detection” and “Manual Data Removal.” Examples of storms removed from consideration include:
    a. Storms without continuous and consistent timestep measurements.
    b. Storms with apparent snow melt, visible through waves in the falling limb of the hydrograph without preceding precipitation, as well as the time of year.
    c. Trench hydrographs with irregular patterns suggesting bad data, for example unnatural linear trends or unusual concavities.

5) From each individual hydrograph, the height of each peak was estimated with the use of an algorithm. Then the duration from the beginning of the storm to the estimated peak was measured. Both the peak and duration were used as input data for a linear model, to be called the "peak and duration" model.
6) The data between the start of rainfall and the peak hydrograph water depth was eliminated, leaving the falling limb of each storm hydrograph. The rising limb was eliminated (limited inflow, primarily outflow) to simplify the mass balance equation. The remaining recession limb does contain some outflow, however, a test was done on the effectiveness of the model if data points were removed from the beginning of each storm equivalent to ten times the time of concentration, and it was determined that the remaining inflow portions had no effect on the modelling process used. Based on the resultant outflow model, without inflow into the system, the change in storage of the system is equal to the outflow from the system. The change of storage can be measured with the height of water in the system alone, and consequentially continuity can be measured in its entirety with only a height measurement.
7) All storm recession limbs were consolidated into one continuous curve superimposed over each other, modelling for the presence of kinks in the graph by partitioning the data into sections. The technical process for overlaying hydrographs will be detailed in the sections "Primary Knot Points," "Splines," and "Hydrograph Consolidation and Knot Tuning." This step ideally creates an averaged falling limb hydrograph, allowing for any subsequent estimation of the system to be based on an aggregation of the available data. The aggregated hydrograph was then modelled using the EARTH modelling system, to be called the "limb shape" model. The EARTH modelling system is discussed further in the "Time Series" section.

For the creation of the forward problem model:

8) The linear model used to measure trench water level hydrograph peaks and durations from the inverse problem section was used to synthesize peak heights and durations based upon existing rainfall data.
9) Each trench water level hydrograph was re-created from the rainfall data, peak and duration model, and the limb shape model. The only field data used to construct the new hydrographs was the existing rainfall data, so the new hydrographs are referred to as "Synthetic hydrographs."
10) Synthetic hydrographs were all mapped onto one continuous time period and compared to the original field data, allowing for a side by side comparison of synthesized and observed trench hydrographs. By comparing the synthetic data to the field data, one can estimate the efficacy of the modelling process.

The forward problem model does not contain a direct solution for hydraulic conductivity. However, the forward model does provide results in terms of inches per hour out the sidewalls of the subsurface gravel trench at all different elevations by taking the derivative of predictive model, which can be used in programs like HydroCAD when modelling the performance of a subsurface trench. The process of applying the results of the forward model in a design capacity will be discussed in the "Field Workflow" section.

B. Layer Equations

When considering an anisotropic trench system, infiltration into the surrounding soil could be considered as a bulb shape, as in Figure 7. Water will exit both the bottom of the trench

and the sides. Water exiting the sides will eventually flow vertically due to gravity, but for the purpose of this thesis, the trench will be considered a black box, only in consideration of the volume exchange occurring through the trench walls and the bottom of the trench, as shown in Figure 8.

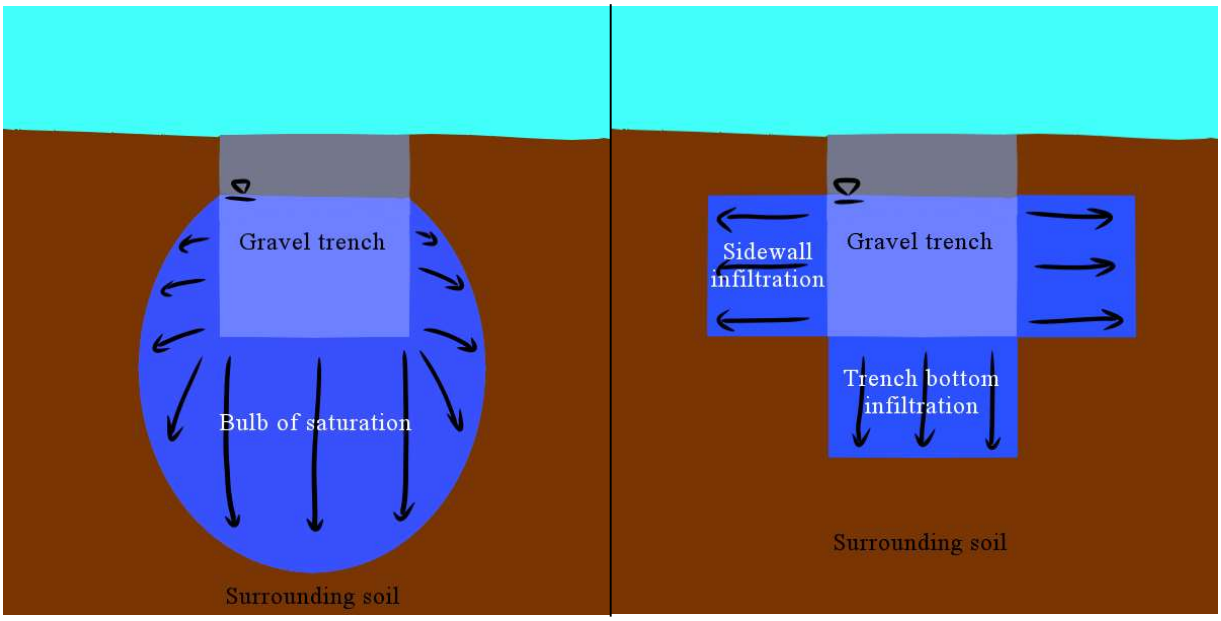

Figure 7: (Left) A depiction of the bulb of saturation surrounding a subsurface gravel trench

Figure 8: (Right) The conceptual model of infiltration from a subsurface gravel trench

With that in mind, the continuity equation (Equation 1) will be satisfied by associating the change in storage directly to the flow out of the trench. The rising limb trench height hydrograph data is removed from all hydrographs. Some flow into the system will still be occurring after the hydrograph peak, but the modelling process is expected to have an averaging effect that cancels out the remaining inflow, and the peak data is too useful a metric to eliminate from the modelling process. Once the model is created, any information derived from the model would be the equivalent of $Q_{in}=0$.

Equation 1. $Q_{in}-\Delta S=Q_{out}$

Q_{in} = Flow in (L^3/T)

ΔS = Change in storage over the time step (L^3/T)

Q_{out} = Flow out (L^3/T)

The trench's overall shape was modelled as a rectangular parallelepiped, or a 3-dimensional rectangle. When considering outflow from the gravel trench, water can be expected to leave the system in one of two ways:

1) Through transpiration/evaporation
2) Through infiltration from the side walls and bottom surface of the trench

Transpiration is a slow process (Balugani, 2016), albeit a significant one, and can be difficult to distinguish from infiltration. For the purposes of this thesis, all water leaving the trench will be treated as infiltration. The justification is made on the basis of the limited existing vegetation on the site, including several small trees with significant dieback (dead sections bearing no leaves), and short, poorly maintained grass in soil compacted by foot traffic. The top of the gravel trench is also partially covered by pavement, which has no transpiration effects at all.

Infiltration in the gravel trench can occur through the bottom of the trench, and through the sides of the trench. Since the bottom of the trench was measured to be low permeability (Appendix J, Infiltrometer Data, A-Lot Area 2), it is expected that very little infiltration occurs through that surface. The sides of the trench would experience infiltration through the urban fill on top of the clay layer. The vast difference of infiltration rate provides an expectation of

anisotropy for the system. Equation 2 shows the expected flow of water from the system during a given timestep.

Equation 2. $Q_{out}=A_s*V_s+A_b*V_b$

Q_{out}=Flow from the trench (L^3/T)

A_s, A_b=Area of trench sides, trench bottom, respectively (L^2)

V_s, V_b=Velocity (infiltration rate) of water through trench sides, trench bottom, respectively (L/T)

The flow out of the sides of the trench can be discretized into individual components. Those components each have their own area and hydraulic conductivity and in the case of the bottom of the trench, a gravitational constant driving pressure. Those individual components can be separated and solved on their own, and flows calculated across each surface can be added together for a total flow out of the trench.

Equations 3 and 4 calculate the area of the sides and bottom of the trench, each being comprised of known quantities, length, width, and height of water in the trench, represented l, w, and h (L), respectively. Note that length and width are added in equation 3 to represent both the side walls of the trench and the end walls.

Equation 3. $A_s =2*(l+w)*h$ (L^2)

Equation 4. $A_b =l*w$ (L^2)

The height of water in the system is a known quantity, as it is measured over time, but has properties suggesting layering effects. To capture the layering effects, 'h' must be discretized into multiple components. Since the height of water in the system is variable, and the layers of soil adjacent to the trench are constant, then the height of water can be described in terms of the exposure to saturation of each individual layer.

Equation 5. $h = \sum_{k=0}^{n-1} h_k + h_{nx}$

n = the layer of soil in which the considered height is located, starting with 0 from the bottom (ordinal)

h_k=the thickness of layer of soil 'k'. (L)

h_{nx} =the saturated portion of the highest saturated layer 'n'. (L)

The volume of water exiting the system at any time is known, since the height changes over time, and a change in height corresponds to a change in volume times gravel porosity. Since the continuity equation during the falling branch of the water height hydrograph assumes no inflow into the system, then flow out of the system is equal to the change in volume over time times porosity. The change in volume is directly related to the change of height of water in the system since the trench maintains the same dimensions throughout the vertical axis. That being said, for volume times porosity to be directly related to height, the height of water must be assumed consistent throughout the gravel trench, as illustrated in Figure 9.

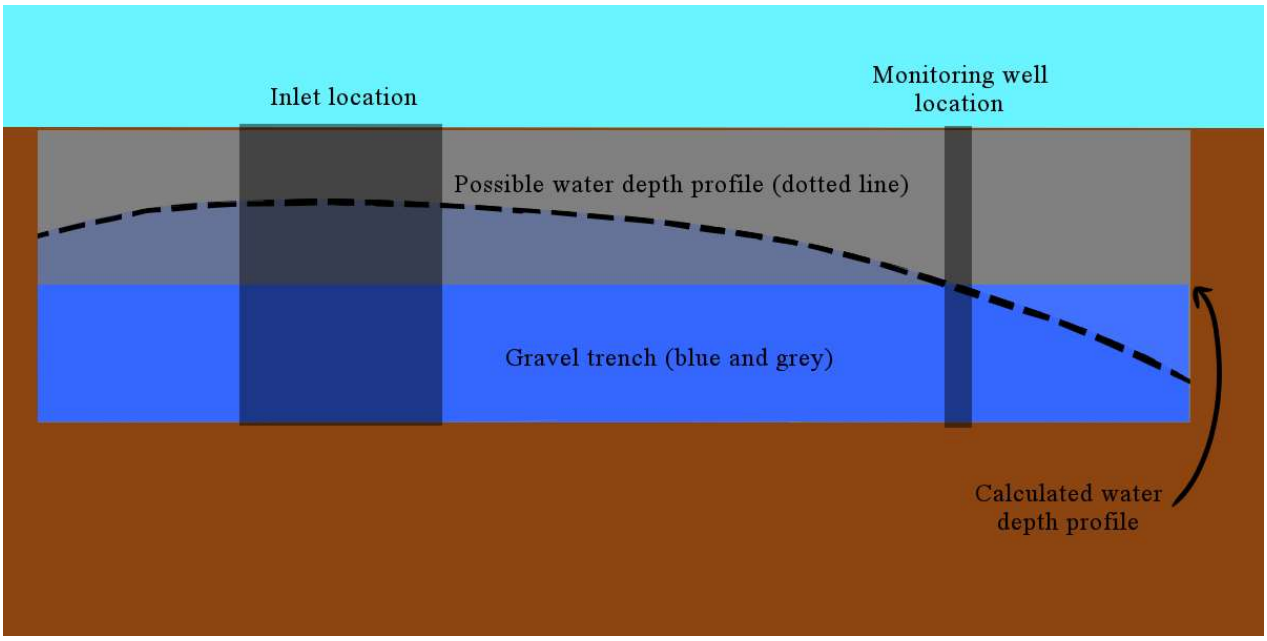

Figure 9: Uneven versus calculated depth profile for partially filled gravel trench

For example, if the water height is one foot at the north end of the trench, it is assumed that the water height at the south end of the trench is also one foot. Note that the timestep is described as ordinal. That is because while timesteps must be consistent relative to each other, timesteps on the aggregate can start or end at any given time. For example, if the timestep chosen for the project is 15 minutes, t_1 can be defined as 0 minutes or 100 minutes, provided t_2 is either 15 minutes or 115 minutes, respectively. Either scenario would have no change to the output.

Equation 6. $Q_{out,t} = (h_t - h_{t-1}) * w * l / \Delta t$

t=timestep (ordinal, but measured in minutes, T)

h_t= Height of water at timestep 't' (L)

With the provided information, one can solve for an aggregate of velocities (infiltration rates) of water exfiltrating the trench, but to understand the individual components of velocity

through each of the sides and bottom of the trench, additional information is needed. Equations 3 and 5 can be used with the area and velocity components of Equation 2 to create an aggregate estimation of flow out the sides and bottom of the trench.

Equation 7. $Q_{out} = l * w * V_b + 2 * (l + w) * \sum_{k=0}^{n-1} h_k * V_k + 2 * (l + w) * h_{nx} * V_n$

Equation 7 can be adapted for the nomenclature of Equation 6 by adapting time dependent variables, in this case "height" to the timestep in question. Also note that since velocities have not been established as being independent of height, and height is directly associated with time, then velocities are also assumed to be associated with the timestep, unless proven otherwise. Since Equation 7 refers to an instantaneous value, and Equation 6 refers to a value over time, both sides of Equation 8 will be considered as approximately equivalent.

Equation 8. $(h_t - h_{t-1}) * l * w \approx l * w * V_{b,t} + 2 * (l + w) * \sum_{k=0}^{n-1} h_k * V_{k,t} + 2 * (l + w) * h_{nx,t} * V_{n,t}$

Equation 8 has several unknown quantities, including the various heights of soil horizons representing the native soil layering surrounding the gravel trench, as well as the velocities of water exiting through the sides and bottom of the trench.

The first unknown quantity that can be solved is the height of horizons in the soil profile. The impetus for suggesting the soil has layering effects in the first place was based upon visible "kinks" in the falling limb of the trench water height hydrograph, and those kinks seem to occur at consistent heights in the trench, so the working assumption would be that the height of a kink

in the height hydrograph corresponds to a height of the soil profile's horizons. Since the trench height hydrograph aside from the kinks has a distinct curve, it will also be assumed that any portion of the falling branch of the hydrograph can be described by a polynomial function. A kink can then be mathematically described as a discontinuity in the polynomial function. Discontinuities in the polynomial function can be found by taking multiple derivatives of the known elevation data in the falling limb of the hydrograph, until the polynomial data derivatives reach a value close to zero, and the discontinuities reach significant non-zero values. As a demonstration of this idea, suppose there is a fictitious trench with a water height of 1 foot like in Figure 10. Then suppose the height of water is measured over 15-minute time steps.

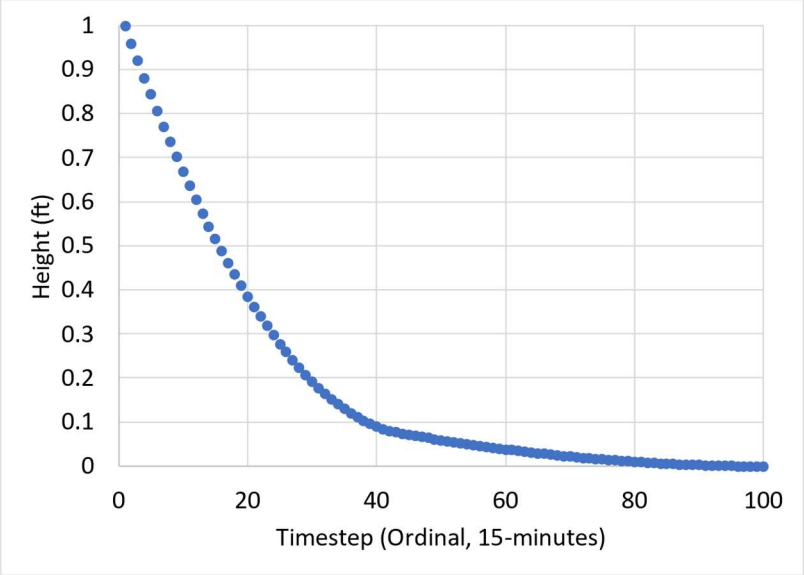

Figure 10: Example of finding discontinuities, part 1

One can clearly identify that the curve has a distinct kink somewhere in the middle, perhaps around timestep 40 at a water height of approximately 0.1 feet. In order to take the derivative of this curve, one need only take the difference of heights between each timestep and divide by the timestep, as present in Figure 11. Figure 12 presents a comparison between the height data and the derivative (velocity) data.

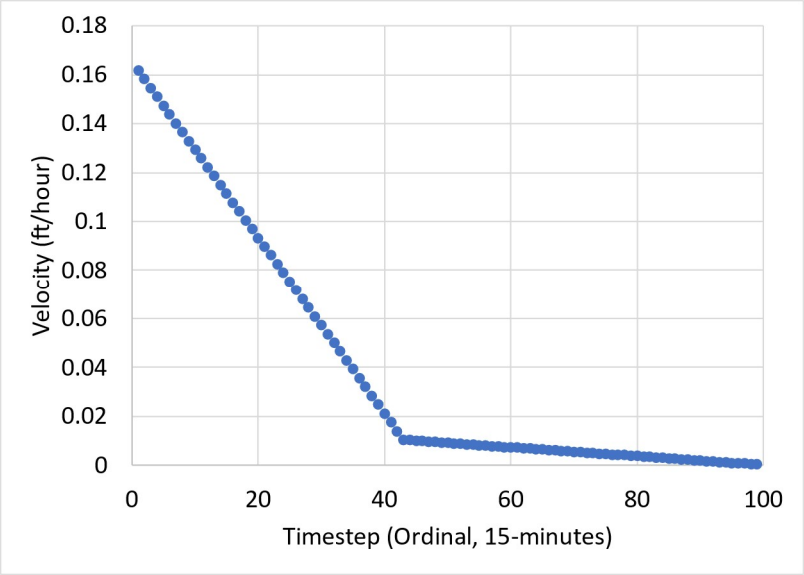

Figure 11: Example of finding discontinuities, part 2

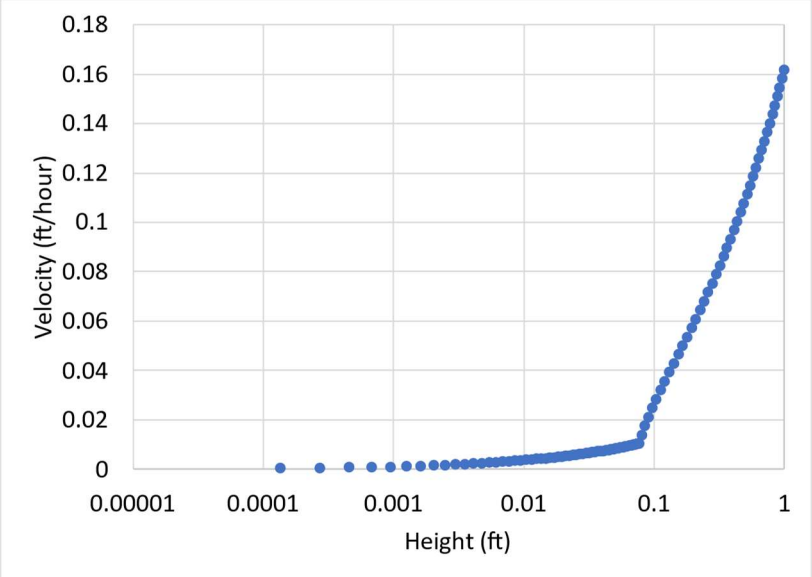

Figure 12: Example of finding discontinuities, part 3

The presence of a kink in the data is now readily apparent. The graph is now representative of rate at which height decreases over time. However, for the distinction to be made mathematically, one needs to take the derivative of the height twice more, from the acceleration at which water height decreases to the 'jerk' at which water height decreases. Jerk is

the technical term for the third derivative of position with respect to time. Jerk is also the derivative at which the kinks in the data would become apparent, as is the case in Figure 13.

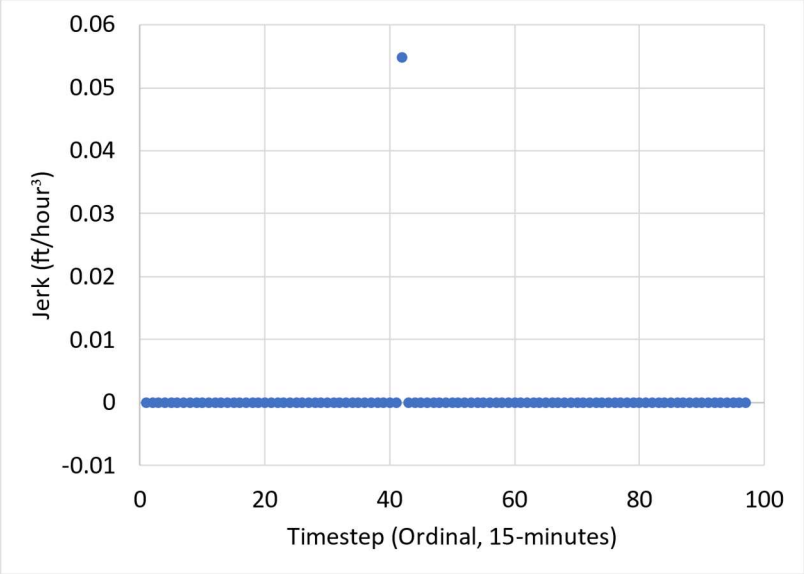

Figure 13: Example of finding discontinuities, part 4

With Figure 13, one could mathematically define a kink in the data as any non-zero point using the third derivative of the falling branch of the example height hydrograph. While the presented example is useful for illustrating the mathematical significance of kinks in the data, real data has lots of noise, and the falling branch of the height hydrograph may not be easily represented by a small-integer-order polynomial equation. To that end, splines were implemented to find the kinks, or "knots" in the data (Albrecht, 2007). "Knots" are the mathematical terminology for kinks utilized by algorithms like EARTH, as discussed in the "Time Series" section. The implementation of splines to find knots is discussed in the "Primary Knot Points" section. The knot points, estimated through the location of the timestep on the falling limb water height hydrograph, is directly related to the height at which distinctions between soil horizons occur.

Once one finds the various locations of each layer of soil horizon, the only remaining unknown variables in Equation 8 are velocities (infiltration rates) of water exiting the trench. Both water velocities through the sides and the bottom of the trench for the saturated condition are based upon the amount of surface area on the edges of the trench. Since the bottom of the trench is almost completely flat, it is assumed that at water elevations greater than very nearly zero, the entire trench bottom is experiencing the same rate of flow per unit area across its surface. If the water level in the trench is nearly zero, it can be assumed that infiltration out the sides of the trench is negligible, since the value of h is so small, severely limiting the capacity of infiltration out the sides of the trench. With that in mind, one may be able to distinguish between velocities out the sides of the trench and out the bottom of the trench by using parts of the water height hydrograph near a height of zero for estimating flow out the bottom of the trench. Since for the purposes of this analysis, flow out of the trench occurs only through the side walls and the bottom, any estimated flow out the bottom can be used with total flow out of the system to solve for flow out the sides of the trench, and subsequently velocity.

Equation 9. $Q_{out} \approx V_b * l * w + 2 * (l + w) * 2 * (l + w) * \sum_{k=0}^{n-1} h_k * V_{k,t} + 2 * (l + w) * h_{nx,t} * V_{n,t}$

With Equations 8 and 9, and the estimation of soil layering heights h_n, one can solve for all velocity components within the gravel trench for each time step. However, since the analysis requires that outflow data be separated into parts, one must find a realistic justification for any model setup capable of separating aggregate outflow from the gravel trench into flow from the trench bottom and lateral flow from each individual surrounding soil layer. In order to achieve

that justification, one must understand the difference in the physical world between infiltration aided by gravity and infiltration flowing perpendicular to gravity, as driven by capillary pressure, also known as imbibition (Chesworth, 2008).

Darcy's Law offers a flow equation describing lateral flow as through a soil column with a constant flow of liquid travelling through it, as in Equation 10 (Bear, 2010), and illustrated in Figure 14.

Equation 10. $Q = k_s A \frac{p_1 - p_2}{\rho g L}$

Q= flow through column (L^3/T)

k_s= Saturated hydraulic conductivity (L/T)

A=cross sectional area (L^2)

p_1=pressure head at start of soil column (F/L^2)

p_2=pressure head at end of soil column (F/L^2)

ρ=density of water (M/L^3)

g=gravitational constant (L/T^2)

L=Length of soil column (L)

The problem with Darcy's equation applied to the gravel trench sidewalls is that there is no suitable length of soil column, as the theoretical framework of the problem specifies that flow through the gravel trench medium is instantaneous, the restrictive medium is the surrounding native soil, and flow into the soil is considered as a planar boundary. There is an important

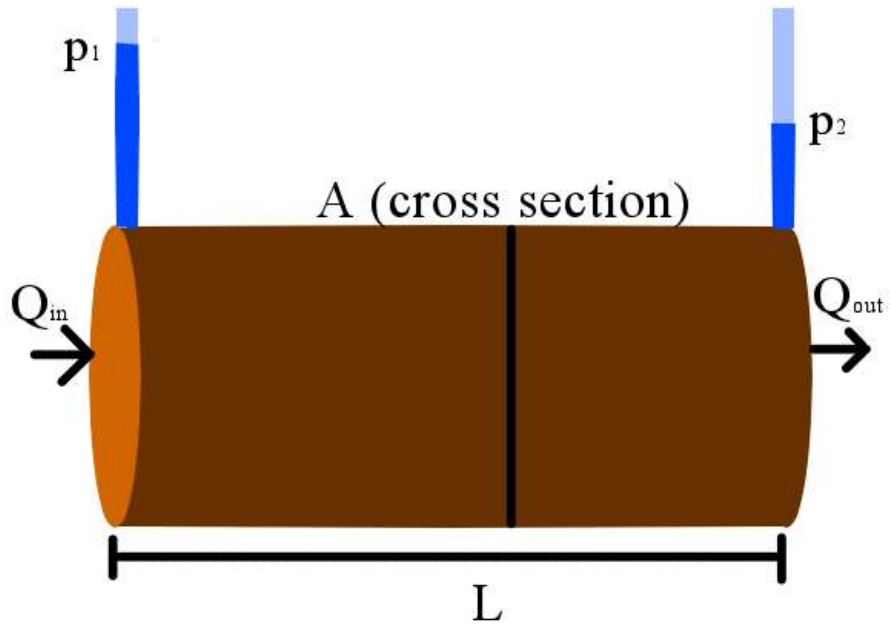

Figure 14: Illustration of Darcy's Law

distinction to be made with Darcy's Law for this case: flow out the side of the trench is not dictated by differences in elevation, only by differences in pressure head and hydraulic conductivity. The pressure head is driven by the surface ponding present at the top of the soil. Since water near the bottom of the trench has the weight of water above it, that water would be driven out of the sides near the bottom faster than near the top.

While there is not enough information available to solve for the soil's hydraulic conductivity out the side walls, there is enough available information to form a theoretical framework for modelling the separate components of flow out of the system.

Flow exiting the bottom of the trench: Flow out the bottom of the trench is driven by both gravity and capillary pressure of the wetting front. The matric suction across the bottom surface and below the gravel trench is assumed to be constant. In the case of the side walls in an anisotropic system, the capillary pressure can change with elevation. In the case of the particular trench system, gravity is assumed to be the driving factor moving water into, through, and out of

the system. As the water height in the trench gets lower, the driving pressure out the bottom of the trench due to gravity decreases with the reduction in weight, but the length of the wetting front below the trench gets longer. As such, it can be expected that the flow from the bottom of the system asymptotes toward a constant rate. In the modelling process, flow exiting the system would therefore resemble a polynomial, as the antiderivative of a linear relationship between height of water and exfiltration rate would be an exponentially decreasing relationship between height of water in the trench and time. If the bottom of the trench is perfectly flat, then the bottom surface area would be infiltrating all the time, and the second order polynomial fitting equation would be applicable until the trench is empty. However, when trying various order polynomial fittings (C_b*x^1 through C_b*x^5, with x representing the spline for the bottom and C_b representing the regression coefficient) it was determined that a third order polynomial fit the field data better at levels below the lowest observable layer of anisotropy.

A possible explanation for a third order fit is that at very low elevations, there may have been slight unevenness in the trench bottom elevation, or unevenness in the water level itself, meaning that only part of the trench was exfiltrating water near the trench's bottom surface. If it is assumed that the unevenness is a linearly sloped bottom (or linearly sloped water depth within the trench), then the unevenness of the trench bottom would correspond to a linear decay in infiltration rate with height. In terms of the modelling process, that would be two decaying factors on top of each other by height, corresponding to a third order polynomial fit of water height over time. This explanation is conjecture, and was not factored into the final analysis.

A slight drawback to this fit is that polynomial fittings tend to have larger errors at the tail ends of datasets, so the fitting will likely slightly overestimate the infiltration rate toward the

extreme ends of the data, but the tradeoff is that it will more accurately model the duration of infiltration time taken by the system, as the trench experiences long periods wherein there is less than an inch of water in the system. Understanding periods with little sidewall infiltration are important in contextualizing the problems with relying too heavily on sidewall infiltration. In the case of the gravel trench, the system spent long periods with low water elevations. By the logic used, a hydrograph can be split into several different height components. Each component can be described as the height of water that will exit the system through its respective exit point. If all height components are added up, it will sum to the total height of water in the gravel trench. Equation 11 describes the equation used to model the height of water exiting the bottom of the trench. There will be additional equations that describe the height of water that exits through each individual soil layer. Since duration is a sensitive component of the analysis, and the model has a floating time variable, constants are added to ensure the final function has a value of zero at the approximated time when the trench should be empty.

Equation 11. $h_b=m_0*((-x_t+C_1)^3)+C_0$

h_b=Partial component of the total height of water in the trench that is expected to infiltrate through the bottom of the trench. (L)

m_0=constant, to be determined in the modelling process.

x_t= "Shaping" variable (to become the third order polynomial described earlier), representative of the decay of water height over time ($L^{1/3}$)

C_0=constant which adjusts height of function so that it ends at a height of zero, to be determined in the modelling process. (L)

C_1=constant for placement of approximated time when trench is empty, to be determined in the modelling process. ($L^{1/3}$)

Flow exiting the sides of the trench: The vertical surface of the gravel trench must be described using an equation for each layer of soil. Each equation can be separated into three sections:

1) Flow through the layer when the water height in the trench is above the layer.
2) Flow through the layer when the water height in the trench is between the upper and lower bounds of the layer.
3) Flow through the layer when the water height in the trench is below the layer (zero flow).

When the water height in the trench is below a layer, there is assumed to be no lateral flow through the layer. When the water height is above the layer, flow through the side walls is dictated by pressure from water depth and capillary pressure. Depth related pressure in the trench scenario is the water pressure directly adjacent to the soil, much like the p_1 given in the Darcy flow example. That would mean lateral flows through a given area of sidewall would increase as the water depth increases. However, the method described in this thesis of discriminating between flows through soil horizons would be much more complicated computationally if the relationship between water depth and increased horizontal flow were taken into account. As such, for the purposes of this analysis, the flow out the sides of the trench will be assumed constant per unit area. Such a method has inherent inaccuracies, but its implementation is not without precedent, as programs like HydroCAD have options to use that very simplification (HydroCAD, 2020).

To solve for the total components comprising the height of water in the trench, one must add the proportion of water stage that will infiltrate through the sidewalls and the bottom of the trench. Equation 12 shows how the sidewalls are divided into multiple components based on the soil horizons.

Equation 12. $h_t = h_b + sum(h_s)$

h_t= The total height of water in the trench. (L)

h_b= The height of water expected to infiltrate through the bottom of the trench, as a component of the total height. (L)

$sum(h_s)$= the sum of all height components expected to infiltrate through the sides of the trench, as a component of the total height. (L)

With the use of equations 11 and 12, if one can create the needed "shaping variables" to mimic behavior of the different horizons of soil with data, one can then develop an equation that separates the infiltration rates through various parts of the trench. The performance of each part of the total soil profile can then be used to predict the observed system's behavior in different circumstances, or can be used to calculate infiltration rates per unit area for a different sized system with a similar soil profile, which can then be used to predict a different system's behavior. For a potential method for calculating infiltration rates of a soil profile, see the section "Field Workflow."

C. Automated Correction and Detection

This section will describe the processes used to ensure the quality of rainfall and height hydrograph data gathered on-site, as well as the processes used to discretize said data into individual storms.

Drift correction - Over time, the height sensor gauge in the subsurface gravel trench tended toward overestimating pressure readings. Figure 15 displays the entire dataset of both the in-trench hydrograph and hyetograph of Lot A. As can be seen at the tail end of the graph, there is about a tenth of a foot of drift.

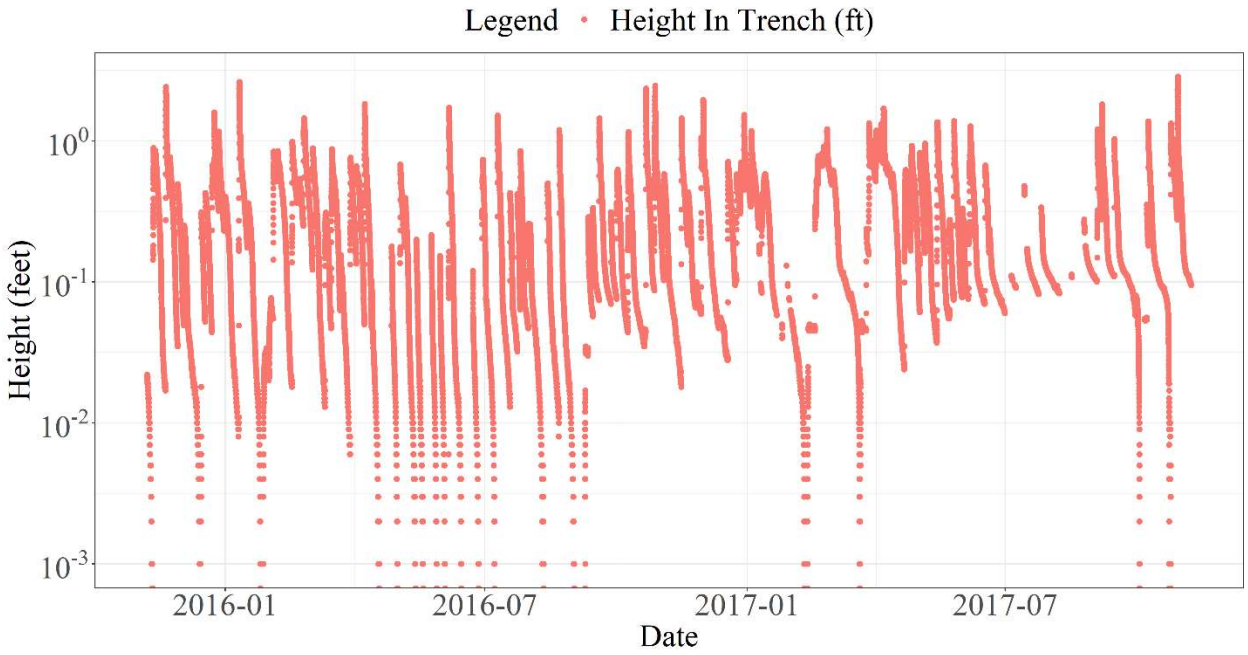

Figure 15: Complete dataset, pre-drift correction, UNH A-Lot

This gradual loss of accuracy in sensors is known as drift. Drift can be corrected by estimating the rate of accuracy loss over time and subtracting the accuracy loss from the dataset. In order to estimate accuracy loss, one must find consistent base points, where the location of the dataset is known. In typical cases, the sensor reference literature recommends calibrating sensors

periodically (Appendix L, HOBO Specifications). If the sensor is not calibrated for an extended period, one can correct for error by calibrating the sensor afterwards and detecting how far off its measurements were, then adjusting measurements proportionally between the starting error and the ending error. In the case of the sensor used, retrieval was difficult and drift appeared to be non-linear, so an alternative method was developed.

The difference between base points and corresponding recorded values is the error. The error can then be estimated between locations of known error using a regression. In the case of the subsurface gravel trench, there are assumed to be base points where the water has totally drained out of the trench, leaving a height of water in the trench of zero. Unfortunately, the sensor itself is not located at a stage of zero and continues to empty past the bottom of the trench with a noticeable dip in sensor readings past the bottom of the trench. While there are approximations for the bottom of the trench, there is no self-evident location in the sensor's data that would describe the stage of the sensor. If the drift correction is to be described computationally, and not using a manual line of best fit, some assumptions must be made using the knowledge of the time history of the trench hydrograph. As the stage of water in the trench reaches a height of zero, its rate of infiltration slows considerably, meaning the slope of the height hydrograph approaches an asymptote. That means that the majority of points will be within a consistent range over the course of time, if not at a stage of zero. Therefore, a highly simplified regression over the complete dataset minus the calculated y-intercept could work as the error, which could then be subtracted from the initial height dataset during periods of drift. In order to remedy the drift, a linear model with exponentials from 1 to 7 was applied to the results, considering height in the trench over time.

Figure 16 displays the drift correction function against the in-trench hydrograph. There are a few considerations for this graph: the first is that the linear model includes a y-intercept factor that is not included when subtracting the drift correction from the original dataset. The linear model must include a y-intercept factor to be excluded from the final correction, so that the initial calibration is not offset by the averaging of the data. The second consideration is that there is no theoretical link between the model used and the data. The model will not be applicable for every dataset, particularly very small ones. Since the model is a seventh order polynomial regression model, and models of that nature tend to predict the center of the dataset better than the tail ends (Gelman, 2014), the ends of the model veer off considerably, as can somewhat be seen on the right side of Figure 16. Note the data is relatively high up there, but the regression veers downward. In the case of the studied dataset, a few storms near the very beginning and end of the dataset will be negatively affected. For a more consistent approach, one might use a first order linear model to calculate drift. Such an approach would not be as form fitting as the seventh order equation, but it would be more consistent when used with different datasets. If one was invested in maintaining the dataset as much as possible, a future investigation would remove and recalibrate equipment more frequently, or might use a drift correction scheme based off a low-pass Fourier transform, as such a scheme is based on combinations of phased sine waves, and would not diverge at the tail ends like a high-order polynomial function.

Figure 17 shows the dataset after the drift is corrected, and all values below zero were set to zero. The bottom is zeroed out because any infiltration below the bottom of the trench is considered outside the scope of this project.

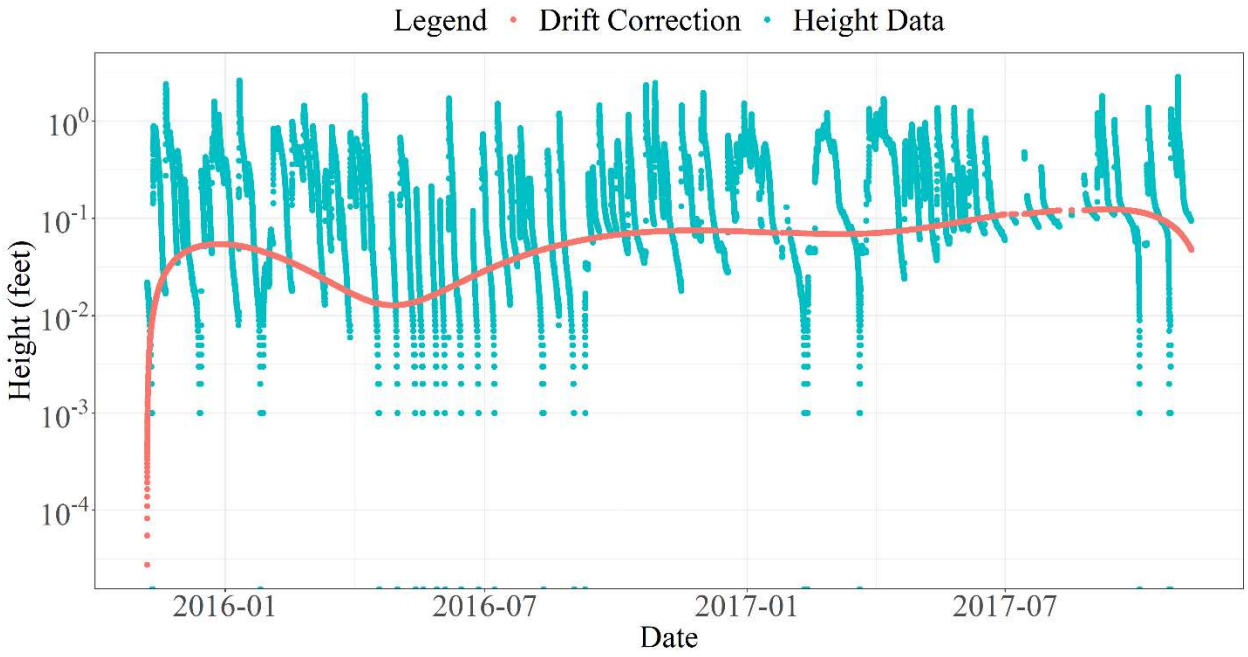

Figure 16: Drift corrected complete dataset, UNH A-Lot

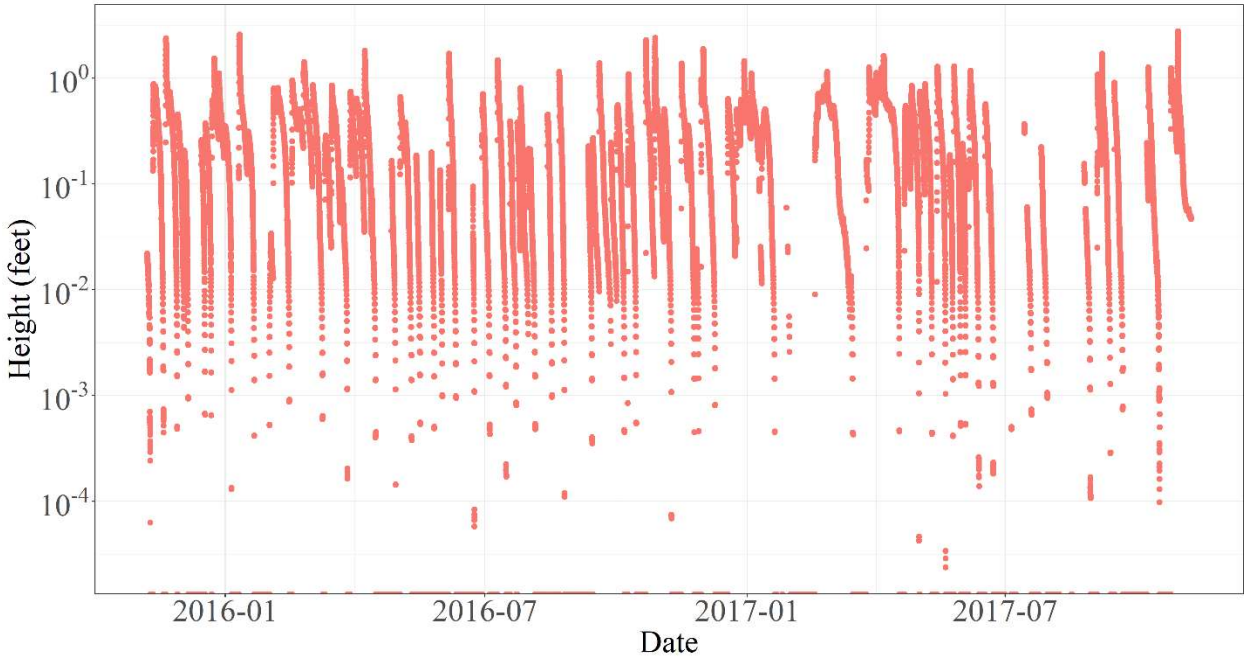

Figure 17: Complete dataset, post-drift correction, UNH A-Lot, depth of water in gravel trench

When considering flow out of the subsurface gravel trench, the system was treated like a black box. Flow was considered in terms of water leaving the sides and bottom of the trench.

Groundwater and soil moisture flow outside the trench system was considered beyond the scope of this thesis. After correcting for drift, any data points below the lower surface of the subsurface gravel trench were set to a trench height of zero.

Peak detection - In general, the impact of storms on a hydrograph have a consistent shape. The hydrograph generally starts at a localized low point. After rain falls, stormwater runs off the parking lot surface. If the runoff rate produced is faster than the bottom of the trench's capacity to infiltrate the runoff, the runoff gradually starts to fill the trench faster than the trench can infiltrate the runoff. After runoff decreases to a rate lower than rate the system can infiltrate, the depth of water reaches a localized high point and inflow into the system is steadily overtaken by outflow from the system, after which the height of water starts to decrease. As the height of water in the trench lowers, the driving factors expelling the water tend to decrease, causing the height of water in the trench to slowly level off towards a height in the trench of zero. In the case of the trench, infiltration decreases as height lowers and the water height levels off to a height of zero. In order to isolate individual storms automatically, one must be able to identify the localized high points of each hydrograph. To reduce noise in the dataset and make peak detection easier, a Savitzky-Golay filter (A. Savitzky, 1964) was used since it was the most ideal for preserving the peaks of the dataset. A standard smoothing function, a rolling average, takes the average of a specified number of adjacent points in a dataset, which would drag the peak of the function down considerably, as well as reducing the skewness of the function, offsetting the true location of the peak. Alternatively, a Savitzky-Golay filter applies a polynomial fitting to each set of points within the entire set, instead of a flat average. In this case, the filter used a first-order polynomial fitting over nine local points. As a result, the points have a smoother fit, but

contain the local extrema provided by polynomial regressions, reducing the effects of smoothing on the dataset's peak and skewness. The peak detection algorithm (the function "findpeaks" from the package "pracma") combined with the smoothing filter estimates a rough location of each storm peak, but the smoothing technique offsets the true location of the peak in the dataset. To finish the process, a temporal buffer around the estimated peak is created, and the maximum height value from the observed data is selected from within that buffer. The local maxima were then used as the peak of the hydrograph for each storm. If a storm had multiple local peaks after the end of rainfall, the last peak on the hydrograph corresponding to the storm was used.

Additionally, periods containing rainfall relevant to the storm and the rising limb of the hydrograph were removed from trench height hydrographs before applying regressions. Periods of mild rainfall after the storm period, but prior to the following storm period, were included in the analysis, as they were not considerable enough to cause a significant change in inflow. The reason the rising limb was removed was because the rising limb requires an additional calculation of inflow in the continuity equation, and was not necessary to predict the outflow behavior of the trench.

Figure 18 shows a subset of the peak detection dataset. In an ideal scenario, any time the in-trench hydrograph rises and then falls again due to precipitation, the code would be able to determine the exact location where the hydrograph is highest. The algorithm is imperfect, due mostly to specific types of variations within the dataset, so there are a couple of partially obscured locations where the peak detection did not find the hydrograph peak. There are also some events where there is a peak present, but such a peak is not immediately obvious to the algorithm. In order to keep the process as repeatable and internally consistent as possible, some of the peak data not captured by the algorithm needed to be removed from consideration in the

rest of the modelling process. The upside to that outcome is that data that was not captured by the peak detection tended to have a lot more noise than the rest of the dataset, and may not have been ideal for the rest of modelling process anyway.

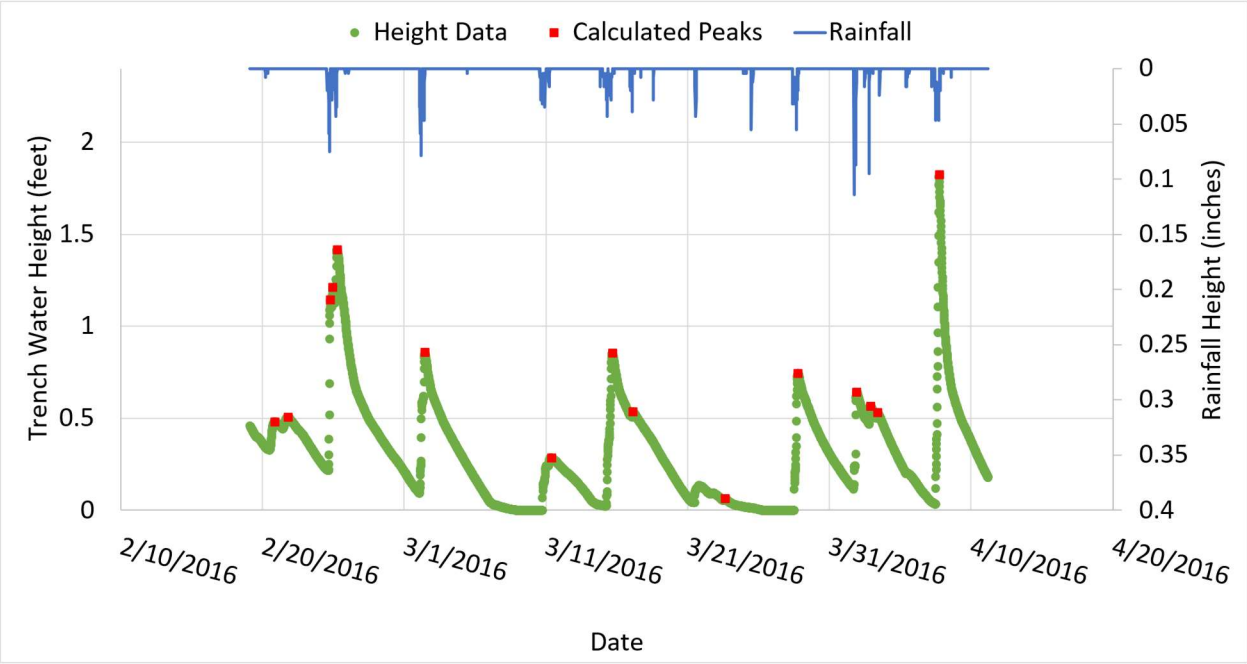

Figure 18: Partial dataset and peak detection, UNH A-Lot

The start of a hydrograph is defined for this project with either t he end of rainfall, or the presence of the hydrograph peak. Both conditions help to ensure that there is either no or limited amounts of water entering the system for any relevant hydrograph system. There may be significant rainfall runoff entering the gravel trench when it reaches its peak water height, however, these hydrographs will be combined together later in this thesis which is expected to reduce the impact of such inflows. Alternatively, the effects of removing water height data from the end of precipitation to ten times the time of concentration were studied, but were found to be insignificant in improving the fit of the final model.

The trench height hydrograph usually rises to a peak, and then drifts downward, reaching a localized minima before the next stretch of rainfall begins. The end of the storm hydrograph is then defined as the beginning of the following rainfall event. The hydrographs for the A-Lot system in particular very rarely reached a trench height of zero, because while high trench heights (like greater than one foot) tended to drain quickly, very low trench heights (like one inch or less) took significantly longer to drain completely, sometimes in the range of several days. It should be noted that some storms do not have defined peaks. Because the trench takes so long to drain, sometimes a storm was small enough that it generated no runoff at all, in which case the entire storm consisted of the "falling limb" of the hydrograph. The falling limb in this case would either be a stagnant height in the trench of zero, qualifying the trench as empty, or would be any remaining water from a previous storm.

Figure 19 shows the trench hydrograph with the recession limb hydrographs isolated. For the purposes of the study, the rising limb of the hydrograph will not be considered in developing the models. The falling limb dataset used is the complete dataset excluding the period of time between the start of rainfall and the peak of the hydrograph, or between the start of rainfall and the end of rainfall for a given storm, depending on whichever period is longer. The exclusion results with each storm's recession limb: a peak height that descends toward the minimum height before the start of the following storm. It should be noted that there may still be water contributing to the in-trench hydrograph at the water level peak, but on the basis that the time of concentration is only six minutes, compared to a typical timestep of fifteen minutes, the number of points on a given graph expected to be offset by inflow is minimal. Additionally, since periods of precipitation totaling less than 0.1 inches are not qualified as individual storms, sometimes precipitation can be seen during a discretized storm after an antecedent dry period. Storms can

also happen in quick succession, leaving short recession limbs that seem incomplete before the next storm starts.

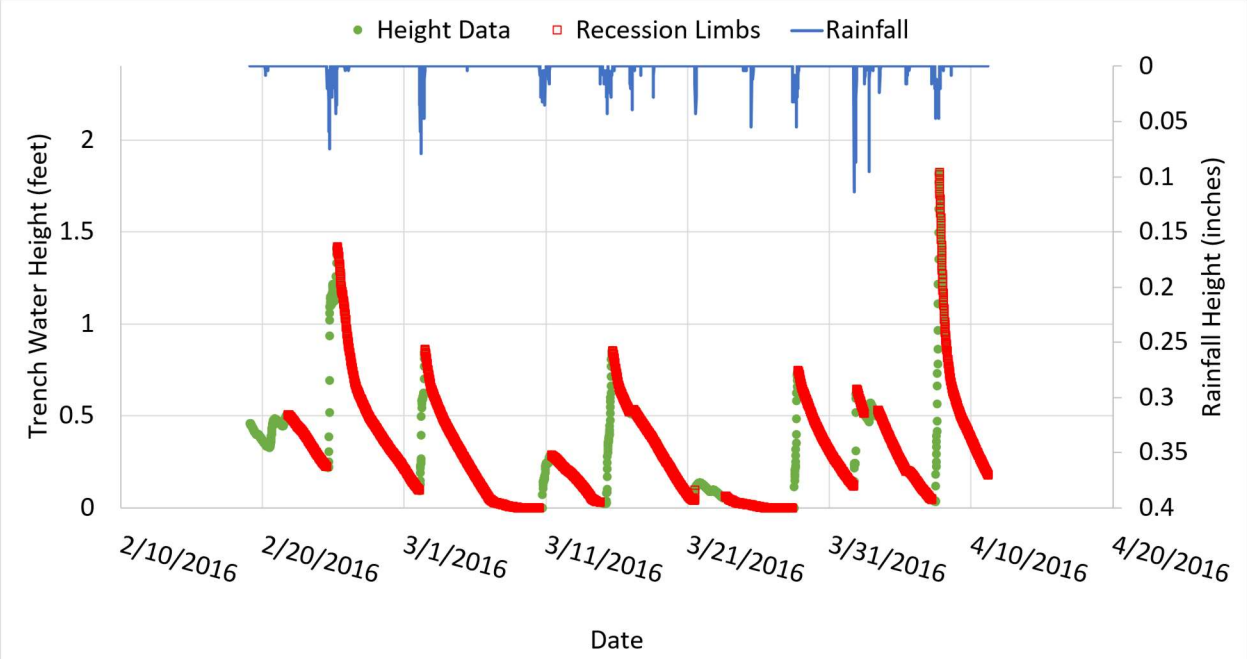

Figure 19: Partial dataset with cropped recession limbs, UNH A-Lot

Automated data removal - Any series of data should always be checked for consistency. If there are unexplained or undesirable inconsistencies within a data set, part of that data may need to be removed from any statistical consideration, dependent on which parts show problems. Such problems do not exclude the entire dataset, as most problems observed from the A-Lot dataset were temporary in nature. This thesis will be referring to such inconsistencies as "bad data." While some portions of bad data need to be removed manually, as only visual inspection can identify them with the limitations of the presented setup, there is at least one instance where automation can find bad data in any storm: the absence of data. If any storm or hydrograph had a temporal gap, defined as any period with greater than 29 minutes between two adjacent timesteps, any rain and stage data collected after the gap and before the following storm was

discarded. The reasoning for removing said data is that anything could be happening in the time gap that could disconnect the following data from the initial event, for example, a storm event that happened during the time gap and was not caught. Some of the data suffered rounding errors on the time scale, which meant an occasional timestep was sixteen minutes, or fourteen minutes, but that was corrected by rounding the time data to the nearest fifteen-minute mark.

Incomplete data tends to happen for a few reasons, including lack of power, insufficient storage, equipment malfunctioning, and human error. The most common example of incomplete data was lack of power, as the Campbell Scientific instrumentation was powered by a deep cycle battery, and the battery was charged by a solar panel. If the solar panel received insufficient light, as could happen during the short daylight cycle winter months, or if the battery lost its ability to hold a charge, the Campbell Scientific would cease to function, and that series of data points would not be collected. Snowmelt could probably be incorporated into the automatic removal phase, as slow, periodic peaks on a hydrograph with no associated rainfall are usually attributable to snowmelt, but time constraints forced this step to be a part of manual data removal.

D. Manual Data Removal

Before any data was removed from the height gauge dataset, the dataset was discretized into individual storms. In order to use height gauge data as effectively as possible to estimate outflow from the gravel trench, some parts of the observed height data needed to be removed on a more subjective basis. Periods of rainfall and storms containing unexplained temporal gaps

were removed automatically. This section discusses data that must be reviewed by a person, as automation proved difficult for the required data discrimination.

The portions of rainfall and stage data removed included either the entire storm event, or any data following an inconsistency in an otherwise consistent storm event. The first event type in the height gauge dataset to be removed was snow melt. Snow melt could be visually identified on a trench height hydrograph as periodic peaks without sufficient explanatory rainfall data, particularly during the colder months. In the event of hydrograph data explained by snow melt, the entire storm event was discarded, as it would throw off the peak height estimations from rainfall data, which in turn would throw off any predictive results of the analysis.

Figure 20 shows an oddly timed spike at the end of the hydrograph. The spike may be caused by snow melt, especially considering the fact that it occurred in early February. While snow melt is a legitimate consideration in any stormwater system's performance, the metrics posed by snowmelt are not within the scope of this project.

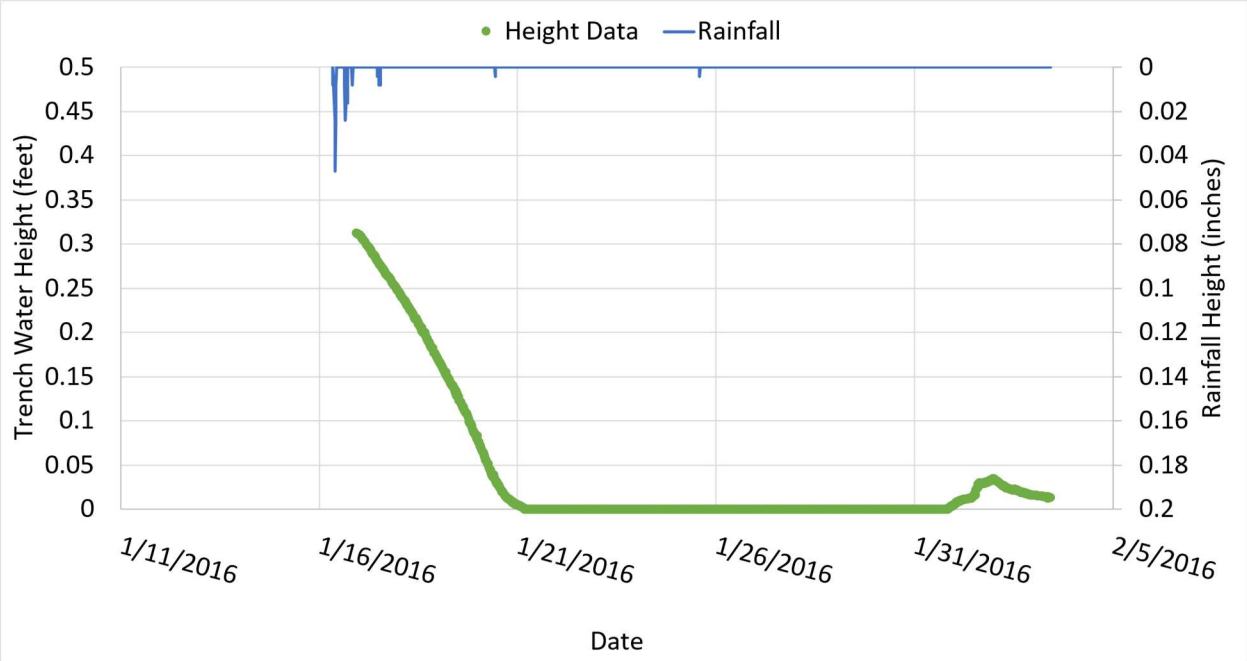

Figure 20: Discarded storm hydrograph, algorithm irregularities, UNH A-Lot

Figure 21 shows a storm which does not initially appear to have invalid data but came across as suspicious due to the long time delay between the initial rain burst (seen during February 3rd) and the final reaction. Since the process of extracting the recession limb removed trench water height data between the start of rainfall and the peak of the water height hydrograph, the extended period without height data represents what the R-code determined was the ”rising limb,” as is similarly displayed in Figure 22. The delayed reaction may result from data removal due to irregularities caused by snow melt. Many cases that should be removed are highly interpretive, hence the requirement that the user review the data before continuing the process.

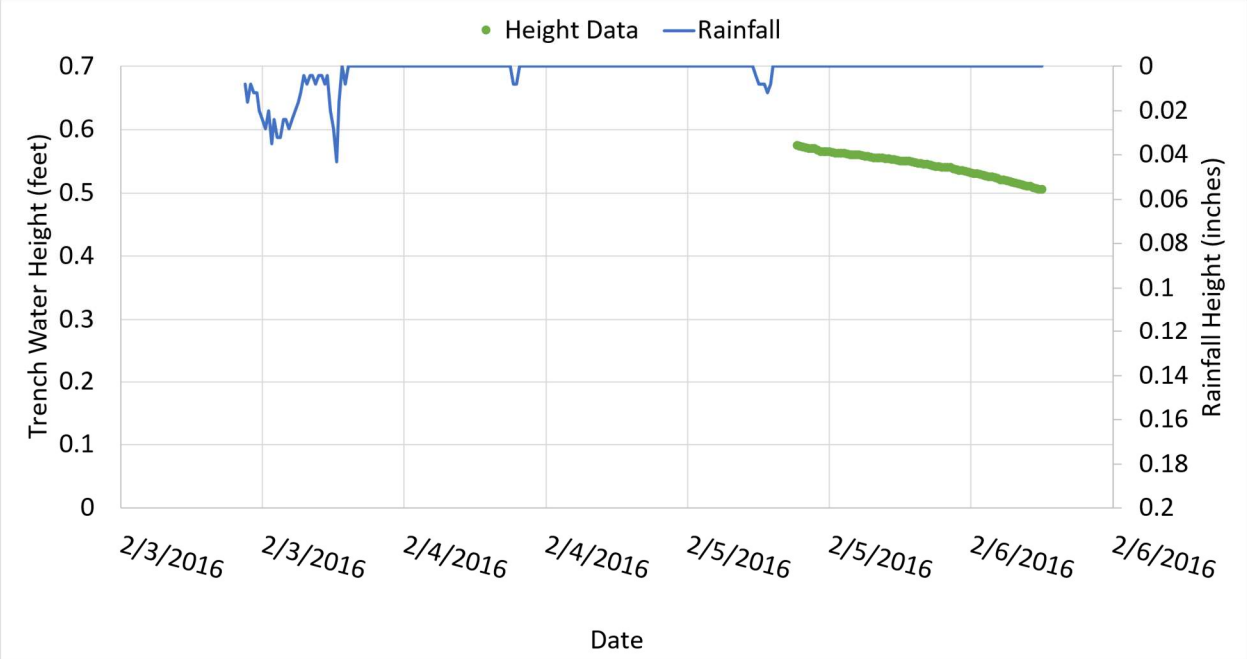

Figure 21: Discarded storm hydrograph, bad data, UNH A-Lot

Figure 22 shows a similar system reaction as Figure 21, however this time there is no preceding rainfall to the peak by over one day. Such an event could occur if additional peaks were created by snowmelt, in which case this storm is outside the scope of the project. This

storm was not used regardless of interpretation, as rainfall from at least 20 hours prior is required to run the height prediction algorithm.

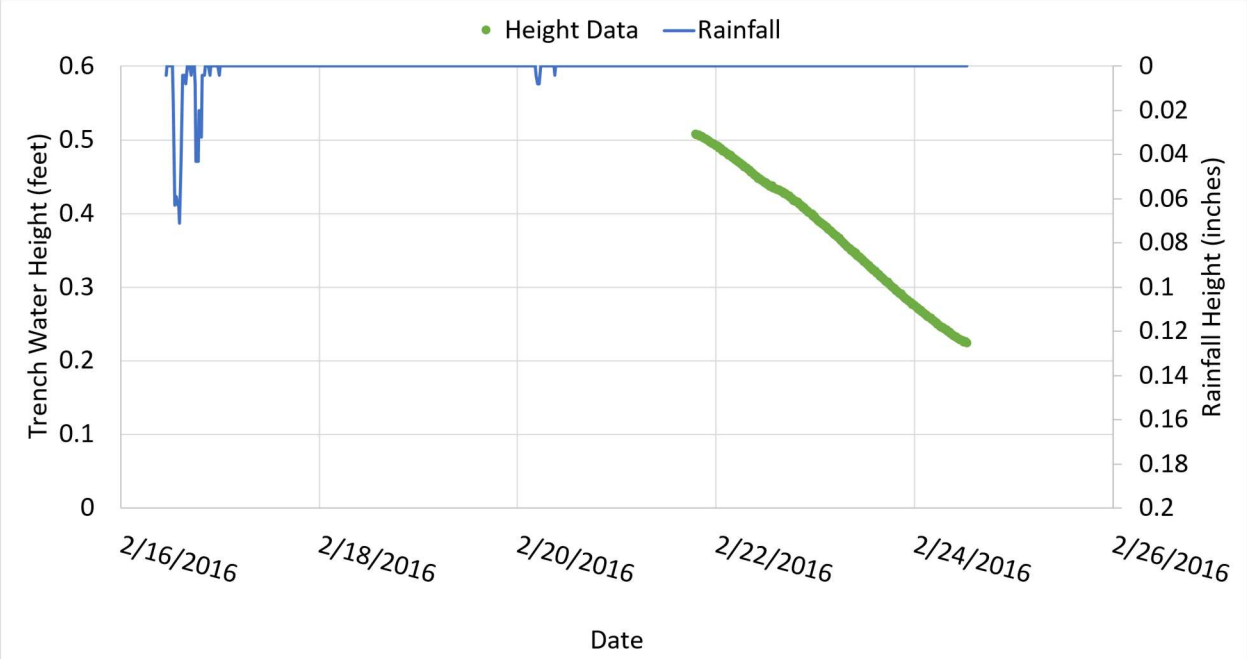

Figure 22: Discarded storm hydrograph, extensive reaction delay, UNH A-Lot

The second event type to be removed is misshapen data. In general, storm events follow a distinct pattern of behavior. As the result of a rain event, the height gauge has a rising limb, a peak, and a falling limb. Sometimes, if a storm is light enough that it does not generate significant runoff, the storm might have only a recession limb, an artifact of a previous storm that had not left the trench adequate time to drain completely. The standard hydrograph pattern is very consistent following an ordinary rain event, so if a storm had considerable irregularities, such as large, instantaneous changes in height, changes in height that could not be explained by rain events, unnaturally flat sections of data, or otherwise unnatural appearing data, the entire storm was discarded. Irregularities could be explained by faults with the sensors, unnatural external phenomenon, or even less easily identified snow melt.

Figure 23 displays a hydrograph determined to best represent the trench system, from a storm on October 9th, 2016. Determining the most ideal storm event is essential to the creation of the modelling process, as such a storm yields a recession limb hydrograph that will display system infiltration details.

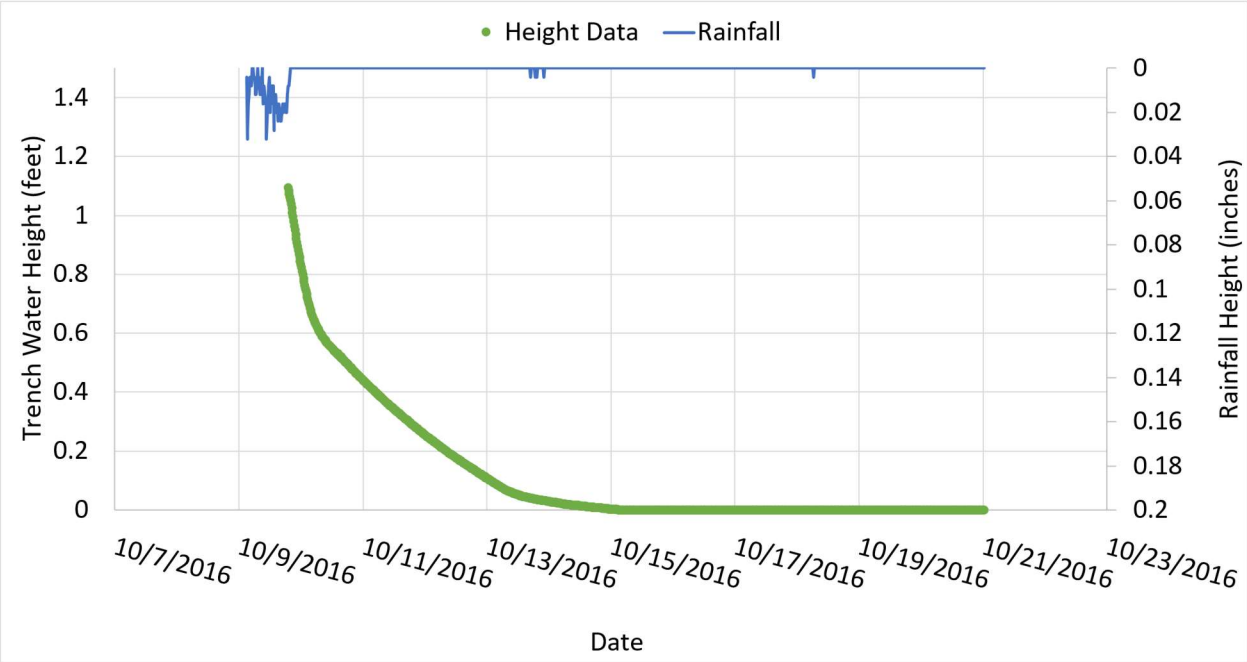

Figure 23: Chosen dataset for initial regression (Oct. 9, 2016, 0.884 inches of rain), UNH A-Lot

Through the process of selecting data for modelling, a significant amount of data was removed from consideration. Of the original 66,134 data points in the process, a total of 40,363 points were used, for a retainment rate of 61.0%. Of the original 108 storms, 86 were used.

E. Time Series

The first major step in creating the predictive model for the subsurface trench height hydrograph was estimating the peak of each hydrograph based upon rain data. Since the inflow to the system is not being calculated, there needs to be a way to gage the response of the water

height in the trench to the inflowing stormwater. This section seeks to explain the process used in the predictive model.

Water height peaks were used as the training data in developing a time series prediction model, using rainfall from multiple time steps as the explanatory variables. If a storm did not have a water height peak, either due to the peak being excluded by the elimination of rainfall time periods, or by the low magnitude of rainfall being unable to produce a distinct peak, then the peak of that storm would default to the first point in the series. It is worth pointing out that the water height peak of the dataset will still have inflow, as it is not the point where inflow stops, but the point where outflow exceeds inflow. It is an assumption of this thesis that once all storms are aggregated for a final regression, those inflow periods will be teased out of the regression by the nature that periods of inflow contain a minority of the data, and occur at random heights relative to the recession limb. Containing the peaks within the analysis will help to assess the performance of the system in extreme conditions.

The dataset consisted of the training data and the explanatory variables. The training data was the peak height of each water height hydrograph. The explanatory variables were rainfall data, specifically 21 timestep lagged variables prior to the end of rainfall. That means the 21 timesteps measuring rainfall prior to the end of the storm would be used in the model to estimate the peak trench height of that storm. There needed to be enough lagged timesteps used that the rainfall entailed therein could characterize the whole storm's rainfall.

For each individual storm, the resulting hydrograph height prediction would be produced from 67 different data points. 21 data points were the lagged rainfall timesteps. Another 21 of the data points were the same lagged rainfall timesteps, but each value was transformed by an exponential function ($e^{rainfall}$). Another 21 of the data points were the lagged rainfall timesteps,

but transformed by a logarithmic function (ln(rainfall)). Finally, the last four data points described the time of day during which the storm took place, and the day of year during which the storm occurred. Since the time of day and the day of the year are most relevant due to temperature and the relationship it can have with a storm, and that temperature tends to cycle, the day and time variables were transformed using a sin function so that every day and every year started and ended at the same value for the time and year variables, respectively. Every storm peak height had a total of 67 data points to explain it. Many of those 67 data points were either correlated or not explanatory, so many of the variables needed to be eliminated to prevent creating an overfitted model. An overfitted model would disrupt the repeatability of using the model on that site. The correlation between many of the used variables was expected because most of the variables were simple transformations of the lagged rainfall data.

The solution to the need for variable reduction was the use of an R package called "EARTH," based off the Multivariate Adaptive Regression Spline, or MARS regression technique. MARS is a registered trademark. The EARTH model is the freely available version of MARS. The method involves creating a regression from multiple linear splines using the fewest number of pivot points, or "knots" possible.

A first order linear regression creates a line of best fit from an entire dataset so that one can use an explanatory variable to estimate a predictive variable. A spline fitting is qualified by subdividing a linear regression into multiple regressions, wherein each regression explains only a portion of the total domain of the explanatory variable. Where two splines meet, they form a point. In the case of the gravel trench recession limb, that point would have a specific time and height. Figure 24 shows a comparison between a set of points estimated with a standard linear trendline (the dotted blue line) versus a three knot linear spline (the solid black line).

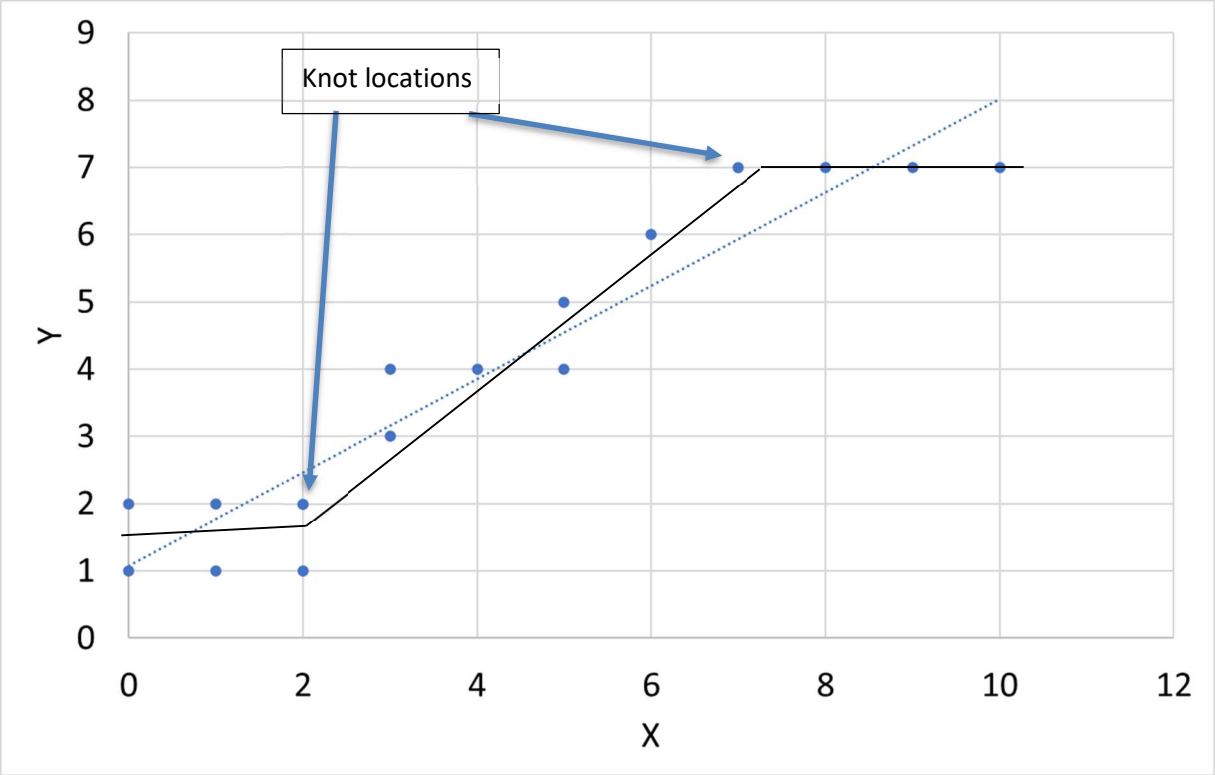

Figure 24: Comparing a linear spline to a general trendline

The number of knots depends on the diminishing returns of higher r-squared values calculated from the regression. The limiting knots factor helped to ensure that the regression automatically limited the number of splines to only the most explanatory ones. (Friedman, 1991)

Figure 25 shows the predicted hydrograph peaks versus the actual hydrograph peaks. The model for the predicted hydrograph peak used rainfall lag variables. The R-squared value is 0.85, which indicates a strong correlation. RMSE is in feet.

Figure 26 displays a screenshot of the resulting model of the height predictor produced by EARTH. (Milborrow, 2021).

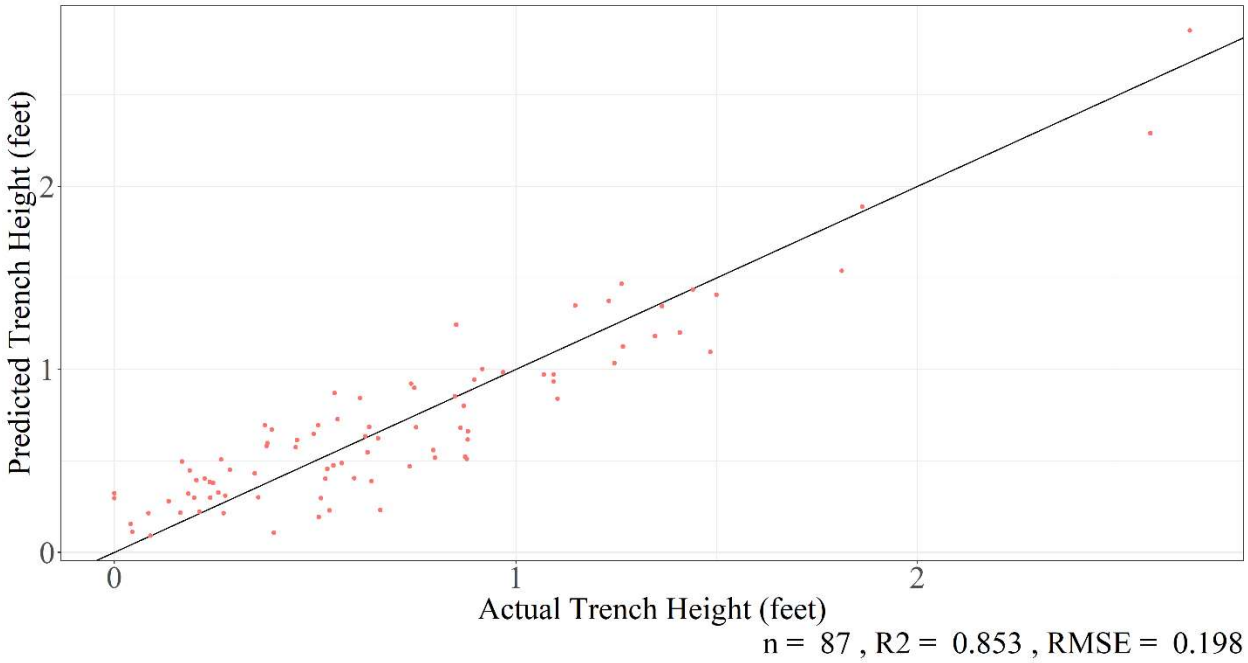

Figure 25: Predicted versus actual trench hydrograph, R-squared, UNH A-Lot

```
-0.2927599
+   0.7437875 * h(rain_01log--2.67365)
+  0.07241055 * h(-3.29684-rain_03log)
+   0.2012484 * h(rain_03log--3.29684)
-  0.05634061 * h(-2.43042-rain_04log)
+   0.3201614 * h(rain_04log--2.43042)
+   0.1482785 * h(-4.34281-rain_10log)
+   0.2919088 * h(rain_10log--4.34281)
+   0.1096916 * h(rain_18log--5.29832)
-    21.18627 * h(1.0202-rain_08exp)
+    3.950304 * h(newhour1--0.866025)
+    3.298773 * h(-0.707107-newhour1)
-    3.888337 * h(newhour1--0.707107)
```

Figure 26: EARTH results for hydrograph peak prediction

How to read this model is as follows:

-The first value (-0.2927599) is the y-intercept.

-The first column is all the coefficients defining the magnitude of each spline.

-The “h” function surrounding the second column is called a “hinge function.” The function solves for the maximum between the variable on the inside and zero. The entire model could be re-written as:

Peak height = -0.2927599 + 0.7437875 * max(0, rain_01log + 2.67365) +…-3.888337 * max(0, newhour1 + 0.707107)

Where peak height is in feet (L).

-Rain variables each have a number attached. The number corresponds to the number of timesteps the rainfall was lagged from the end of the storm. For example, “rain_03” would represent the rainfall that occurred 3 timesteps from the end of the storm. The reason for the backwards naming convention is that number of lags can be adjusted without renaming any of the variables.

-Variables that end with “log” had a natural log function transformation by taking the natural log of the original rainfall value (ln(rainfall)). Note that all but one of the rain variables used were log transformed variables. A log transformation may be sufficient in using time series rain data for peak height predictions. A possible reason for the prominence of log transformed rainfall in the EARTH model may be that the transformation created a “dampening” effect on the rain data, similar to rainfall routing practices.

-Variables that end with “exp” had an exponential transformation by raising e to the power of the rainfall value ($e^{rainfall}$).

-Variable newhour1 was one of the day and time variables described earlier, in this case, describing the time of day the storm took place.

Figure 27 shows the number of knots used versus the resultant best fitted R-Squared value. The graph (as well as Figure 28) is a direct export of the EARTH package, and is a little tricky to

understand without the appropriate context. An increase in the number of terms (as shown in Figure 26) leads to an increase in the final R-Squared value, the red dotted line (Milborrow, 2021). The chosen model is marked by the vertical black dotted line. A term is equivalent to a line segment derived from one of the contributing predictors. The model is chosen based upon the peak GRSq value. The GRSq line describes how the number of terms used in the model affects the model's generalized R-Squared value. The difference between R-Squared and generalized R-Squared is that the generalized R-Squared method applies a penalty as terms are added to a model. As the effects of adding terms to the model diminishes, the GRSq line will peak and then curve downward, representing a loss in model effectiveness. The "out-of-fold" lines utilize cross validation data. The faint red lines represent the subsets used for validation, and the heavy red line represents an average of all the validation subsets. As can be seen, the selected model has very diminished re-usability, with a Cross-Validated R-Squared of .2807, compared to an R-Squared of .8534.

Figure 28 compares the fitted hydrograph peak water height (in terms of feet of water under the "fitted" axis), against the residual errors (the difference between observed values and predicted values, in terms of feet of water on the "Residuals" axis). The red line on the graph is a moving average (Milborrow, 2021). The variance of all peak predictions appears to be consistent across the range of height predictions, ranging from -0.4 feet to 0.4 feet. Several outliers are highlighted on the graph with red numbers.

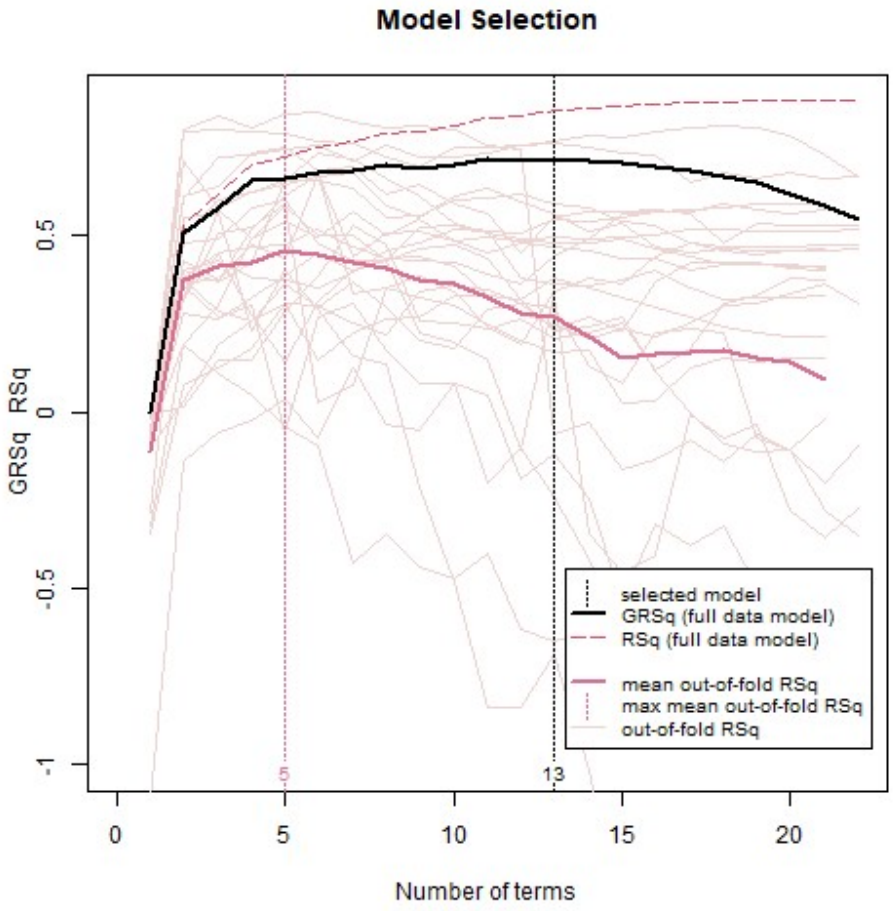

Figure 27: EARTH model selection, UNH A-Lot

F. Drainage Prediction

This section will discuss the formation of a statistical analysis process for developing the falling branch of a subsurface gravel trench hydrograph, including possible locations of soil horizons through kinks present in the hydrographs. The process will require several steps so that one may move from one hydrograph dataset containing multiple storms to one reference master hydrograph containing an average of all hydrographs, over the entire potential range of water heights in the gravel trench. The master hydrograph can be used with any storm height to predict

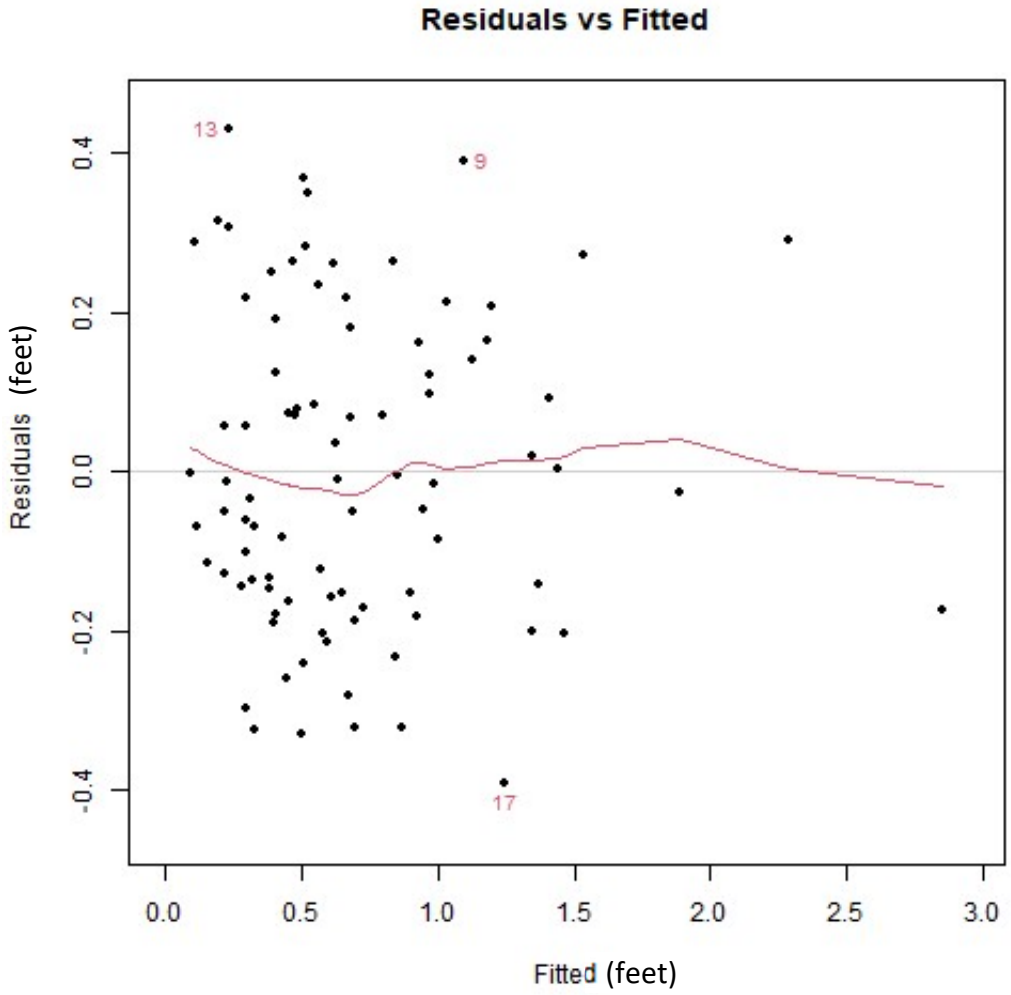

Figure 28: EARTH residuals (ft) versus fitted water height values (ft), UNH A-Lot

the overall pattern of the falling branch of that hydrograph. The use of a floating time axis on the master hydrograph allows one to replace the initial height location and any following points with the appropriate timestamps. The following points on the master hydrograph can then be mimicked directly as the predicted data. For example, if one predicted a peak height estimation of 0.85 feet, the master hydrograph would be shifted so that the corresponding height of 0.85 feet on the graph would start at timestep 1. All points on the master hydrograph prior to timestep 1 would be removed, and all points following timestep 1 would be replicated as the rest of the

height prediction for that storm. In effect, observed data created the master curve, and the master curve created all predicted hydrograph curves. Any storm with a starting height of 0.85 feet would have an identical prediction to any other storm with a starting height of 0.85 feet, though as results may show, that may not be an accurate statement. Figure 29 shows an example of what a master curve juxtaposed against a derivative secondary curve would look like. Note that the master curve extends above the elevation of the trench (2.4 feet). When using the master curve to predict the behavior of the trench, the top elevation of the trench should be kept in mind as elevations above it represent the trench's inability to store the entire runoff volume. In the development of the statistical model, an upper bound for water level was not included.

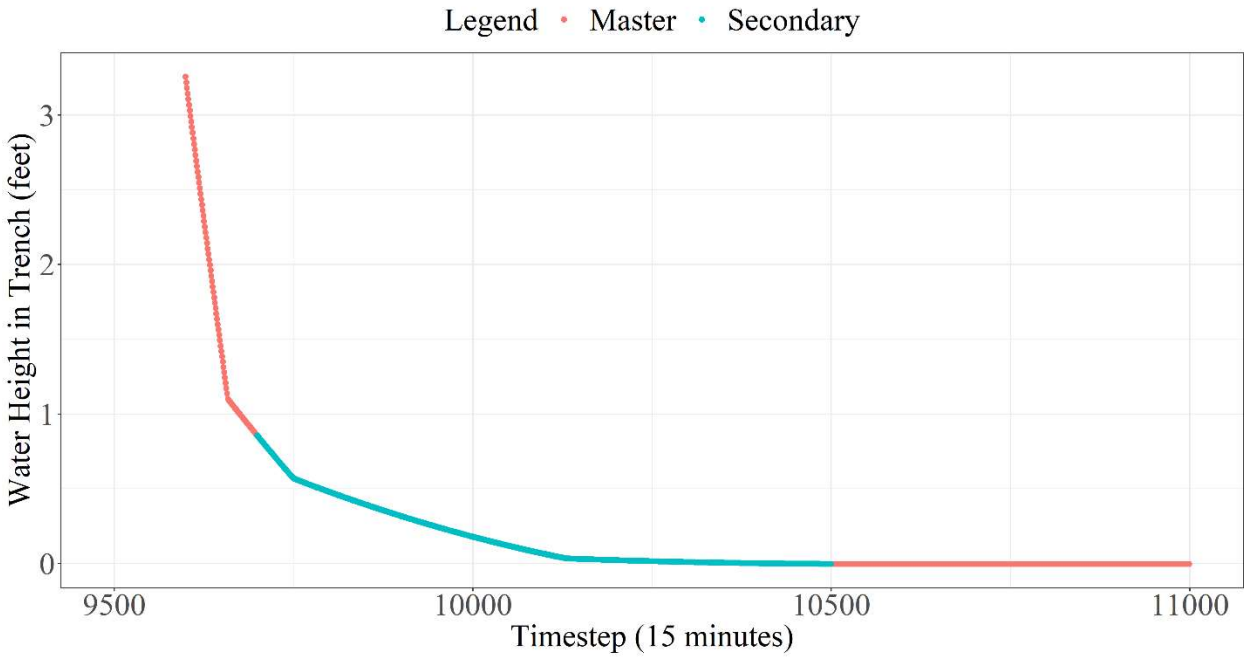

Figure 29: An example of a master curve and a derivative secondary curve

One can also use a given storm height, for example the water height in the trench corresponding to the Water Quality Volume (the runoff from one inch of rainfall over the area of the watershed), to predict the amount of time the storm will take to totally empty from the system. The combined observed hydrograph data can be used to predict the time where the

gravel trench is completely empty, which would then be used to further refine the master curve, and subsequently all other synthesized hydrographs. Since a minimum 24-hour emptying period is required for the design process as per the New Hampshire Stormwater manual, the process used for predicting emptying time is not trivial. A process that includes sidewall infiltration and anisotropy considerations may shorten those duration estimations considerably.

Once the EARTH model is created, any individual spline, as opposed to the summation, could be used to estimate how much flow from the trench could be due to infiltration from that one simulated layer.

G. Primary Knot Points

When forming the master hydrograph curve from which other hydrograph recession limbs will be formed, the first task is to determine the approximate temporal locations of each kink in the recession hydrograph. While the kinks themselves are a vertically occurring phenomenon, storms must be shifted along the time axis so that storm peak heights can overlap with the estimated model. The kinks will be used as the locations for knots. While the x-axis of the master hydrograph is representative of time, it is not representative of a specific time, but rather a series of successive times, relative to each other, but not the real world. In the case of the A-Lot hydrograph, every monitored consecutive water height point is separated by 15 minutes. One does not need to solve for a timestamp of every knot point from which one forms the splines, but rather, all the knot points must be solved for their location relative to each other.

One of the desired features of the modelling process to measure soil horizons was to somehow average all storm hydrographs together and then measure the heights of any kinks in

the data as they appear in the aggregate. The only way to superimpose storms over each other was to shift each storm's time axis so all storms overlapped, as shown in Figure 30. Figure 30 shows the results of overlapping 87 water height hydrographs (n=40,363). If all storm recession limbs were overlapped at the beginning, then their peak water heights would all be different, so more robust layering qualifications were needed. One storm recession limb could be chosen as a lookup table, and all other storms' recession limbs could be matched to that storm by the first data point, but a theoretical dataset might not have a recession limb with the wide range needed to encompass the first points of all other recession limbs. Additionally, such a method would not account for how the system performance changes over time, as any chosen "lookup table" storm might be from a period of high performance, causing any recession limbs with a low performance to stick out awkwardly when graphed against each other.

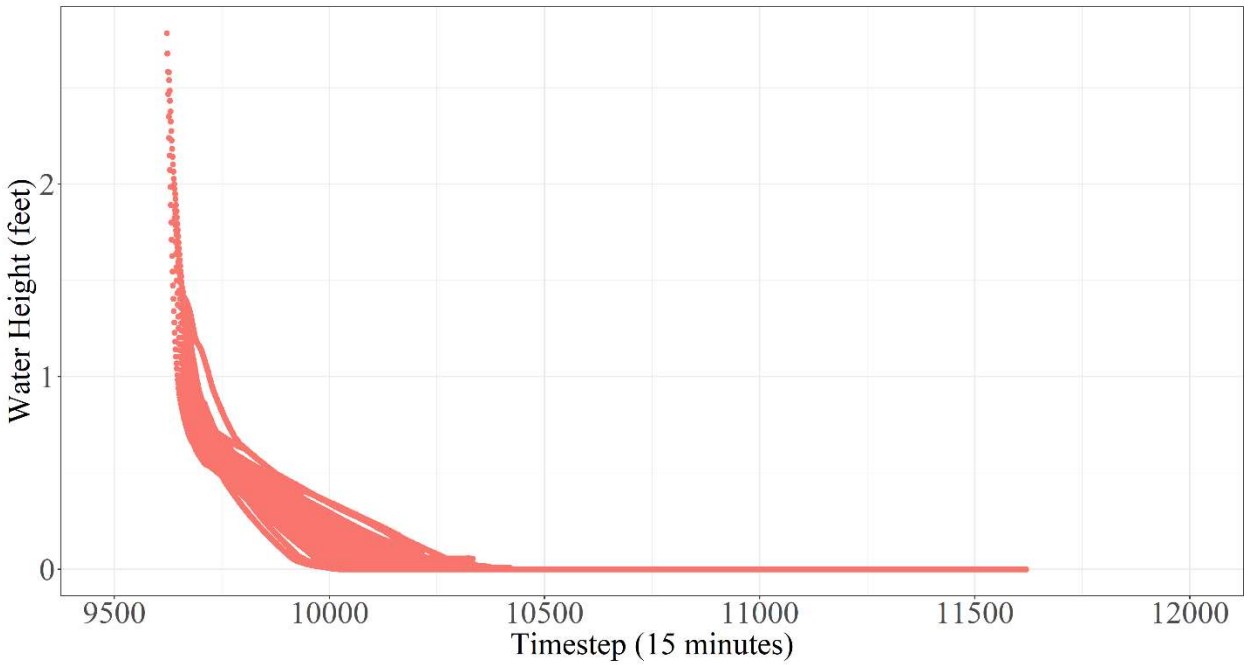

Figure 30: All water depth hydrographs overlapped, UNH Lot A gravel trench

The modelling methodology for estimating the horizon elevations in the soil profile involves the following:

1) Choose an initial storm that well represents the elevation range of the system as a whole.
2) Create a model that matches the initial storm appropriately. The model must contain separate sections, representative of changes in the soil's performance relative to soil horizons.
3) Extrapolate both ends of the model forward and backwards in time to cover all possible peak storm heights. It does not matter how far the model extrapolates provided the physical limitations of the system are kept in mind for analysis, such as the top and bottom elevations of the trench itself.
4) Use the created model as a lookup table to match against the first points of the recession limb of every storm.
5) Recalibrate the model, updating for all data points for all storms.
6) Repeat steps 3 and 4 iteratively until all storms are superimposed over each other in a consistent manner. The final model can then be used in conjunction with predicted hydrograph peaks to create an estimation of the system's performance in a given scenario.

Estimating the elevations of soil horizons in the system through kinks present in the hydrographs is difficult. Creating splines on the basis of height directly is impossible for this method, since the corrective element for adjusting each storm recession limb's relation to one another is the starting time step of the limb, not the water height. Fortunately, the relation of the recession limb is one-to-one (one explanatory value for every response value, and vice versa) , so one can use the described modelling process to find the elevation of soil horizons indirectly by finding the location of a timestep consistent with a sharp change in infiltration rate that occurs

consistently through all storms, and that timestep aligns with a specific soil depth. At first, the process of locating the correct timesteps is achieved by partitioning the data. When the data of all storms was combined later on, an EARTH model was used for finding horizon elevations.

Figure 31 shows the initial estimations of soil horizon locations (abstractly as a temporal phenomenon) within the system. The "ideal" storm chosen earlier in the process is used as a starting point for estimating anisotropy in the surrounding soil. The model works by creating multiple splines, each joined at specific points, or "knots." The location of those knots are determined by splitting each dataset in two parts, forming the splines around each part, and then checking the r-squared value for each set of splines. That process is repeated for every timestep in the storm. Note that knots 2 and 3 occur approximately at kinks in the trench water level hydrograph. There is a kink at 0.6 feet in the hydrograph that is not captured by the knot forming process, but that is due to the insufficient number of knots used, as was specified in the program, a problem which will later be resolved by the use of EARTH. The reason EARTH was not used in this part of the process was because it was undetermined how to make custom splines with EARTH (as described in section H, "Splines").

For example, if the hydrograph is 200 points long (in 15 minute timesteps), the data will initially be split at timestep 20. The 20 step duration was chosen arbitrarily, and could be changed as the need exists. All the points before timestep 20 will form a group, and all the points after timestep 20 will form a group. A first order linear regression is then formed for both groups, creating two lines-of-best-fit for each water height hydrograph subset. The mean error of the total regression is recorded. The process is repeated with a split at timestep 21 and continues until timestep 180. A 20 step buffer is left at the beginning and end of the dataset to prevent errors resulting from forming a linear regression with too few data points. The list of errors is

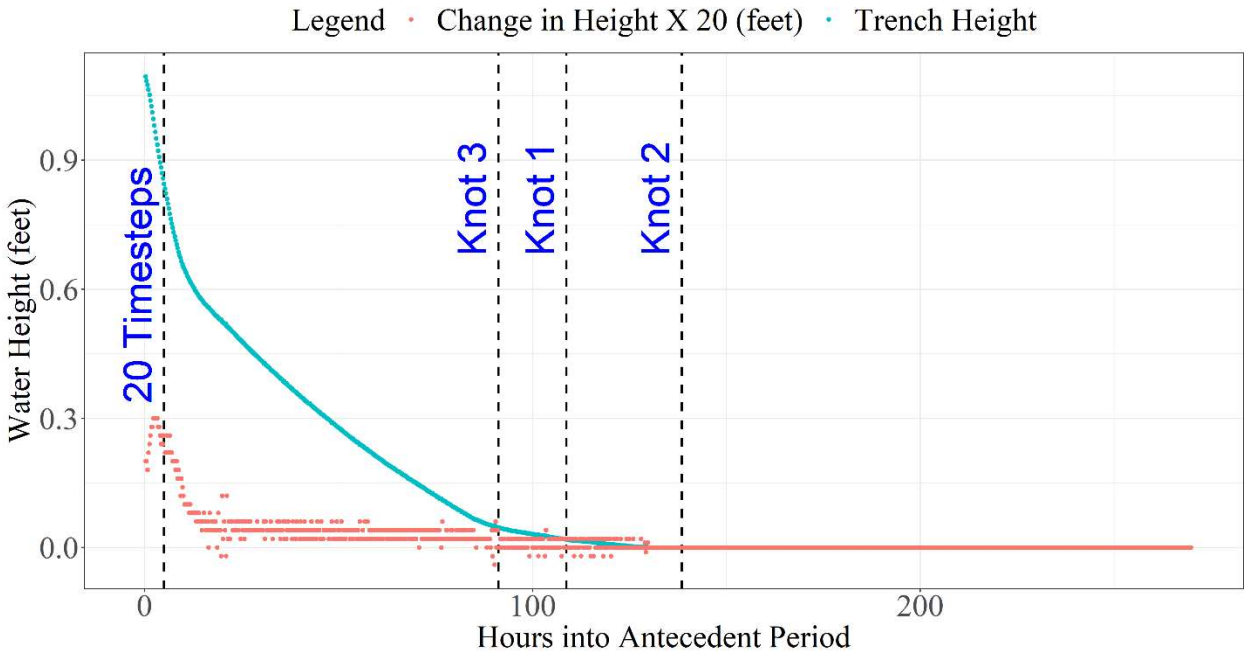

Figure 31: Demonstration of knot points on hydrograph, UNH A-Lot

compiled and the timestep with the smallest error is used as a knot. The entire dataset is split in two using the newly generated knot, and the two new datasets are run through the same splitting process described above, creating two more knots, one for each spline created from the previous split. The final two knots, on the graph above called “Knot 2” and “Knot 3” are used to subdivide the data. “Knot 1” is removed from the process as it was used as a starting point for the creation of the final knots. As can be seen, the process is imperfect because perhaps the most obvious knot at around stage 0.6 feet was missed entirely. That imperfection can be attributed to there being a predefined number of knots when any potential dataset has an undefined number of soil layers. The problem of not having enough layers for every dataset, or too many for that matter, is solved with the introduction of the EARTH model later on.

H. Splines

After the derivative knots are calculated for one storm, their temporal location can be adjusted to account for the change in trench performance over time. This was achieved in the following section "Hydrograph Consolidation and Knot Tuning" by combining all storms together so that they overlapped, and creating an additional fit with all storms together. In order to create an overall average of all storms, initial splines must be created to represent each section between knots, so that storms can be adjusted relative to each other.

The following splines were created to mimic the behavior of flow out of a trench when water is above a given soil layer, intersecting the layer, and below the soil layer. Once the splines are used together in a model, they will have water height values associated with them, directly from the model.

The first spline, or Spline 1, consists of natural numbers, from 1 to the end of the dataset n, representative of all the timesteps in the dataset. This spline is only used for the flow out the bottom of the trench, and is used for the "cubic fitting variable" described later in this section.

Spline 1: $f(x) = n - x, \ if \ 0 \leq x \leq n$

n=The ordinal number of timesteps in the considered dataset

x=The timestep in the series of consideration

The second spline, or Spline 2, is used in the regression curve to model the hydrograph height component of the top layer of soil, as described in the "Layer Equations" section by Equation 12.

Spline 2: $f(x) = \begin{cases} m - x, \ if \ 0 < \ x < m \\ 0, \ if \ m \ \leq \ x \ \leq n \end{cases}$

m= The ordinal timestep of the location of knot 1

The third spline, or Spline 3, consists of three parts and is used to model the hydrograph height component of a middle layer of soil, below the layer described by spline 2, and above the layer described by spline 4.

Spline 3: $f(x) = \begin{cases} 0, \ if \ k < x \leq n \\ k - m - x, \ if \ m \leq x \leq k \\ k - m, if \ 0 < x < m \end{cases}$

k= The ordinal timestep of the location of knot 2

The fourth spline, or Spline 4, is used in the regression curve to model the bottom layer of soil.

Spline 4: $f(x) = \begin{cases} n - x, \ if \ k < x \leq n \\ n - k, \ if \ 0 < x \leq k \end{cases}$

Each spline contributing to lateral flow has its antiderivative taken as the splines were created to model infiltration rate, and the antiderivative of a rate is a position, in this case the position of the water stage. The antiderivative of each spline is calculated using the "diffinv" function in R's "stats" package. The linear regression equation to which future falling limb models will be fit is written below:

Regression Curve $f(x) \sim \text{Intercept} + C_1*(\text{Spline } 1)^3 + C_2*\text{diffinv}(\text{Spline } 2) + C_3*\text{diffinv}(\text{Spline } 3) + C_4*\text{diffinv}(\text{Spline } 4)$

Figures 32 through 34 describe the three distinct sequences used in the estimation of the curve. When forming the final r egression limb for the chosen storm, the three characteristic curves will be used like individual variables, each with an associated constant value that will dictate each of their relative contributions to the infiltration process. Recall that the knot locations depicted are analogous to those of Figure 31, and that Knot 1 was removed from consideration because it was used as a starting point for knots 2 and 3.

Figure 32 shows the first characteristic curve to be used on the dataset. Knot 3 is used as a separation point between a second order spline and a constant portion with a value of zero. In the final linear model, the first characteristic curve will ideally capture the resultant stage decrease due to infiltration from the highest layer of soil. Note that since the characteristic curves are designed to create a particular shape, and not yet a particular magnitude, the y-axis does not contain values relevant to the hydrograph yet, hence the y-axis in Figure 32 being labelled "Unadjusted." Figures 33 and 34 share a similar predicament. When this curve is multiplied by a constant dictated by the regression, the output will reflect the height of the hydrograph.

Figure 33 shows the development of the second characteristic curve, with the first characteristic curve included for reference. Note that all characteristic curves are continuously differentiable. The curve left of knot 3 is a non-zero first order spline. The portion right of knot 2 is a constant value of zero. The portion of the curve between knot 3 and knot 2 is a second order spline, designed to be continuously differentiable with the other two splines. The second

characteristic curve is representative of hydrograph water heights attributable to the second highest elevation soil layer.

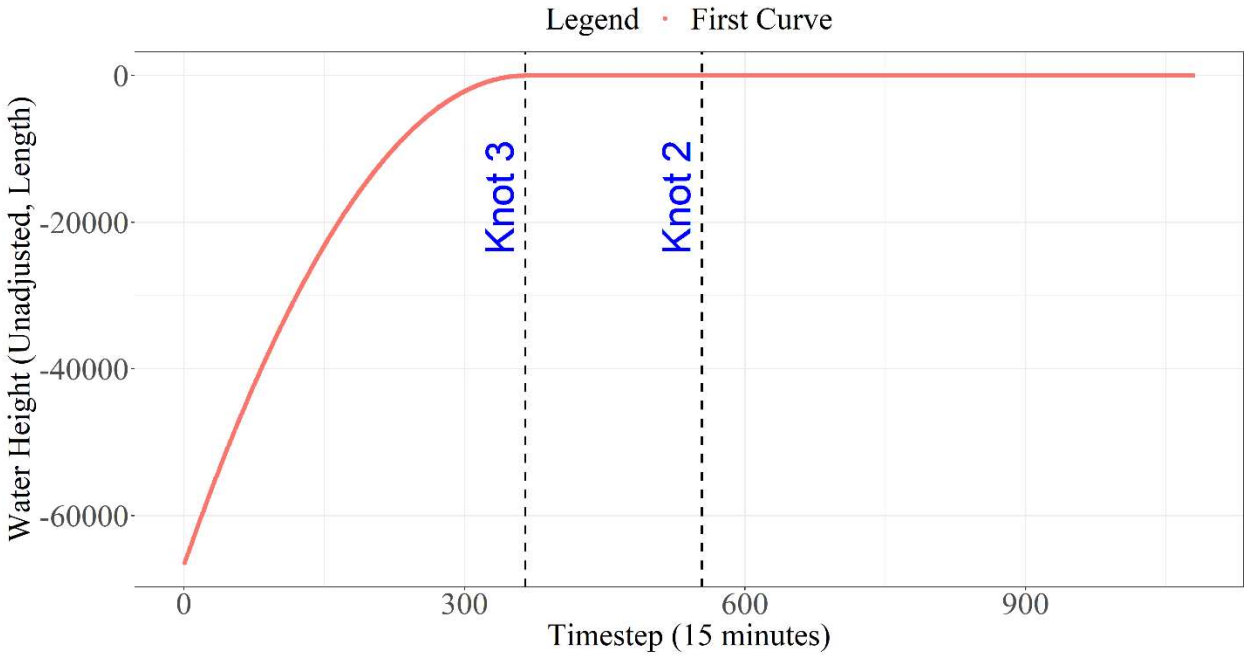

Figure 32: First knot characteristic curve, UNH A-Lot

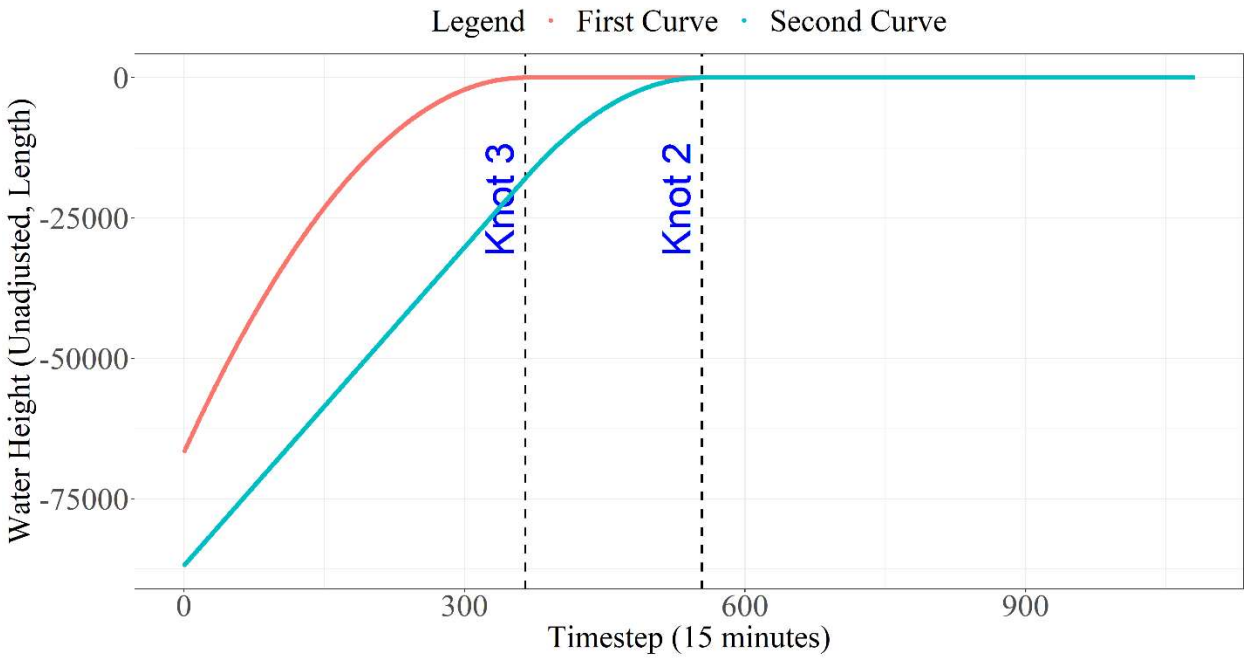

Figure 33: Second knot characteristic curve, UNH A-Lot

Figure 34 shows the third characteristic curve, representative of the height of the hydrograph attributable to infiltration through the sides and the bottom of the lowest soil layer, as well as the first and second characteristic curves, included for reference. It is worth noting that in order to get the parabolic section of this curve to flatten out to zero on the right side of the graph, an estimation needs to be taken of when the trench is completely empty. In order to estimate the approximate time when the trench is empty, a linear regression is used with the series of points close to a height of 0 feet. The time-intercept from the regression is then used as the "empty point." For the third characteristic curve, the empty point is used as the location where the parabolic section of the graph flattens out to zero.

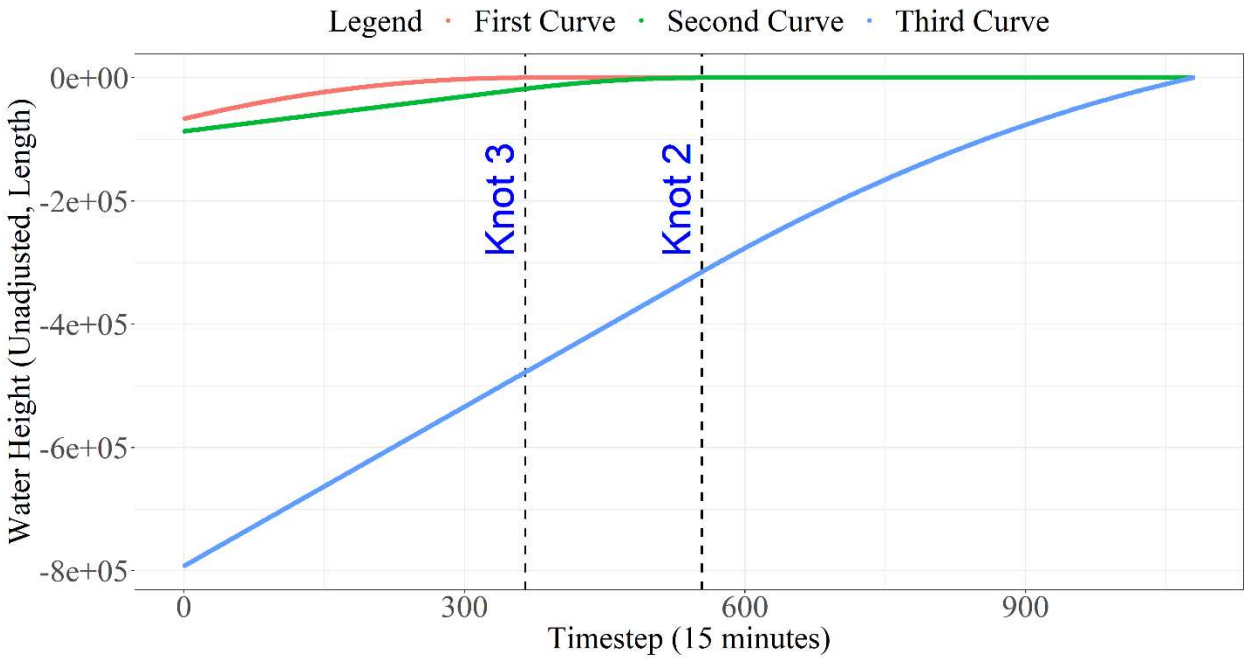

Figure 34: Third knot characteristic curve, UNH A-Lot

Figure 35 shows the fitted curves over the ideal storm hydrograph. This graph was formed around observable characteristics within the hydrograph through the use of the spline equations, but not with the use of any soil parameters. Note that the knot position that was not

identified from earlier (the one at 0.6 feet) is the cause of the greatest variance between the complete model ("All layers" on the graph) and the observed hydrograph ("Water Height in Trench" on the graph). Also note that an extra layer was installed in the linear regression model, here called "Cubic Fitting Variable." That cubic fitting variable was included to help keep the function one-to-one (one explanatory value for every response value, and vice versa), in the event a problem with the fitting resulted in the final curve veering upwards slightly at the end. Because the end of the hydrograph is so level, slight variances in the data could potentially lead to the lowest layer having a positive slope, which would not be conducive to a realistic simulation, so the cubic variable was added to preserve the "one-to-oneness" of the graph, taking advantage of cubic functions' similarities to a hydrograph. Unfortunately, the correlation of the cubic variable to a real life scenario is tenuous at best, as it was created by systematically testing polynomial fittings ranging from orders 1 to 5. The variable is more of a safety measure to ensure the process works smoothly, and as is seen on the final graph, is a minor contributor to the performance of the model in this case. The additional layers in the graph are representative of the calculated infiltration resultant from each specified soil layer in the trench. For example, if the soil has three layers of stratification, the "Layer Below Knot 3" graph can be used to describe the water stage decrease due to combined infiltration of the middle layer and the bottom layer of soil. The "Layer Below Knot 2" graph describes stage decrease from infiltration in the bottom layer of soil. Vertical infiltration is difficult to separate from horizontal infiltration right on the graph of knot 2, but horizontal infiltration at that stage would be negligible, due to the low side-surface area of that layer of soil. Included on the graph are two horizontal lines, representing the estimated soil horizons predicted by the two knots. Note that one of the estimated horizons is at only 0.06 feet, which is barely distinguishable from zero feet on the graph.

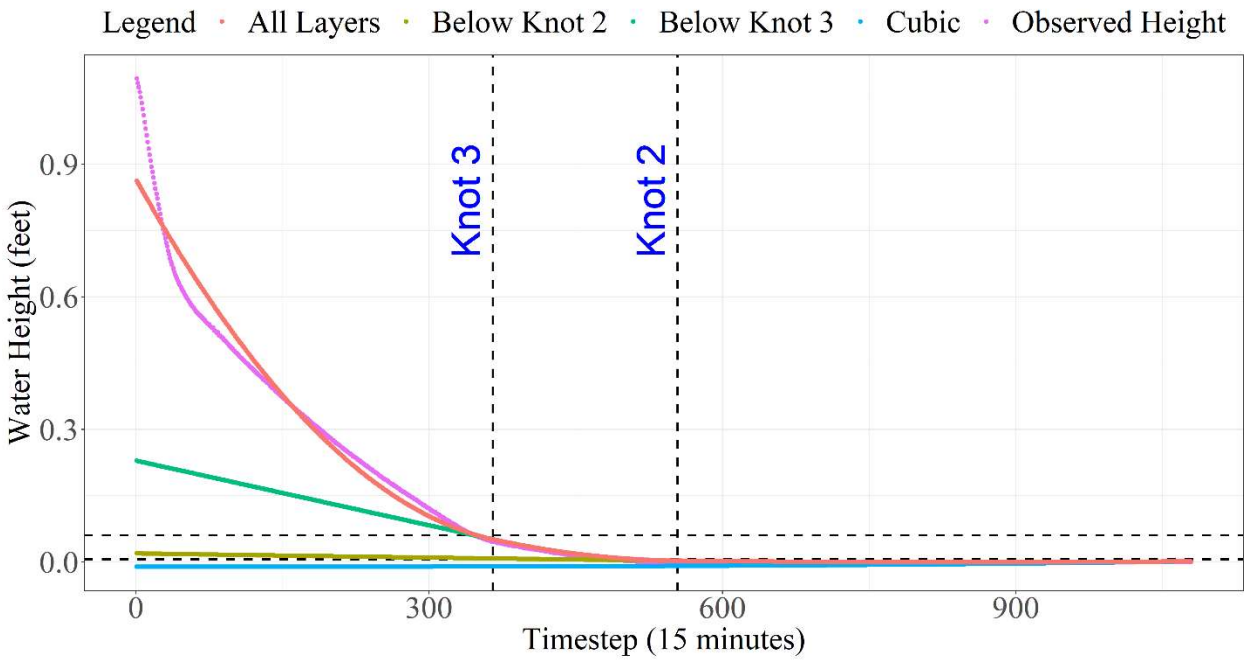

Figure 35: Practice storm fitting, A-Lot

Figure 36 shows the derivative of the results from Figure 35. Note that the cubic spline does not appear in the figure, as the cubic spline had either zero or slightly negative values that would place it outside the log scale used for the y-axis. The results appear to match very closely to the observed data, though at the low end of the scale, the observed data quickly loses resolution.

I. Hydrograph Consolidation and Knot Tuning

Once the splines have been created, the knots k and m have been initialized, and the first linear regression test has been run with the manually selected hydrograph, the knots as well as the linear regression can be finely tuned with the addition of subsequent storm data. This is done through an iterative process described in this section and the EARTH package. The purpose of this section is to explain how to set up the master hydrograph so as to overlap all storm hydrographs with each other in a logical manner.

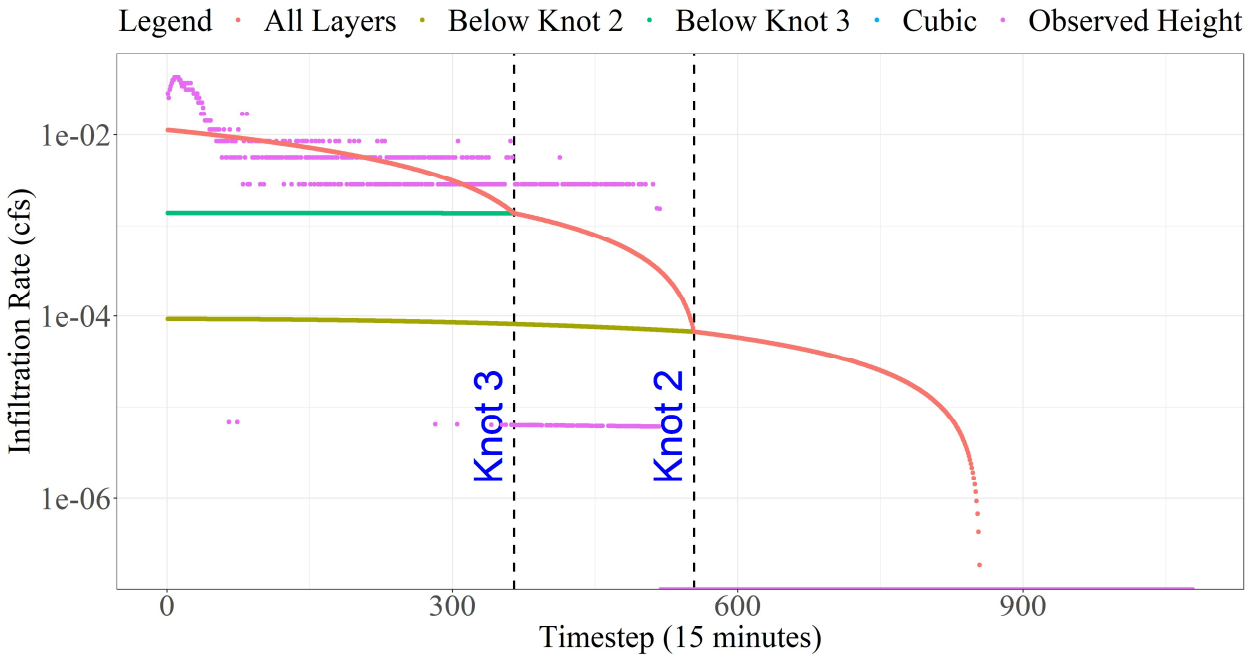

Figure 36: Infiltration rates from practice storm fitting, A-Lot

First, all storms must have the three relevant columns of data, the height of water in the trench, a column marking the numbered timestep in the storm, and a column with the number of the storm itself. The number itself is not necessarily relevant in this case, but the ability to distinguish between separate events is relevant.

A prediction of the linear regression results must be computed for comparison. To form the regression results, a vector containing a range of consecutive integers, representative of a floating time scale is created of greater quantity than the number of observations of the original selected hydrograph. In the case of this thesis, the vector created listed the range of numbers from 1 to 20,000 15-minute timesteps. The range must include extrapolation beyond the range of the original selected hydrograph, as the intended master hydrograph will be matched against hydrographs outside the original selected hydrograph's height range. The master hydrograph was formed by shifting the regression from Figure 35 to the middle of the 20,000 point time scale, and extrapolating the results at both ends with respect to time. The left end extrapolation is

expected to have accuracy issues at height values above the top of the trench, but any instances where the trench is flooded above the top can be considered a failure condition outside the scope of this research.

Figure 37 shows a section of the "master hydrograph." The master curve is meant to predict the behavior of a trench hydrograph at any particular height. The ideal storm from earlier does not need to contain the most extreme values expected from a trench, as those values should be interpolated automatically, and adjusted by EARTH when storms are consolidated. Since the graph in Figure 37 is strictly being used as a reference curve, this graph would not be used as a final result, but more like a lookup table for estimated hydrograph curves.

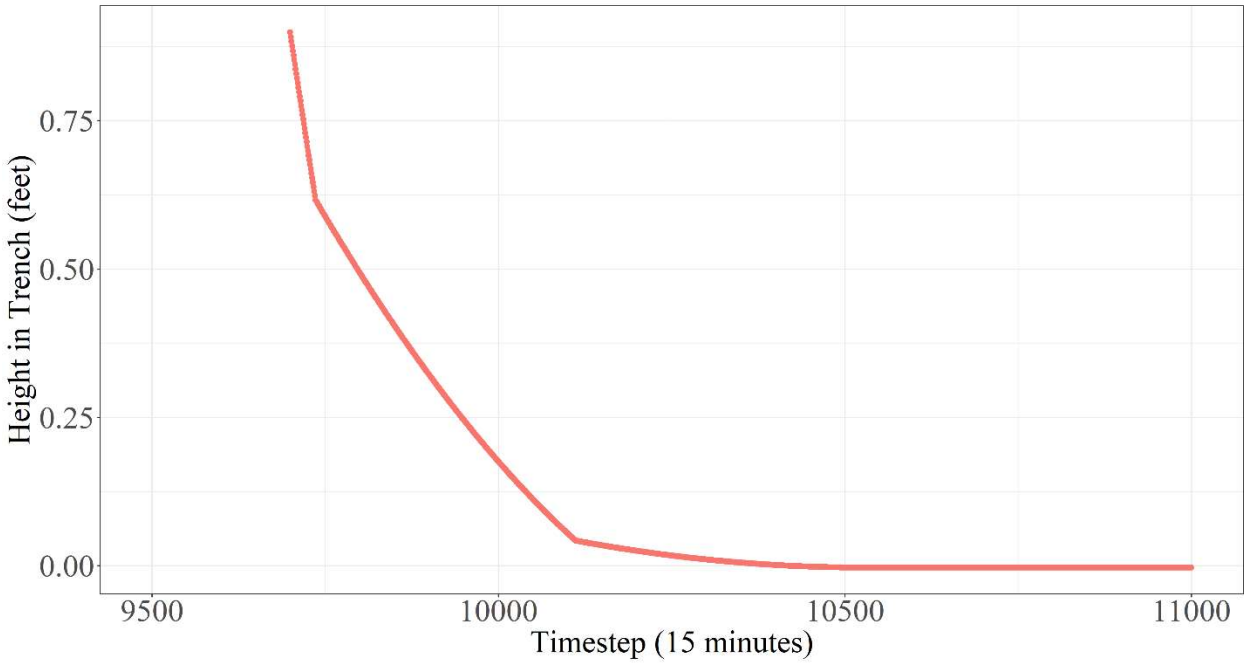

Figure 37: Master curve after adjustment iteration 8, UNH A-Lot

Figure 37 makes mention of "Iteration 8" because the graph was formed from multiple regressions in iterative fashion. The first iteration of the master curve was derived from the original regression, the "All Layers" curve made earlier in Figure 35. Then all individual storm

hydrographs were aggregated, pieced together by matching the hydrographs' respective first points (their peaks) to the appropriate time step on the master curve. Then the EARTH analysis was run again with all storms consolidated together. That new EARTH regression would become the new master curve, storms were realigned to the new master curve, and the process would begin again.

The first points of each storm following the peak were left in the analysis, despite the knowledge they contained residual inflow. This did not prove problematic for the method since the time of concentration for the lot is only six minutes, and the data points are each representative of a 15-minute time step.

Recall that all the storms were placed on the same graph with the natural numbers set. The first value of every storm hydrograph (also the highest point) will be checked against the master hydrograph. If the first height value of a storm hydrograph is lower than the master hydrograph height at their corresponding timestep values, then that storm's timestep values will be shifted upwards until their heights match. If the height value of the storm hydrograph is lower than the master hydrograph height when matching timesteps, then that storm's timestep values will be shifted downwards until the storm's first value matches the height of the master hydrograph at the corresponding time step value. That process is repeated for every storm until all storms are lined up with the master hydrograph results. The time axis of the master curve is floating, it can be any value provided timesteps and heights are consistent relative to one another.

Figure 38 shows the predicted model compared to the entirety of the dataset. Figure 38 shows the results of overlapping 87 water height hydrographs (n=40,363). The regression model used for the entire dataset was an EARTH model, an open source version of Multiple Adaptive Regression Splines (MARS). The EARTH model is used to create the minimal number of knots

necessary to estimate the outflow curve. In that manner, EARTH can be used to determine the number of layers of stratification in a trench's profile. As is seen in Figure 37, EARTH determined there was stratification at the approximate heights in the trench determined earlier (stages of 0.6 feet and 0.06 feet). Additionally, EARTH determined there was a layer of stratification at height 1.1 feet in the trench. That stratification is less evident in the dataset, due to smoother transitions between sections. Lines are depicted on Figure 38 showing the approximate location of all soil horizons, as estimated by EARTH.

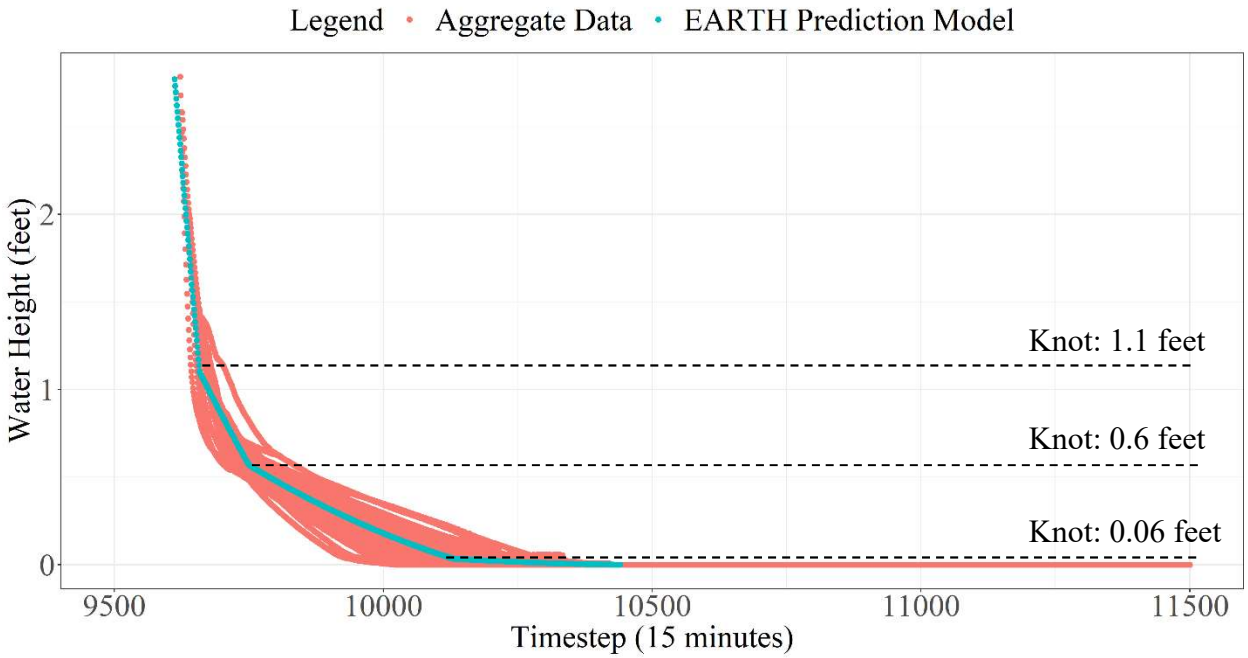

Figure 38: Comparison of adjusted aggregate data to EARTH model, UNH A-Lot

Figure 39 shows the model produced by the EARTH regression. The results are organized in a similar fashion to those of Figure 26. The variable "zeroCount1" was a second order polynomial spline that extends upwards preceding the estimated location where the hydrograph hits a height of zero, resembling Figure 32 earlier on in this thesis, but levelling off

at the estimated empty point of the hydrograph. Because the spline used as an input for EARTH was partially a second order polynomial, the numbers represented in the maximum function used by earth are of extreme magnitudes, meaning the value comparison (like 172,225 in the first spline) was large, and the coefficients used to adjust the magnitude of the spline (like $9.47*10^{-7}$) will be small.

```
0.1330999
+ 9.474485e-07 * h(zeroCount1-172225)
- 2.142807e-07 * h(632025-zeroCount1)
+ 2.497939e-06 * h(zeroCount1-632025)
+ 1.648321e-05 * h(zeroCount1-786769)
```

Figure 39: EARTH model for master curve

For this particular model, the R-Squared was 0.9413, the Generalized R-Squared was .9410, the Residual Sum of Squares was 141.57 from the number of observations n=40,363. While what qualifies as a good fit is subjective and often dependent on not only the level of error but the shape and repeatability of the data, the high R-Squared value would suggest the model is a good fit, and the large number of observations would suggest the model has high accuracy.

Figures 40 and 41 show the number of knots used versus the resultant best fitted R-Squared value, and the residuals versus the predicted height of water in the trench, respectively. Note that the difference between R-Squared values (RSq, obscured by GRSq in the graph) is not very large, from 0.89 to 0.94, meaning that most of the variance in the dataset can be predicted with one knot, presumably a steep downwards spline and a shallow downwards spline. The GRSq is identical to the R-Squared values because there was no validation data used in this case. The GRSq line describes how the number of splines used in the model affects the model's

generalized R-Squared value. There is only one predictor variable used for “NBR Preds” (time), so EARTH’s capacity for selecting variables is not utilized.

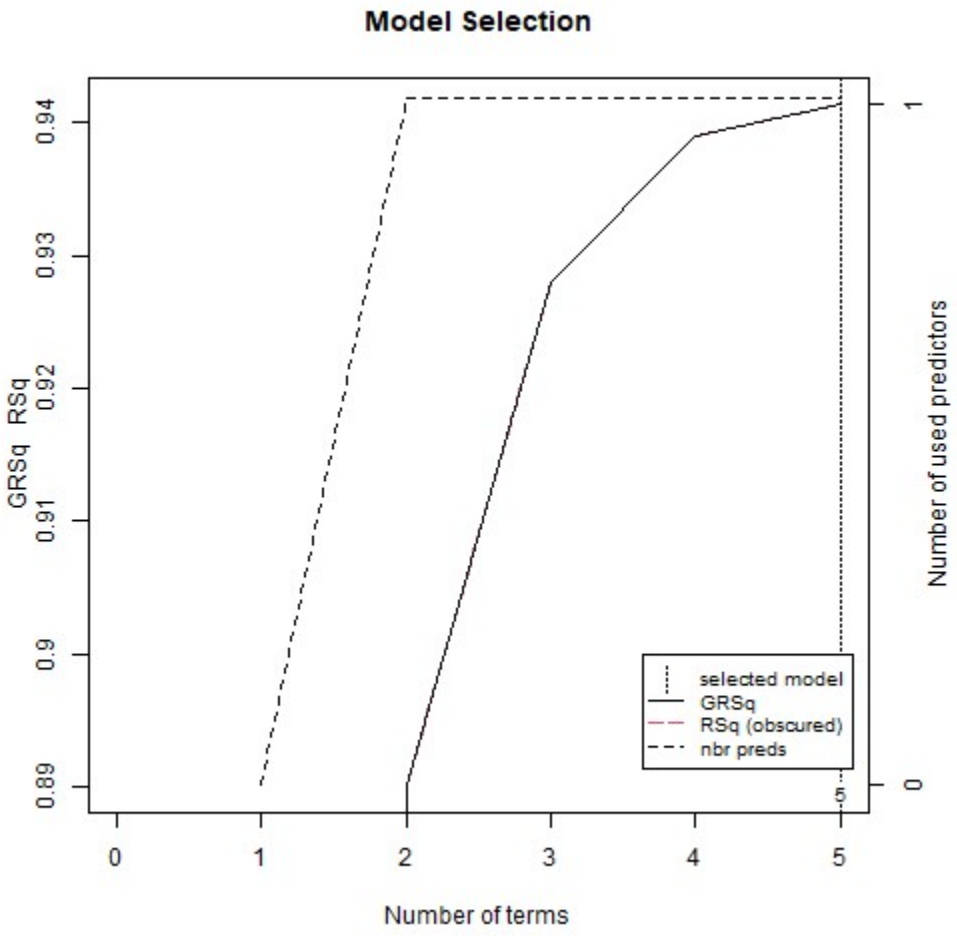

Figure 40: EARTH model selection, UNH A-Lot

Figure 41 compares the fitted hydrograph peak depths (in terms of feet of water under the “fitted” axis), against the residual errors (the difference between observed values and predicted values, in terms of feet of water on the “Residuals” axis). While the higher predicted values have the most variance (which is to be expected since there is significantly less data to describe the higher values), most of the variance is explained by the lower predicted values. That can be seen in Figure 38, where the graph is thickest around the 0.06 ft to 0.6 ft height range. That variance is

most easily described as a difference of slopes in that height range between separate storms. The cause of the variance is unknown but guesses as to the cause might include a change in performance over the lifespan of the trench, error from the drift correction, inflow into the system, and seasonal effects. Note the presence of an outlier storm between -0.6 and -0.4 feet on the residuals axis. Such an outlier is likely due to the minimal data of higher hydrograph heights.

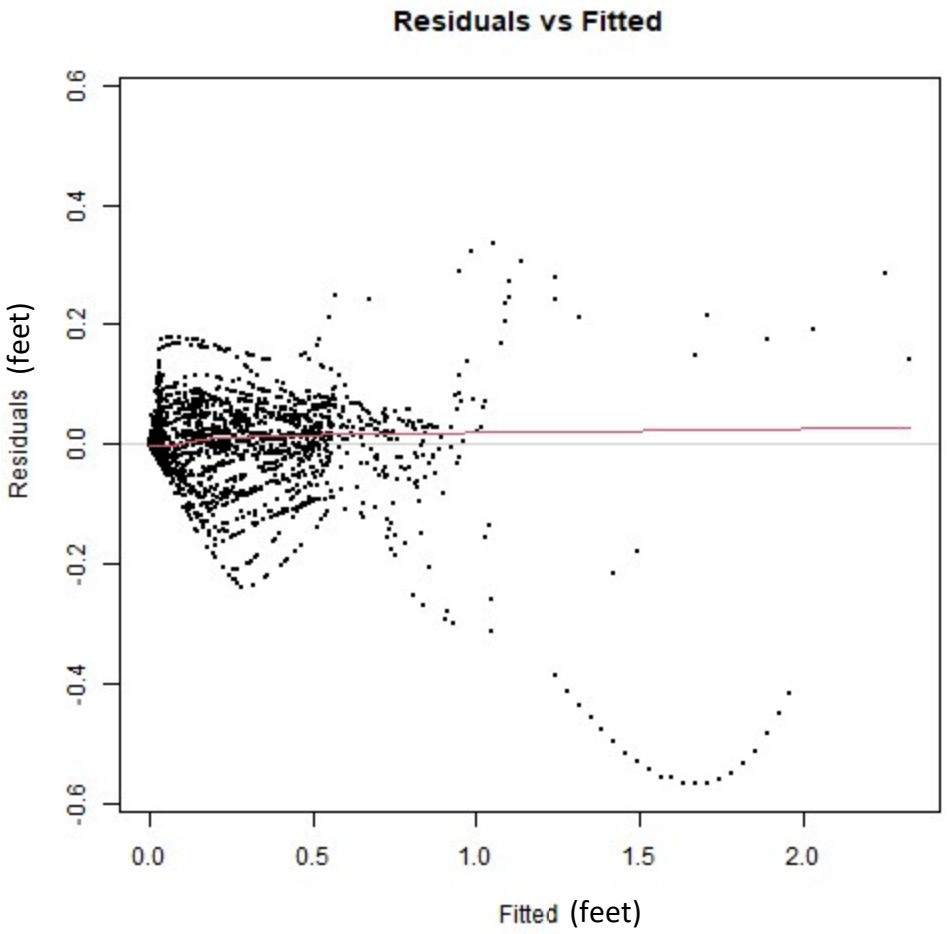

Figure 41: Trench height EARTH residuals (ft) versus fitted trench height values (ft), UNH A-Lot

Figure 42 shows the R-squared performance of the predicted height versus the actual height of water in the gravel trench. Note that there are multiple curved humps on the upper half

of the R-squared line (particularly the curve in the 1.2-2.0 foot fitted range). Those humps indicate a problem with the fit used. The problem with the fit is that a continuous second order line was used in conjunction with the Earth model, instead of the multiple curvilinear segments used for modelling the "ideal" storm hydrograph earlier in the process. As a result, the curve used for modelling in EARTH (Figure 38) was not ideal to properly display the qualities of the trench. A solution to this problem might be to use EARTH to predict the knot locations, and then implement the splines from the "ideal" model for the final model, provided that the "ideal" model is correct. RMSE is in feet.

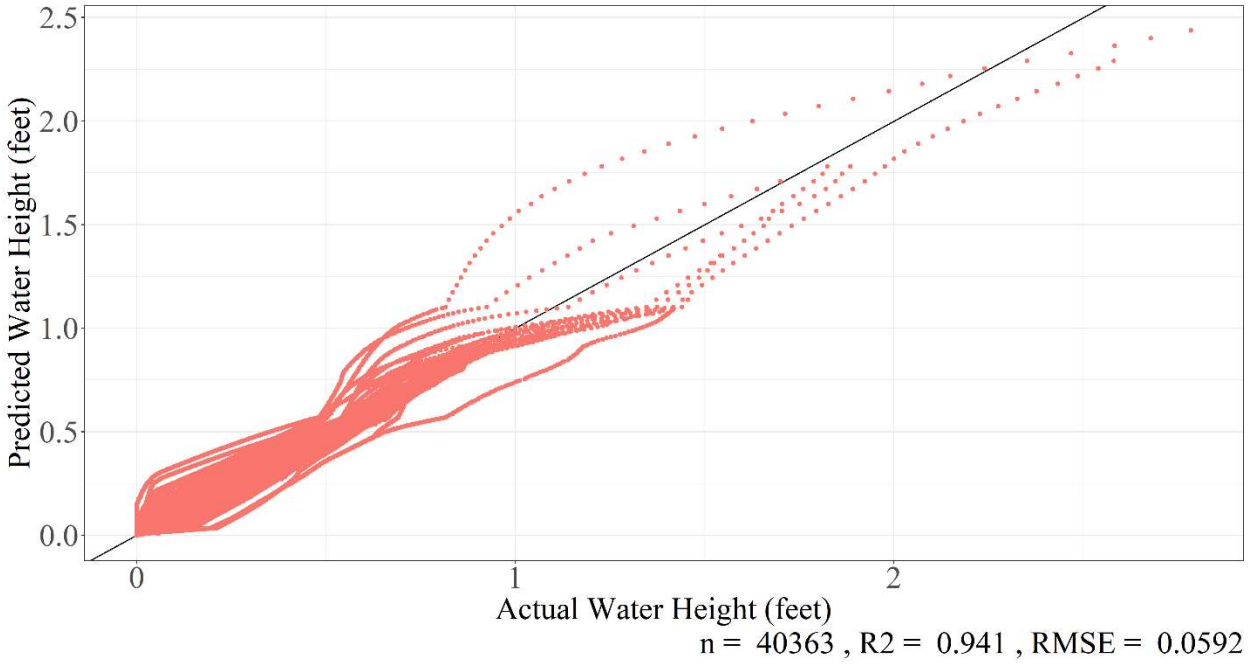

Figure 42: Predicted versus observed water height in trench, UNH A-Lot

RESULTS

1. Recreating Original Data with Model

Once the final master hydrograph curve is created, it can be used in conjunction with the predicted storm heights to recreate the entirety of the original height hydrograph data. The purpose of recreating the data is to juxtapose the predicted components of the hydrograph against the observed data to see any systemic errors within the predictions. This section will briefly review the components of both the original data and the predictive process, then will discuss the process to replicate the original data using the predictive process.

The original data consists of three parts: timestamps, rain gauge data, and water height gauge data. Recall that the water height gauge represents the height of water in the trench at any given time and corresponds directly to the volume of water in the trench itself. The height gauge data has been corrected and trimmed in several ways to leave only the falling branches of characteristically representative storms. The corrected height gauge data can be overlayed on the original set of timestamps on one continuous vector.

The predictive process has three components: trench peak magnitude prediction, trench peak temporal prediction, and the master hydrograph regression curve. All three components are predicted using models derived from observation data. The peak magnitude prediction predicts the peak of the hydrograph in the trench before or after the end of rainfall. The peak temporal prediction predicts the number of timesteps separating the end of rainfall and the peak of the hydrograph. If the peak occurs before the end of rainfall, then the prediction defaults to one timestep after the end of rainfall. Starting the peak of the storm following rainfall would be consistent with the design approach, since peaks that occurred during rainfall were cut off in the

“peak detection” phase of editing the data. The master hydrograph curve is considered to contain all states of height within the trench as is possible with the pre-existing data. The y-axis of the recession curve describes the height of water in the trench. The x-axis of the recession curve is treated as a floating time variable. All consecutive points on the x-axis are 15 minutes apart, but no point has a specific time stamp tied to it. The recession curve's importance is in how different heights of water in the trench relate to each other over time. Note that in the creation of each the trench peak magnitude predictors, trench peak temporal predictors, and the regression curve, all the original data is required for the process, but once the predictors are created, only the timestamps and rain gauge data are required for the predictive process. Timestamps and rain gauge data can be created to predict how the system will react in particular circumstances, or the original timestamps and rain gauge data can be used with the predictors to estimate the accuracy and precision of the predictions against the original dataset.

The process to take timestamps and rain gauge data and turn it into trench water height prediction data using the predictive elements is as follows:

1) Discretize the rain gauge data into individual storms. The process for converting rain data into individual storms can be found in the "Storms" chapter.

2) Run each individual storm rainfall event through the trench peak magnitude and trench peak temporal regression equations. This thesis used 20 hours worth of lagged data in EARTH, but alternate setups can use longer time periods in consideration of longer storms. Once the setup of the data is complete, each regression can be run with the time series variables to predict both the peak magnitude and peak temporal locations for each storm.

3) Once the hydrograph peaks are estimated, then the master regression curve can be used to predict the falling limb of each storm's hydrograph.

The master regression curve is matched to the estimated peak heights. Any timesteps on the master hydrograph preceding the predicted peak are not considered when recording the results of the predicted storm, while the points proceeding the estimated peak are used for the falling limb of the predicted hydrograph. One may consider any storm prediction a subsection of the entire master hydrograph. The peak results are then translated to the appropriate position on the timestamp dataset, as well as the corresponding falling hydrograph limb. Any falling limb data that extends into the temporal range of the following storm is cut off. The result is an estimation for every storm's falling limb hydrograph, with empty spots during any rainfall where inflow to the system is too significant, empty spots for any storm excluded from the analysis, and empty spots preceding the estimated temporal location of any peak. It is outside the scope of this thesis to estimate what happens during any empty periods. Once the hydrograph data is estimated, it can be compared against the original data for an R-squared estimate and any further analysis.

Figure 43 shows a selection of the dataset superimposed against the predicted data. In the presented instance, the prediction is consistently deeper than the actual performance, suggesting a consistent source of error. The increased performance, denoted by steeper water height hydrograph slopes from the observed field data, might indicate seasonal effects as March and April would have had the highest infiltration rates due to increased soil moisture resulting overall wetter spring periods. The sample was also taken from a dataset early on in the trench's productive life (data points 10000 to 15000 out of a dataset containing over 50000) which might explain an increased performance, if somehow the sidewalls were to become clogged with sediment as time went on. In a more ideal performance modelling scenario, factors like temperature, soil moisture, time of year, or even time since the trench began its productive life

could be incorporated into the model to predict what causes the change in performance. Soil moisture, temperature, and time of year incorporations could explain changes in performance due to changes in the soil's conductivity. Measuring performance over the trench's life could explain how performance of the gravel trench degrades over time, as the surrounding soils lose conductivity due to sediment. One might potentially measure those differences by separating out storm data by year, creating master curves for each year, and then comparing the results of the master curve from year to year, to see if the slope of the master curve becomes more shallow over time. Those factors, however, were beyond the scope of this project.

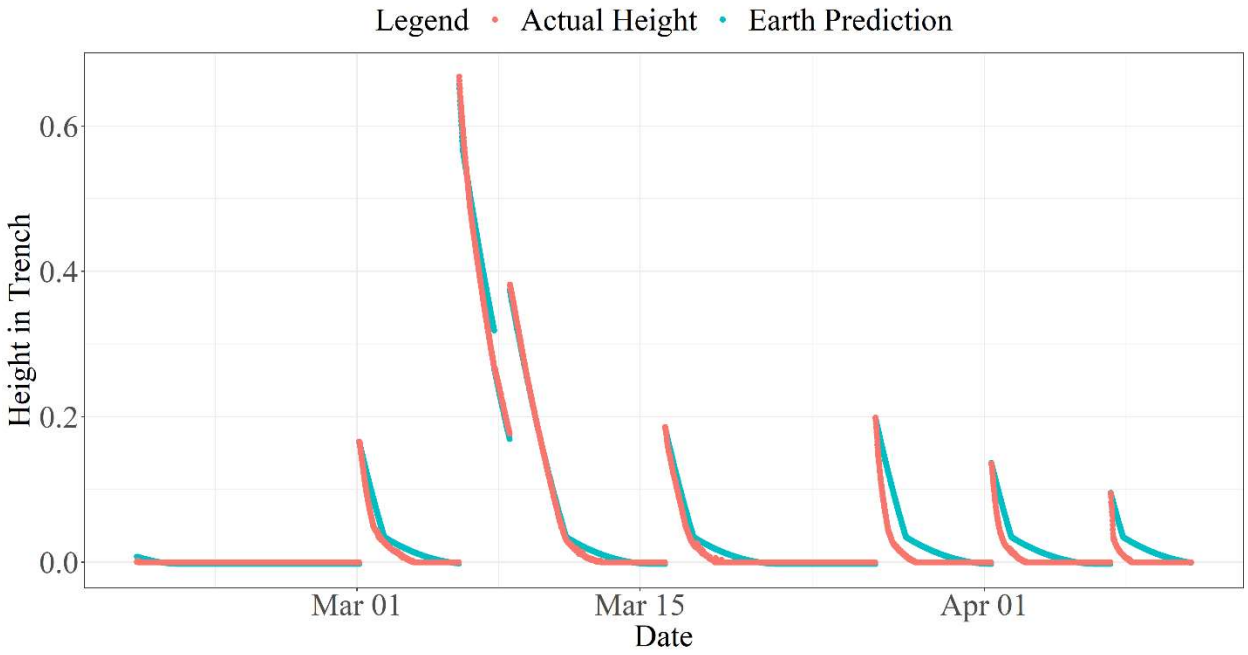

Figure 43: Comparison of EARTH to actual data, partial dataset, UNH A-Lot

Once the EARTH model has been lined up to match each individual storm, the EARTH model itself can be divided into separate hinge functions, as described in Figure 26. The most shallow hinge function describing the water level in the trench, as seen in Figure 39 was "-2.142807e-07 * h(632025-zeroCount1)." Because the function is the most shallow, reaching an

elevation of about 0.06, and by extension has the least amount of sidewall area to infiltrate, it is a fair assumption that the infiltration due to that function is almost exclusively infiltrating through the bottom of the trench. By taking the differences in height between the hinge function at the start and the end of each storm, one may estimate the amount of infiltration through the bottom of the trench. The rest of the water that exits the system is assumed to leave through the sidewalls. The amount of water that infiltrates through the sidewalls can therefore be calculated as a percentage of the total water that leaves the system. This process was done for every storm, and is displayed as a box plot in Figure 44. It should be mentioned that since the EARTH model was based on a collection of storms, it is hypothetically possible for this graph to return unrealistic values. For example, if the trench experienced poor performance with a peak at a low elevation, the total amount of infiltration might be smaller than the amount of infiltration predicted by the model. While that did not happen in this case, such an event is possible, and future results should be considered with that context in mind.

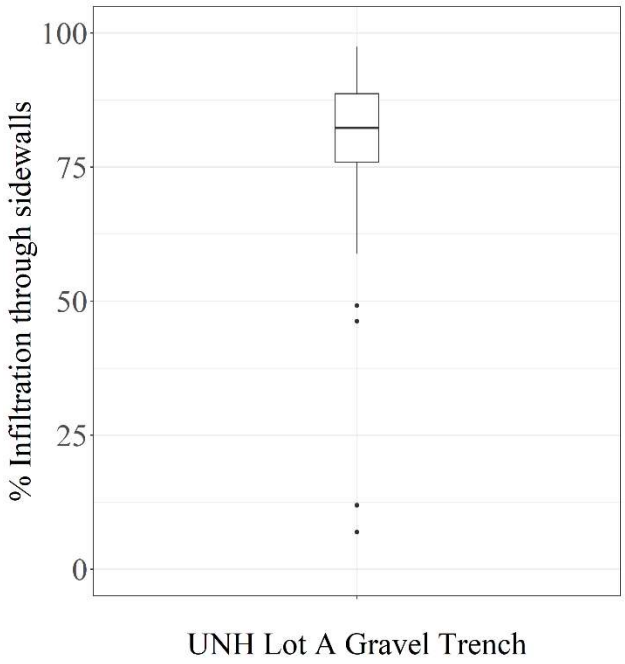

Figure 44: Sidewall infiltration as a percentage of total infiltration

The average infiltration out the sidewalls is 85.7%. The quartiles for the plot are 75.9%, 82.3%, and 88.7%. It is expected that there are outliers near the bottom of the graph, as some smaller storms may reach very low trench heights, and as such have limited access to sidewall area. The storms which received the highest percentage of infiltration through the sidewalls tended to be the storms which reached the highest water height, as they had a much higher level of sidewall area exposed to water. Since infiltration through the bottom is slower than the sides, pressure resultant from higher water depths also resulted in a higher proportion of sidewall infiltration. Since the depth of water in the trench is related to the total depth of rainfall, the percentage of sidewall infiltration can be associated with the total depth of rainfall, as is seen in Figure 45. Note that as the rainfall depth increases, the percentage of sidewall infiltration also increases. The RMSE and fit equation are in terms of percentage points, and the rainfall depth has been transformed with a log 10 function.

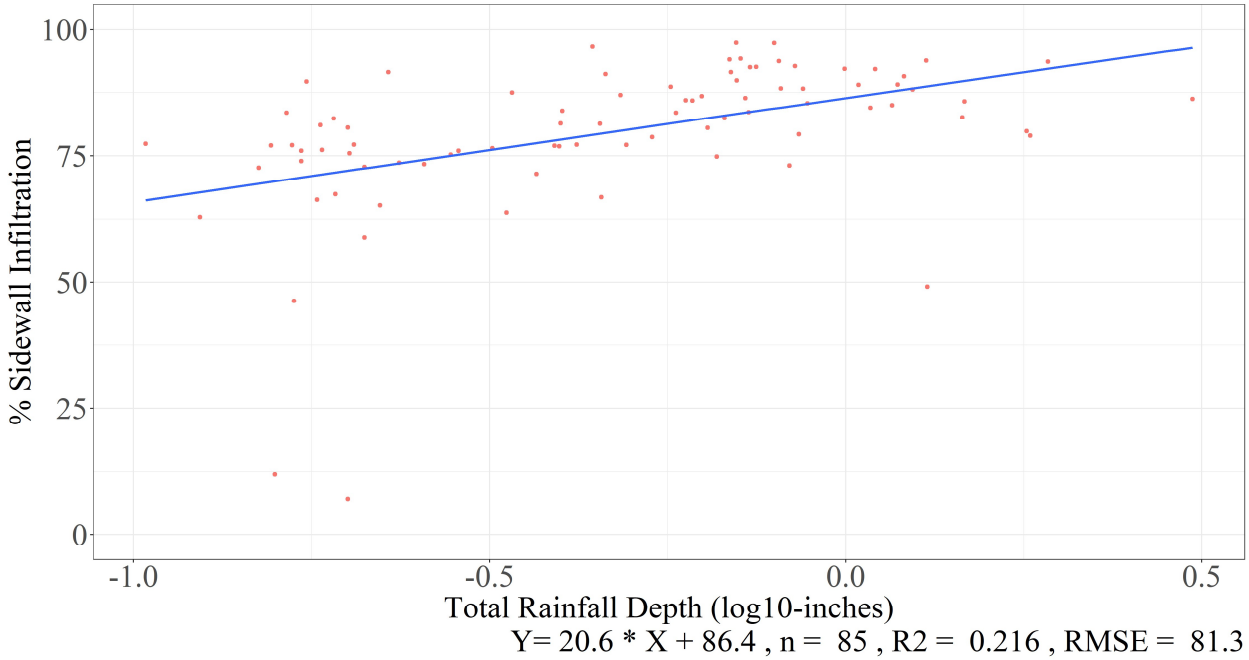

Figure 45: Rainfall depth (log10-inches) versus percent sidewall infiltration, UNH A-Lot

With the estimate of sidewall infiltration, it is worth discussing the validity of the claim that the subsurface gravel trench is an anisotropic system, in terms of the estimation process used. Before creating the model, there was already suspicion that the system was anisotropic, as the Double Ring Infiltrometer tests gave an infiltration rate on the bottom of the system close to zero inches per hour, and the trench system itself had higher performance than expected. The fact that the recession limb decelerates over time is also not unique to anisotropic systems, isotropic systems exhibit the same behavior due to the continuous loss of pressure head, so a model that predicts that the recession limb will decelerate is not sufficient evidence of anisotropy in the system. The evidence of anisotropy within the system, as demonstrated by the observed data and the EARTH model, is the significant change in deceleration (or jerk) exhibited by the data. This phenomenon is shown graphically with Figures 10 through 13 earlier in this thesis. The change in deceleration is made even more significant through the fact that it is observable across storm events, always occurring at the same water heights. If the change in performance of the system occurs consistently at specific heights, it stands to reason that the change in performance is not due to infiltration out the bottom of the system. Since the bypass out of the system was capped as well as the underdrain, the only other route for water to exit the trench which is sensitive to elevation was the sidewalls. Differences in infiltration performance out the sidewalls due to height differences would be most easily explained by soil stratification, which is definitionally an anisotropic soil profile. It is for this reason that it is believed both that the observed data shows performance attributable to anisotropy, and that the EARTH model is a sufficient method for detecting changes in performance due to anisotropy.

Figure 46 shows the EARTH predicted recession limb (combining the predicted peak height and master hydrograph) versus actual height of water in the trench. The dataset has an R-

squared of 0.79. Note the large amount of variance for lower predictions. It is assumed that the majority of the variance is attributable to the peak height prediction algorithm, which has an R-squared of 0.85, as opposed to the master curve which has an R-squared of 0.95. The peak delay prediction, despite having a very poor R-squared of 0.04, should have had a minimal effect on the overall prediction considering all it does is offset the peak by a few timesteps. RMSE is in feet.

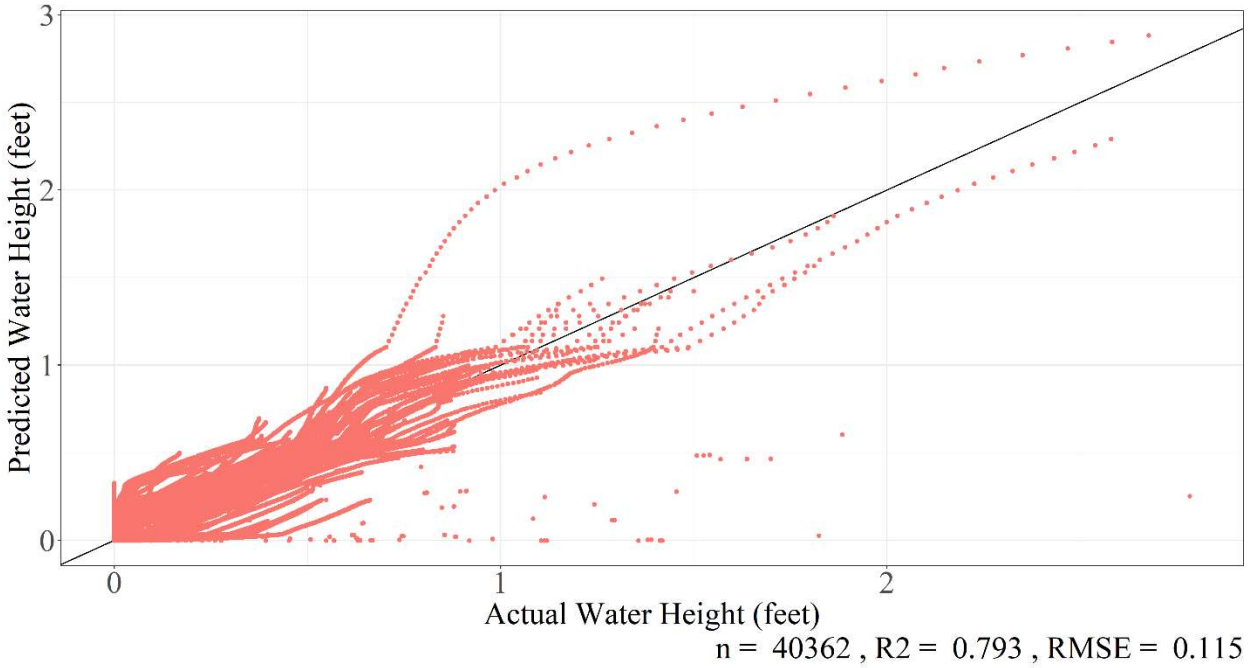

Figure 46: Synthetic hydrograph versus actual data, UNH A-Lot

Figure 47 shows a synthetic prediction hydrograph over the actual height dataset. One of the overarching goals of the project was to create a synthetic hydrograph using modelling parameters, rain data and timestamps. The peak height in trench predictions were made from a model using lagged rain data, and the master curve was created from the EARTH model. Using those, one could create a predicted hydrograph from rain gauge data and timestamps. The result is a height prediction with minimal physical connection to its real life counterpart. The results are imperfect, but closer than one might expect given its source. While there appears to be lag from

some of the storms in this graph, those storms actually do start at similar times, but the height difference is enough to make them appear off.

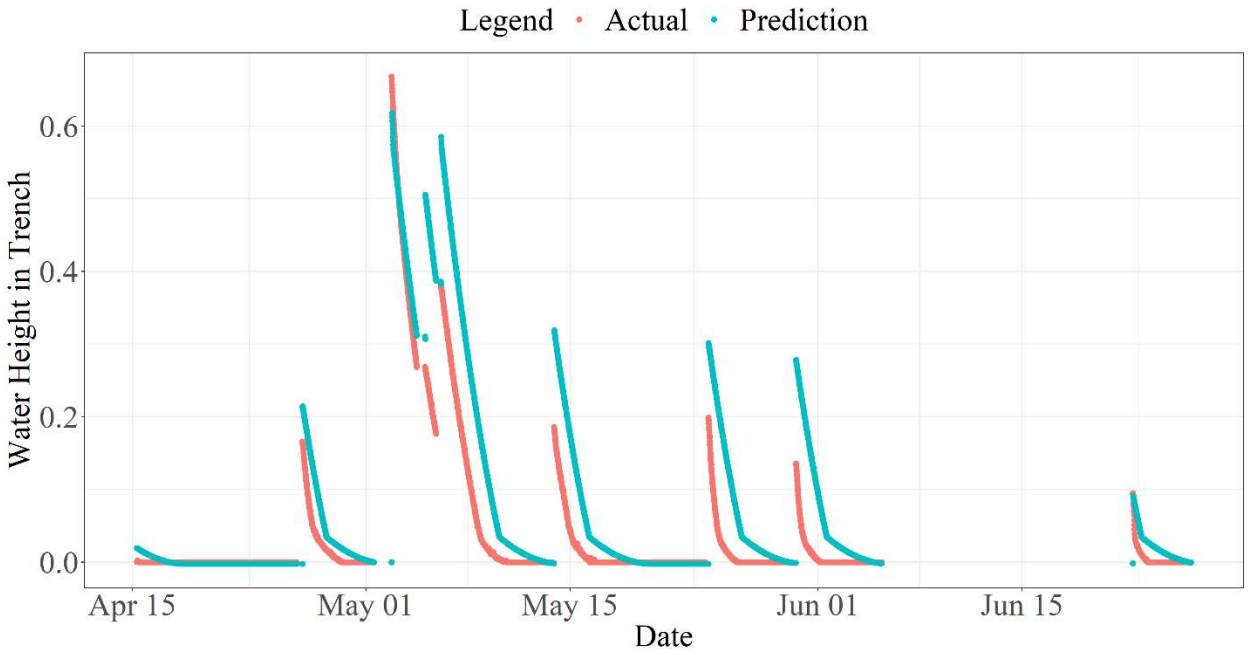

Figure 47: Synthetic and actual hydrograph of UNH A-Lot, partial dataset

Figure 48 shows the prediction curve of a synthetic 1-inch storm, which is a common design element in a static design, as opposed to the more random nature of actual rainfall . The height prediction based on the simulated burst of rainfall was around 2.1 feet in the trench, which is not far from the true expected height of about 2.4 feet, for which the trench was originally sized. The duration prediction is around 203 hours.

Figure 49 shows the infiltration rate estimates across the 1-inch storm. Each portion of the piecewise function represents the total infiltration resultant from adding soil layers up from the bottom. For example, the second section, the set of values around 0.0075 cfs , represents the summation of the infiltrations of the bottom (0 feet), second (0.01 to 0.06 feet) and third (0.06 to 0.60 feet) soil layers. In an ideal scenario, this function would be continuous, but as depicted there are clear separations between layers. Fortunately, an assumption made by this thesis is that

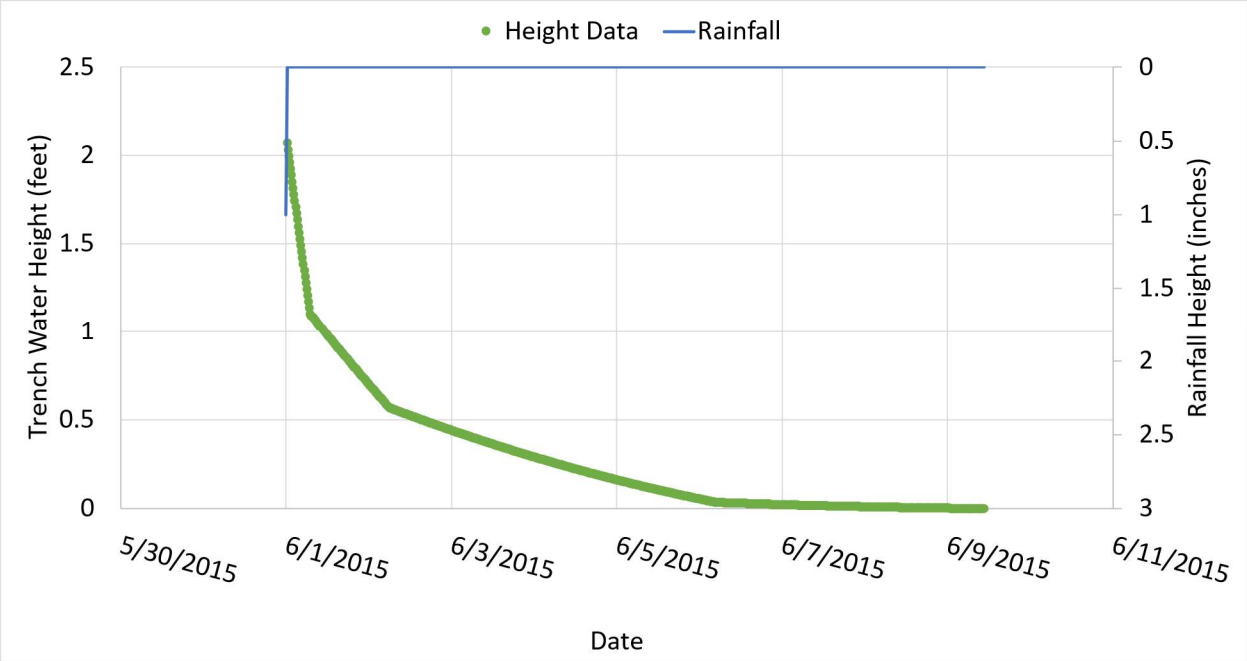

Figure 48: One-inch storm hydrograph estimation, UNH A-Lot

water infiltrating the sides of the trench does so at a constant rate, which is not accurate to reality as the increasing length of the wetting front out the sides of the trench would cause the infiltration rate to decrease over time, but is supported in modelling software such as HydroCAD (HydroCAD, 2020). HydroCAD only has functionality in support of a decreasing infiltration rate out horizontal surfaces, not vertical surfaces. Having infiltration rates in distinct stages as presented makes it easier to estimate the inputs for each layer. Note the exceptionally high level of the highest presented infiltration value, at over 0.04 cfs. Remember that this value represents an average infiltration rate over the height of the trench, and not an infiltration rate for any individual layer, because Figure 49 is a derivative of the complete hydrograph of Figure 48. Also note that the infiltration rate decreases over time, instead of being multiple constant values. The slope in infiltration segments is due to the decreasing height of water in the trench. Since the higher levels have higher aggregate conductivity, then as the water level rises a greater

proportion of higher conductivity surface area is exposed to the water in the trench, resulting in a higher aggregate conductivity.

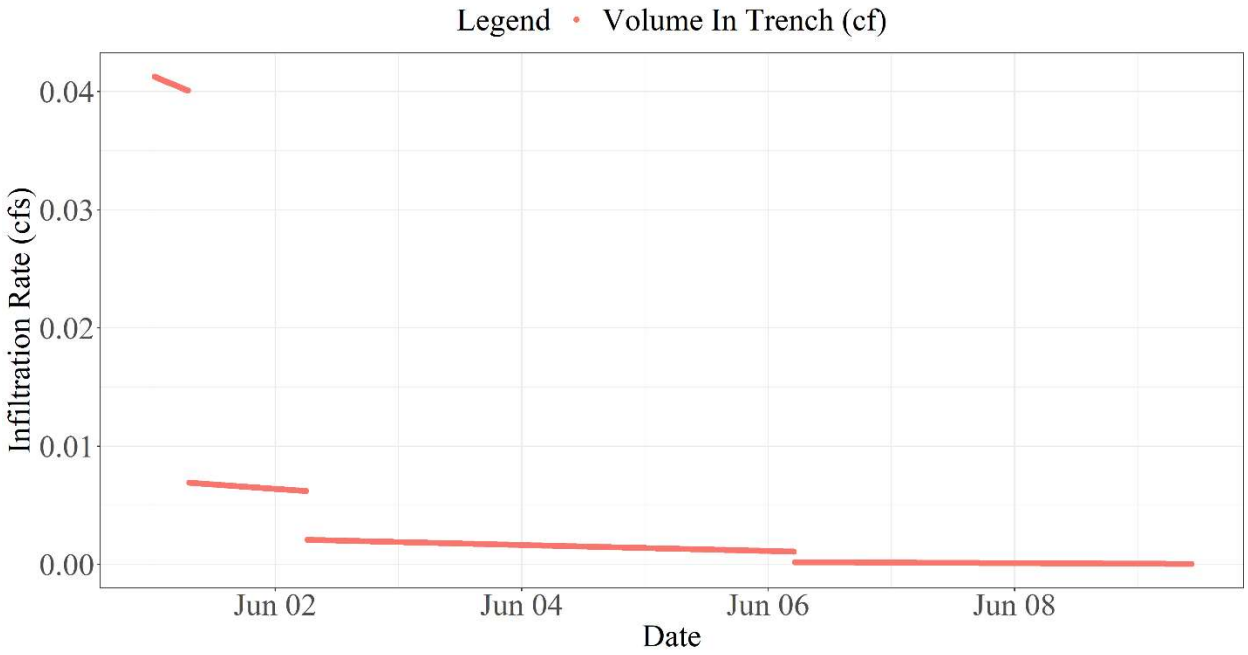

Figure 49: One-inch storm hydrograph system average infiltration rate, UNH A-Lot

Figure 50 shows the average infiltration rate when compared directly to elevation in the gravel trench. Note the bottom infiltration rate is near the start of the graph, where the elevation in the trench is zero.

Infiltration rates were derived from the data in Figure 50 by taking the average height of each plateau. Each plateau is representative of a layer of soil exposed to water, in addition to all soil layers beneath it. While Figure 50 is not well representative of the actual infiltration rates of the trench, as such a graph would be continuous, the well-defined plateaus can be used for estimations of infiltration rates. Equation 13 shows a method for turning aggregate infiltration rates into infiltration rates specific to each layer.

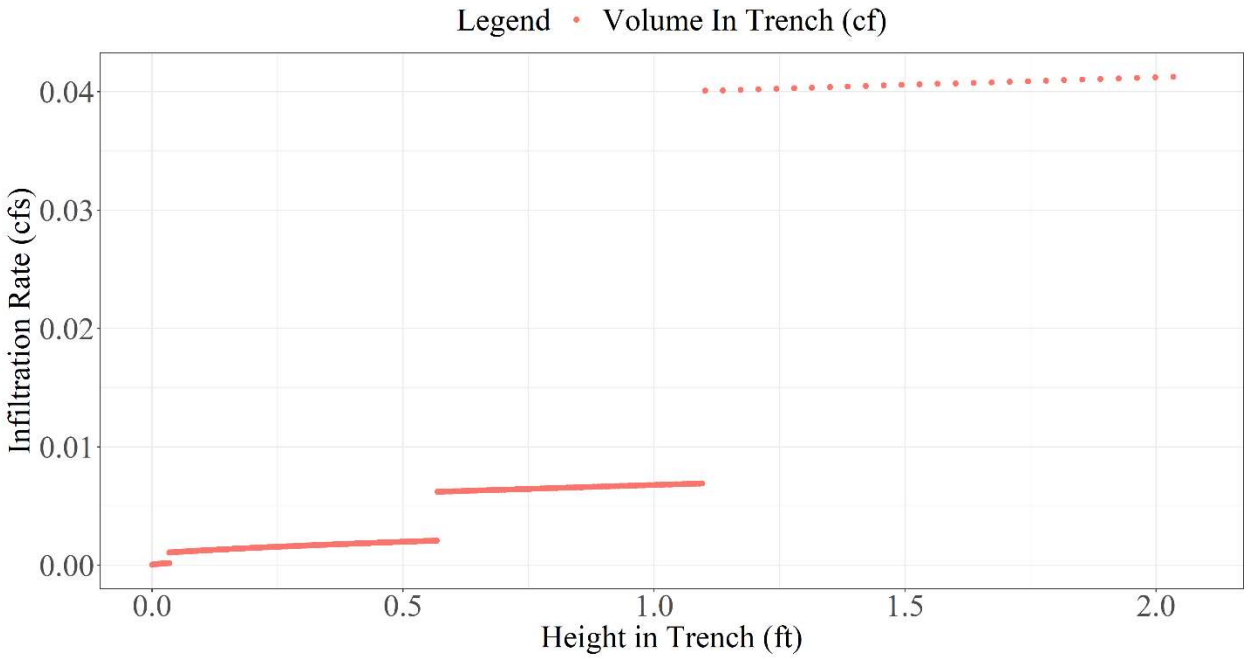

Figure 50: Height in gravel trench vs. system average infiltration rate, UNH A-Lot

Unfortunately, the modelling method chosen does not separate the infiltration out the bottom of the trench from infiltration out the bottom layer in the trench, as the slopes of water height around calculated knot positions determine how each layer is teased out. Since there is no knot that separates the horizonal plane from the vertical one, the bottom horizontal layer is consolidated with vertical flow. In order to tease out the difference between infiltration through the bottom of the trench, and infiltration through the bottom layer of soil surrounding the trench, a HydroCAD model was implemented to mimic the infiltration performance of the design storm, adjusting the rate of infiltration out the bottom of the trench to best simulate the duration the trench takes to empty completely. This was accomplished by using the average infiltration rate component for the sidewalls of the lowest layer (which was less than 0.05 feet high, so it contributed next to nothing), and then performing a trial and error process for the infiltration rate out the bottom of the trench until a satisfactory drainage time that matched with the synthetic one-inch hydrograph was produced. This guess and check system was not difficult, because

matching closely with the infiltration rates produced by the double ring infiltrometer, the rate of infiltration out the bottom was between 0.001 and 0.000 inches per hour, the lowest possible values for infiltration produced by HydroCAD. Because having no infiltration out the bottom would effectively prevent the trench from ever emptying, a value of 0.001 inches per hour was used. Table 1 displays infiltration values calculated by taking the information from Figure 50 and calculating the contribution of each layer using the following equation (with the HydroCAD model being used to estimate the bottom velocity):

Equation 13: $I = (q_2-q_1)/((h_2-h_1)*Perim)$

I = The infiltration rate of a soil layer

q = The aggregate infiltration rate for a given soil horizon (L^3/T)

h = The top and bottom horizon elevations of a soil layer (L)

Perim = The perimeter of the trench (L)

Table 2: Infiltration rate profile of Lot-A subsurface gravel trench estimated from HydroCAD

Height of Soil Layer from Bottom of Trench (feet)	Estimated Infiltration Rate (inches/hour)
Bottom of trench (0 feet)	0.001
0.01 to 0.06	0.150
0.06 to 0.60	2.970
0.60 to 1.10	10.830
1.10 to 2.40 (top)	124.40

The results from an infiltration rate profile like this could be incorporated into a HydroCAD model in the design process when looking to ensure a proposed trench drains within the 72 hour time frame specified by the NH Stormwater manual, if the state allowed sidewall infiltration in the design process. A HydroCAD model can incorporate lateral infiltration through the sidewalls of the trench by specifying in the infiltration options that the wetted area be used for infiltration. Since the wetted area changes over time, the HydroCAD model is also sensitive to the amount of sidewall area exposed to water in the trench. Additionally, one may specify in HydroCAD that infiltration can only take place above and below specific elevations, allowing the user to create multiple infiltration parameters, each specifying a specific layer through which infiltration can take place. Included in appendix E is the HydroCAD results for the 1-inch storm and the 1-year storm, both of which the trench passed without flooding the system. Additionally, the HydroCAD analysis includes results for the same system if only vertical infiltration were considered, using the highest double ring infiltrometer vertical infiltration rate measured in the field, for comparison. Figure 51 shows the results of the trench with only constant infiltration out the bottom of the trench (0.05 cfs), while Figure 52 shows the results of constant infiltration out the bottom and the calculated rates for the layered infiltration in sides of the trench. Both Figures use a storm with one inch of produced runoff.

Since inflow into the system was identical in both cases, both reach a peak inflow of 0.90 cfs. The distinction between infiltration results is immediate. Infiltration through the sides of the trench in the model seemed to decrease the detention time from over 200 hours to around 110. The graphs do not display the results for the sidewall infiltration well, as from 65 to 110 hours, the trench does not appear to be infiltrating at all, but the trench is infiltrating very slowly. Infiltration rates from the model utilizing sidewall infiltration reached 0.11 cfs while the

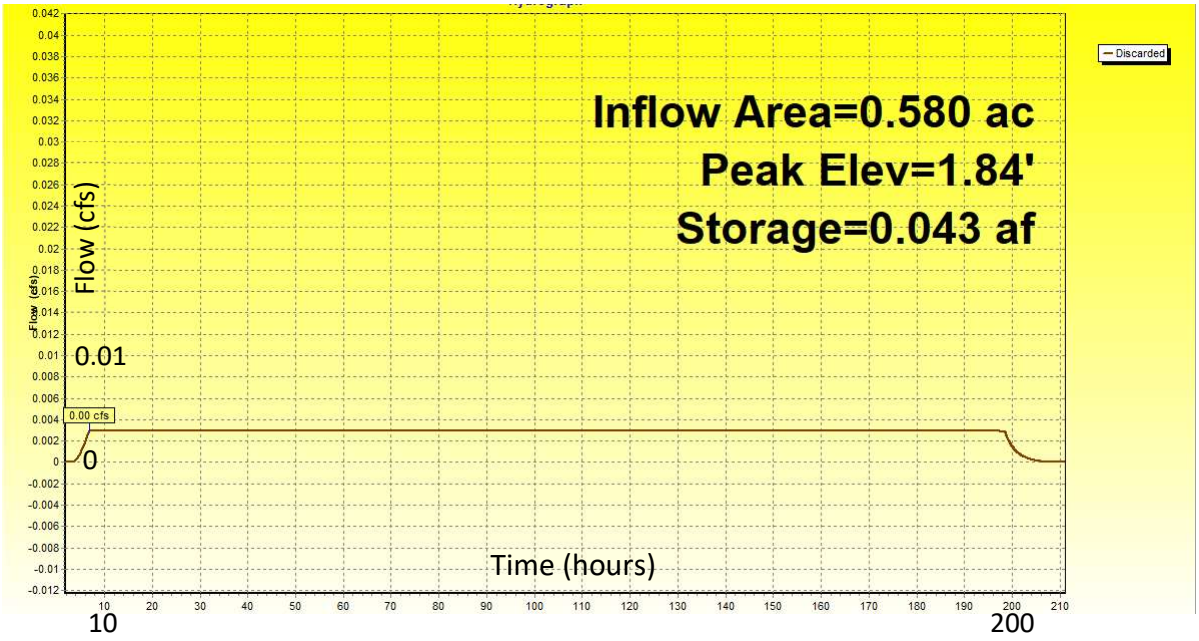

Figure 51: HydroCAD infiltration through bottom of gravel trench, A-Lot

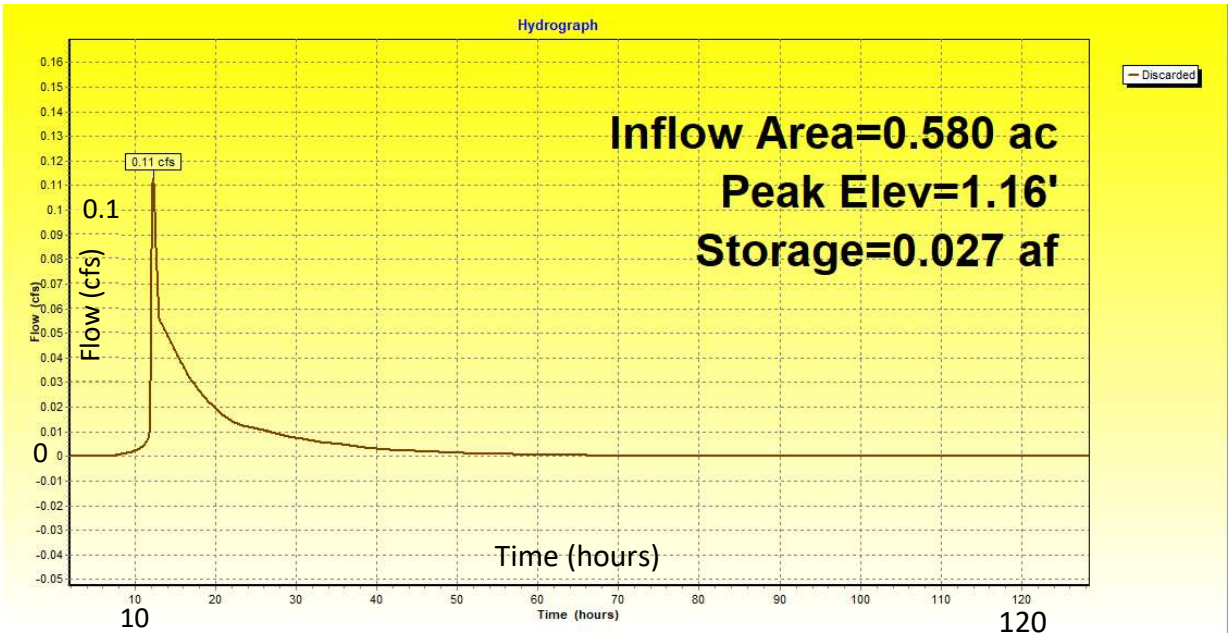

Figure 52: HydroCAD infiltration through bottom and sides of gravel trench, A-Lot

bottom infiltration did not register above 0.00 cfs. The result of side infiltration matches somewhat to the observed data, as at one point a 0.884 inch storm took six days to infiltrate completely in the trench. In terms of the continuity equation, low elevations of water in the trench may not have a large impact on the performance of the system, as any storage it removes

for future storm runoff may be compensated by additional infiltration capacity from the higher water stage in the trench. However, there may be practical disadvantages to having standing water in a gravel trench for extended periods, such as creating a breeding ground for insects. Additionally, the estimation of sidewall infiltration might be too vigorous as predicted by Table 2, as the trench only reaches a height of 1.16 feet, where the statically sized model predicted the trench would fill up to the design height of 2.4 feet. The estimation coincided much better with the observed data, however, which showed the trench fills to 1.1 feet with a 0.88 inch storm. The trench does fill up more with greater intensity storms, as well.

In regards to this thesis's hypothesis, the objective of this thesis was to determine through an explanatory model if sidewall infiltration could explain subsurface gravel trench performance that vertical infiltration could not by itself. The results of the methodology presented here show promise toward that end, but are ultimately imperfect for a number of reasons. Sidewall infiltration was modelled as a constant value, which in reality would tend toward zero as the wetting front out the side walls increases, but a constant infiltration value allows HydroCAD to model infiltration through the sidewalls. Additional points should have been removed from the beginning of each hydrograph to completely eliminate inflow into the system, and there is doubt as to how much inaccuracy that introduced to the results. The modelling technique for creating the master hydrograph may have been done backwards, as EARTH would have been far better suited to estimating knot point locations within the system, and the compound splines created in the "Splines" section may have been better suited to produce the final master hydrograph. Additionally, as an implied goal of this thesis was to produce a statistical estimation product that could be used when collecting data from a site, the product created would be too difficult for an outside party to use accurately. To the methodology's credit, the generated EARTH models did

manage to predict the hydrograph results with an R-Squared of 0.94, predicted the peak height of each hydrograph with an R-Squared of 0.85, and with those models, created an estimation of the trench hydrographs using only rainfall data with an R-Squared of 0.79. The HydroCAD model created has some level of inaccuracy, but demonstrates that theoretical detention time in a proposed trench system can be reduced significantly with the introduction of sidewall infiltration. There are pieces of this methodology which would complement the goals of the hypothesis well, but those pieces would be better served as contributions to a new project with the same ultimate goal in mind, rather than a continuation of this one.

2. Field Workflow

This section will provide an outline into a potential design process with current regulations for subsurface gravel trenches and incorporating sidewall infiltration.

The primary existing regulatory consideration for the subsurface gravel trench design process as pertains to this thesis is the drain time of less than 72 hours, as the consideration of sidewall infiltration introduces an additional outlet for infiltration and would reduce the amount of time water takes to infiltrate into the surrounding soil. Anisotropic conditions does not change the design volume of the system as systems are statically designed according to the WQV. A number of methods could be used to estimate the effect soil layering has on the infiltration time of a trench. The method presented here is based on the context of which this research was conducted, as a composite estimation of flow out of individual soil layers.

1) Drill several boreholes or backhoe excavations to multiple depths for each test performed, preferably to depths where there is a noticeable change in soil consistency.

2) Perform slug tests or double ring infiltrometer tests at each depth, in order to determine the saturated hydraulic conductivity, or at least the infiltration rate of that layer. Note that a slug test will produce a composite saturated hydraulic conductivity, while a double ring infiltrometer will produce a vertical saturated hydraulic conductivity.

3) Each layer can be treated like its own soil horizon. If one wishes to model the system in HydroCAD, the saturated hydraulic conductivity will need to be converted to a constant rate. The constant rates would then need to be implemented as exfiltration outlets, one for each soil layer. The bottom of the trench, meanwhile, can still be modelled using a conductivity instead of a constant rate.

4) Alternatively if one wishes to model the system using the Green-Ampt method in the long form, they may do so by modelling the bottom infiltration rate using the traditional equation, and model the sides by neglecting the wetting front length on the top of the equation. That way, the only contributing factors would be matric suction and pressure resultant from ponding. Note that with this method, an additional column would be needed specifying the wetted surface area on the sides of the trench for each layer. Additionally, the ponding distance would need to be calculated to the center of each layer, as each layer would experience different ponding pressure.

There are limitations to this methodology. Since the double ring infiltrometer measures vertical conductivity, it has limited usefulness for anisotropic soil layers. The soil layers themselves must be isotropic. A borehole test is generally unreliable for producing a consistent saturated conductivity vector when in the presence of anisotropy. For example, it was found that if one uses a constant head borehole test in anisotropic conditions, and the results are

extrapolated to a theoretical zone of all lateral infiltration, the resultant infiltration rate may be negative.

Unlike the methodology presented in the thesis, this method cannot find exact locations of soil horizons. Locating soil horizons can be done visually, or one can treat the elevation of each infiltration test as its own soil horizon in the modelling process, for calculation purposes. Also, HydroCAD cannot use sidewall infiltration for saturated hydraulic conductivity, only constant infiltration rates. When choosing a test for this process, keep all tradeoffs in mind.

The functional result of this process would be a trench system with a more accurate infiltration rate, which in turn would prevent the need for a larger bypass at the bottom of the system. The system may still require a bypass, as infiltration trenches with a low performance through the bottom surface but high sidewall infiltration will take much longer to infiltrate at very low elevations, due to the lack of exposure to the sidewalls. However, the bypass would be smaller in size compared to a system not utilizing sidewall infiltration, or compared to a system utilizing sidewall infiltration at the same rate as the bottom surface, which as mentioned in this example, is very low.

3. Future Recommendations

Upon review of the project, changes in the algorithm analyzing and reproducing trench outflow behavior could have resulted in a greater quality product. Such changes could still be made to this thesis's algorithm but were outside the scope of this project. The proposed changes are listed below, in order of most to least severity of importance.

1) The EARTH analysis and initial ideal hydrograph analysis should not have been conducted with the raw height values, but rather with the derivative "change in volume over time" values. The change in volume graph, which would be directly correlated with the Ksat hydrograph in this case, would reflect reality more accurately as a continuous function.

2) The master curve suffers from inconsistencies caused by how the infiltration rate of the trench changes over time. The EARTH model for the trench could be supplemented with additional terms in the model such as sine curves representing seasonal changes, or a first order linear equation representing the age of the system.

3) The peak height fitting curve could be improved with additional considerations. For example, daily maximum and minimum temperature readings could be derived from the available temperature readings, and the prior ten days could be considered for the time series analysis, to consider possible snow melt.

4) The "delay to peak" variable in its current form is essentially a random variable, with nothing useful worth extracting. However, if the patterns of rainfall could be simplified, possibly generalized as a triangular-shaped simplification of rainfall depth over time, perhaps the temporal distance from any localized rainfall peaks to the peak on the trench hydrograph could be estimated.

5) One of the most important attributes of this thesis is its connection to the real world. However, the algorithm has minimal applicability to real world soil variables, like saturated hydraulic conductivity, or even an automated estimate for a sidewall infiltration rate. An infiltration rate could have been calculated automatically if the piecewise function contained upper and lower bounds for each segment, but the idea was discarded due an inability to extract knot locations from the EARTH model, as present in the master falling limb hydrograph.

6) There were multiple methods by which the product could be made more user friendly, the first of which would be to create an executable with a user interface. In its current form, one must understand the basic features of the programming language R to use the program.

7) The drift correction process is imperfect. If the process were to be repeated, the drift equation may be limited to a single order polynomial for consistency. The option might also be included to make drift correction optional, for datasets with few points.

8) The original fitting process to the "ideal" storm is imperfect because the current system only allows for three distinct layers. If the fitting algorithm were revised, knots would be added to the ideal storm fitting until a certain threshold of diminishing returns to the r-squared value was met.

CONCLUSION

Layering in soils can be advantageous when it comes to the infiltration of stormwater from a subsurface gravel trench. The EARTH model was used to estimate the percentage of total infiltration in the UNH A-Lot system due to sidewall infiltration for each individual storm. The quartiles for sidewall infiltration were 75.9%, 82.3%, and 88.7%. The average infiltration out the sidewalls overall was 85.7%.

The primary difficulty to incorporate the effects of soil layering is understanding the infiltration rate of each individual soil. A method for measuring infiltration rates for each soil layer was proposed in this thesis. The proposed method involves using a subsurface structure with void space, like a trench or a borehole, introducing a volume of water to the structure, and measuring the rate at which water descends, preferably with precision equipment like a pressure sensor. The data can then be analyzed by fitting multiple lines to the measured recession limb, as to estimate the elevation of any soil horizons through the presence of kinks or "knots" resulting from the fitting process. The proposed method for measuring soil horizons and measuring soil layer infiltration rates utilizes software which can aggregate multiple recession limbs, allowing for more robust estimations.

The anisotropy measurement method described was used at a subsurface gravel tree trench system located at the University of New Hampshire's parking lot A. The EARTH analysis estimated 4 levels of stratification with horizontal Ksat values from 0.15 to 124.4 inches/hour. The vertical saturated conductivity measured with the double ring infiltrometer achieved results between 0.00 and 0.03 inches per hour. The high rate of anisotropy allowed the trench to exceed performance expectations in terms of the infiltration of large storms, but the low vertical Ksat

caused the trench to underperform in terms of drainage time. Long drain times could pose problems with creating standing water conditions, as exemplified by the presence of insect larvae in the monitoring wells.

The R code created for the purposes of this paper is capable of taking long sequences of data in the form of rain gauge data and hydrograph data, correcting for drift, discretizing that data into individual storm events, splicing storms together as to preserve hydrological properties and stratification, model the resultant hydrological curve, and utilize that curve to predict how a storage system would react to any particular storm event.

The analysis of the A-Lot system seems to reflect one important result about the system itself: infiltration out the sides of the subsurface gravel trench is significant, but not exhaustive. When water reaches a high enough stage in the trench, water exits the trench very quickly, enough to handle most significant storms. The trench experiences a loss in effectiveness at the very low elevations. The loss in effectiveness of infiltration is likely attributable to a decrease in surface area over which the exfiltration takes place. At the highest heights of the trench, water exfiltrates at an extremely high rate, at an estimated 120 inches per hour. At the lowest stages, water flows out very slowly, at about 0.08 inches per hour. At least part of the loss specified is attributable to flow out the bottom of the trench, meaning that flow out the sides is even slower than 0.08 inches per hour. The problem with the slow outflow at the end is that it extends the duration of water in the trench by entire days, when in the given 1-inch storm example, almost 7/8ths of the water has infiltrated in the NH BMP minimum 24 hours, the trench empties to less than 100 cubic feet in 5 days, while the time to empty the trench completely is over 8 days. In spite of the tremendous retention time, the system has managed to infiltrate all but 4 storms over

two years without exceeding the bypass height. That would indicate a tremendous amount of untapped potential in the design process.

The potential for increased infiltration rates overlaps with three opposing design features in the current NH Stormwater design manual:

1) The trench must have enough volume to hold the Water Quality Volume (WQV), or the resultant runoff volume from a 1-inch storm. The logic guiding the volume requirement is that the majority of contaminants on impermeable surfaces wash off into the stormwater during the first inch of rainfall. Since infiltration into the surrounding soil is considered a treatment process, then having a trench hold the 1-inch storm helps to ensure that the most contaminated water is treated.

2) The trench must be able to drain completely within 72 hours (New Hampshire Stormwater Manual Part 2, 2008, page 87). Presumably, the logic guiding the drainage time surrounds the possibility that successive storms might overload the system, or that the system might create potential for standing water.

3) The maximum allowable infiltration rate is 10 inches per hour (New Hampshire Stormwater Manual Part 2, 2008, page 19). Infiltration rates are associated with the number of interactions a water molecule has with the surrounding medium. In a soil with a high infiltration rate, the soil has a low surface area, usually the result of a low percentage of finer materials. In a low infiltration rate soil, such as clay, the amount of surface area is very high, and the water will have many collisions with soil particles, leading to a decrease in velocity. The surface area factor is relevant because surface area is also the primary component of the filtration process, as contaminants can get trapped on those surfaces. As a result, the water that reaches the water table

is filtered to a degree dependent on the infiltration rate. If the infiltration rate is too high, the water is less filtered by the time it reaches the water table.

The preceding list is not exhaustive but presents realistic examples for why anisotropic soils might not receive credit for infiltration. One could form counter arguments as to why the listed problems are not necessarily relevant to a trench system with high anisotropic conditions:

1) If a trench is sized by conventional standards, specifically the static sizing method, there are unrealistic assumptions made about such a system. All water during such a storm fills the trench as one solid block during one timestep. It would be more realistic to design to an adaptive model with longer period design storms, during which time, significant infiltration would occur. The design storm could be even larger than 1-inch, if one were concerned that the WQV needed to be treated specifically, and not get diluted and flow out the top of the system. Or one could dynamically size the trench using a modelling system like HydroCAD. Some manufactured high flow bioretention systems have already started using dynamic sizing to decrease the footprint size (ACF Environmental).

2) A system with low vertical infiltration but high horizontal infiltration has the potential to leave standing water (which might explain why many of the height sensors were frequently found with bug larvae), but in terms of the possibility of multiple storms hitting the system and overloading it, if the system were capable of withstanding the exaggerated model mentioned in item 1, it would seem very plausible that it could withstand multiple storms in a row.

3) The maximum infiltration rate according to the regulations applies to vertical infiltration and not horizontal infiltration as it stands now, but one could easily see the argument being applied to infiltration out the sides of the trench. Such a consideration might be relevant in the instance where the surrounding soil requires remediation, but if the bottom of the trench meets the 10 inches per hour requirement, and there is every indication that the surrounding soil is of a similar quality, then any stormwater leaving the sides of the trench would eventually have to make its way through the correctly rated soil before it reached the water table, during which time it would have travelled through even more media then the water that left the bottom of the trench.

Of the presented arguments, the only one that did not present an immediate justification or potential solution was the possibility of standing water in the trench. At particularly low heights, the amount of infiltration in the trench would slow considerably and present a more suitable environment for bug larvae. One solution might be a drainage orifice flush with the bottom of the trench, but that would detract from the site's suitability as an infiltration practice. With that consideration in mind, the possibility of utilizing anisotropic conditions should not be discounted, as it would provide the possibility of reducing the footprint of many subsurface infiltration systems. If subsurface systems could be reduced in size, then cities would require less scarcely available land to utilize stormwater technology and pay less money to install such systems.

One of the most difficult parts of the analysis during the project was the measurement of anisotropy. Determining an appropriate Ksat value is difficult to do without the use of costly or time consuming procedures. The most accurate way presented by modern, realistic technology

was to extract a core sample of the soil and send the sample to a lab. That method would not work with rocky soils, since it would make retrieving a structurally representative core sample almost impossible.

The next method for Ksat measurement would be either an Amoozemeter or Guelph Permeameter. The theoretical principle is that when measured at different depths, the infiltration rate would go up proportionally to the infiltration rate of the newly saturated profile. Such a notion does not work in a real life situation. In fact, the infiltration rate can veer toward the negative in anisotropic soils. (Jabro, J. and R. Evans)

Possibly the easiest method of measuring anisotropy would be to measure a soil's particle size distribution (PSD) at multiple levels. Each individual soil could be thought of as isotropic, with the combined effect of an anisotropic soil. The method has problems with accuracy due to the disturbance of the soil's structural formation.

One of the more accurate anisotropy measurement methods is a borehole pump test. The results would have better numerical methods for teasing out anisotropic features from pump tests (HydroSOLVE, Inc.), but such tests are expensive.

Considering the poor suitability or heavy cost of most anisotropy measuring methodologies, this thesis proposes a statistical method involving a borehole test, as proposed in the "Field Workflow" section.

LIST OF REFERENCES

ACF Environmental. “FocalPoint Biofiltration System: Bioretention Pond Alternative: ACF.” *ACF Environmental*, 11 Sept. 2020, acfenvironmental.com/products/stormwater-management/filtration/focal-point/.

Albrecht. (2007). Key concepts and techniques in GIS. SAGE.

Alfakih, E, et al. “A Study of Stormwater Infiltration System Feasibility and Design.” *Water Science and Technology*, vol. 39, no. 2, 1999, https://doi.org/10.1016/s0273-1223(99)00034-7.

Allaby, M. (2008). A dictionary of earth sciences. (3rd ed. / edited by Michael Allaby.). Oxford University Press.

A. Savitzky and M. J. E. Golay, "Soothing and differentiation of data by simplified least squares procedures", *Anal. Chem.*, vol. 36, pp. 1627-1639, 1964.

Balugani, E., Lubczynski, M. ., & Metselaar, K. (2016). A framework for sourcing of evaporation between saturated and unsaturated zone in bare soil condition. Hydrological Sciences Journal, 61(11), 1981–1995. https://doi.org/10.1080/02626667.2014.966718

BATU, V. (2012). Solving vertical and horizontal well hydraulics problems analytically in Cartesian coordinates with vertical and horizontal anisotropies. Journal of Hydrology (Amsterdam), 414-15, 72–85.

Bear, & Cheng, A. H.-D. (2010). Modeling Groundwater Flow and Contaminant Transport (1st ed. 2010.). Springer Netherlands. https://doi.org/10.1007/978-1-4020-6682-5

Bouwer, Herman. “Measuring Horizontal and Vertical Hydraulic Conductivity of Soil With the Double-Tube Method.” *Soil Science Society of America Journal*, vol. 28, no. 1, 1964, pp. 19–23., doi:10.2136/sssaj1964.03615995002800010019x.

Burack, Thomas S, editor. *New Hampshire Stormwater Manual*. 1st ed., vol. 2 3, New Hampshire Department of Environmental Services, 2008, www.des.nh.gov/sites/g/files/ehbemt341/files/documents/2020-01/wd-08-20b.pdf.

Chesworth W., Perez-Alberti A., Arnaud E., Morel-Seytoux H.J. (2008) Imbibition. In: Chesworth W. (eds) Encyclopedia of Soil Science. Encyclopedia of Earth Sciences Series. Springer, Dordrecht. https://doi-org.unh.idm.oclc.org/10.1007/978-1-4020-3995-9_286

D. Moret-Fernández, B. Latorre, L. Lassabatere, S. Di Prima, M. Castellini, D. Yilmaz, R. Angulo-Jaramilo, Sequential infiltration analysis of infiltration curves measured with disc infiltrometer in layered soils, Journal of Hydrology, Volume 600, 2021, 126542, ISSN 0022-1694, https://doi.org/10.1016/j.jhydrol.2021.126542. (https://www.sciencedirect.com/science/article/pii/S0022169421005898)

“ECFR :: Title 40 of the CFR -- Protection of Environment.” *Code of Federal Regulations*, National Archives, 22 Mar. 2022, https://www.ecfr.gov/current/title-40.

Ely. (2019). *Infiltration Characteristics of Subsurface Gravel Filtration Systems for Stormwater Management*. ProQuest Dissertations Publishing.

Gelman, Andrew and Guido Imbens. “Why High-Order Polynomials Should Not Be Used in Regression Discontinuity Designs.” *Journal of Business & Economic Statistics* 37 (2014): 447 - 456.

Green, W.H. and G. Ampt. 1911. “Studies of soil physics, part I – the flow of air and water through soils.” *J. Ag. Sci.* 4:1-24.

Hans W. Borchers (2019). pracma: Practical Numerical Math Functions. R package version 2.2.9. https://CRAN.R-project.org/package=pracma

HydroCAD Software Solutions, LLC. “HydroCAD Stormwater Modeling.” *HydroCAD Stormwater Modeling Software*, 2020, www.hydrocad.net/index.htm.

HydroSOLVE, Inc. “Neuman Solution for Unconfined Aquifers.” *Neuman Pumping Test Solution for Unconfined (Water-Table) Aquifers*, www.aqtesolv.com/neuman.htm.

Jabro, J. and R. Evans. “Discrepancies Between Analytical Solutions of Two Borehole Permeameters for Estimating Field-Saturated Hydraulic Conductivity.” *Applied Engineering in Agriculture 22* (2006): 549-554.

Jeppesen, & Christensen, S. (2015). A MODFLOW infiltration device package for simulating storm water infiltration. *Ground Water*, 53(4), 542–549. https://doi.org/10.1111/gwat.12255

Macadam. (2018). *An Improved Infiltration Model and Design Sizing Approach for Stormwater Bioretention Filters Including Anisotropy and Infiltration into Native Soils*. ProQuest Dissertations & Theses.

Milborrow, Stephen. *Earth Notes - Milbo.org*. 1 June 2021, http://www.milbo.org/doc/earth-notes.pdf.

“National Stormwater Calculator.” *EPA*, Environmental Protection Agency, https://swcweb.epa.gov/stormwatercalculator/.

R Core Team (2020). R: A language and environment for statistical computing. R Foundation for Statistical Computing, Vienna, Austria. URL https://www.R-project.org/.

"Regulations." Philadelphia Water Department, 27 Aug. 2021, https://water.phila.gov/regulations/.

Sengupta, & Jammalamadaka, S. R. (2003). Linear models an integrated approach. World Scientific.

Singh, S. K. (2004). Drawdowns due to Intermittent-Pumping Cycles. Journal of Hydraulic Engineering (New York, N.Y.), 130(6), 568–575. https://doi.org/10.1061/(ASCE)0733-9429(2004)130:6(568)

Stephen Milborrow. Derived from mda:mars by Trevor Hastie and Rob Tibshirani. Uses Alan Miller's Fortran utilities with Thomas Lumley's leaps wrapper. (2020). earth: Multivariate Adaptive Regression Splines. R package version 5.3.0. https://CRAN.R-project.org/package=earth

Tsihrintzis, V.A., Hamid, R. Modeling and Management of Urban Stormwater Runoff Quality: A Review. *Water Resources Management* 11, 136–164 (1997). https://doi.org/10.1023/A:1007903817943

Virieux, J., Brossier, R., Métivier, L. *et al.* Direct and indirect inversions. *J Seismol* **20,** 1107–1121 (2016). https://doi.org/10.1007/s10950-016-9587-3

Zijl, W., De Smedt, F., El-Rawy, M., & Batelaan, O. (2018). The Double Constraint Inversion Methodology Equations and Applications in Forward and Inverse Modeling of Groundwater

Flow (1st ed. 2018.). Springer International Publishing. https://doi.org/10.1007/978-3-319-71342-7